

THE EFFECTS OF BETA ADRENERGIC RECEPTOR AGONISTS IN CONTROL AND
MYOSTATIN KNOCKOUT MICE ON ADIPOCYTE APOPTOSIS, AND BODY
COMPOSITION

by

KAREN ANN PAGE

(Under the Direction of Clifton A. Baile)

ABSTRACT

Oral administration of beta-adrenergic receptor (β -AR) agonists to animals causes increased muscle and decreased fat mass in various combinations across species. Myostatin, a member of the transforming growth factor beta super family of growth factors, inhibits muscle growth. Researchers have created a mouse with the myostatin gene knocked out, which results in a double muscled phenotype with decreased fat mass and is an important model for both the agricultural and biomedical fields. Our objectives were to first determine if ractopamine, a β -1 or clenbuterol, a β -2 adrenergic receptor agonist would have similar, different, or any effects on the body composition of control mice. After discovering that clenbuterol had the same effect as ractopamine but at a lower dosage, the oral clenbuterol treatment was then tested on myostatin knockout mice. Our findings showed in both studies that fat pads were reduced, skeletal muscle mass did not change, and adipocyte apoptosis was increased when clenbuterol was administered.

INDEX WORDS: Myostatin, Beta-adrenergic receptor agonists, Clenbuterol,

Ractopamine, Adiposity, Apoptosis, Mouse, Double-Muscled

MYOSTATIN INHIBITION AND BETA ADRENERGIC RECEPTOR AGONISTS

by

KAREN ANN PAGE

B.S., The University of Georgia, 1997

A Thesis Submitted to the Graduate Faculty of The University of Georgia in Partial Fulfillment of
the Requirements for the Degree

MASTER OF SCIENCE

ATHENS, GEORGIA

2004

© 2004

KAREN ANN PAGE

All Rights Reserved

MYOSTATIN INHIBITION AND BETA ADRENERGIC RECEPTOR AGONISTS

by

KAREN ANN PAGE

Major Professor: Clifton A. Baile

Committee: Michael Azain
Roger Dean
T. Dean Pringle
Dorothy Hausman

Electronic Version Approved:

Maureen Grasso
Dean of the Graduate School
The University of Georgia
May 2004

DEDICATION

For my mom and dad. Without their love and support this would have never been possible.

Also for my granddad who knew, anything was possible.

ACKNOWLEDGEMENTS

I would like to thank Dr. Clifton Baile for his support, enthusiasm, patience, and for enjoying the game. My thanks also goes to Diane Hartzell for teaching me how to avoid and solve problems and how to pay attention to detail to make our research the best possible. I would also like to thank Drs. Michael Azain, Roger Dean, Dean Pringle, and Dorothy Hausman for various forms of technical support, and to Mary Anne Della-Fera for writing support. I want to express my appreciation for the assistance I received from our lab group – especially my good friend Ji Lin who never seemed bothered by my endless questions. A special thanks goes to my Joseph for his never ending patieces, for always believing in me, and most of all, no matter my mood, for always making me laugh. Finally, I am fortunate to have one thing that always makes me smile at the end of the day – a perfect mutt named Sydney.



TABLE OF CONTENTS

| | Page |
|--|------|
| ACKNOWLEDGEMENTS..... | v |
| LIST OF FIGURES..... | viii |
| LIST OF TABLES..... | x |
| CHAPTER | |
| 1 INTRODUCTION..... | 1 |
| 2 MYOSTATIN..... | 3 |
| History..... | 4 |
| Structure..... | 7 |
| Physiology and Function..... | 9 |
| Implications..... | 11 |
| 3 β -1 AND 2 ADRENERGIC RECEPTOR AGONISTS..... | 14 |
| Beta 1 Adrenergic Receptor Agonists and Ractopamine..... | 16 |
| Beta 2 Adrenergic Receptor Agonists and Clenbuterol..... | 17 |
| 4 CLENBUTEROL IN VITRO..... | 18 |
| 5 β -ADRENERGIC RECEPTOR AGONISTS INCREASE APOPTOSIS OF ADIPOSE TISSUE IN MICE..... | 21 |
| Abstract..... | 22 |
| Introduction..... | 23 |
| Methods..... | 23 |

| | |
|--|-----|
| Results..... | 26 |
| Discussion..... | 31 |
| References..... | 34 |
| 6 EFFECTS OF CLENBUTEROL ON MUSCLE, ADIPOSE TISSUE AND | |
| ADIPOCYTE APOPTOSIS IN MYOSTATIN KNOCKOUT MICE..... | 37 |
| Abstract..... | 38 |
| Introduction..... | 38 |
| Methods..... | 40 |
| Results..... | 43 |
| Discussion..... | 48 |
| References..... | 51 |
| 7 CONCLUSION | 54 |
| REFERENCES..... | 56 |
| APPENDICES..... | 59 |
| A P27 KNOCKOUT MICE; REDUCED MYOSTATIN IN MUSCLE AND ALTERED | |
| ADIPOGENESIS..... | 59 |
| B MELANOCORTIN RECEPTORS MEDIATE LEPTIN EFFECTS ON FEEDING AND | |
| BODY WEIGHT BUT NOT ADIPOSE APOPTOSIS..... | 75 |
| C EVALUATION OF ADIPOCYTE APOPTOSIS BY LASER SCANNING | |
| CYTOMETRY..... | 95 |
| D COMPARATIVE 2D DIFFERENCE GEL ANALYSIS OF HYPOTHALAMUS | |
| PROTEIN EXPRESSION PATTERN OF MYOSTATIN KNOCKOUT MICE | |
| WITH CLENBUTEROL TREATMENT..... | 113 |

LIST OF FIGURES

| | Page |
|---|------|
| Figure 2.1: Belgian Blue Cow..... | 5 |
| Figure 2.2: GDF-8 Knockout verses Control..... | 6 |
| Figure 2.3: TGF- β Activation..... | 7 |
| Figure 2.4: Myostatin Protein..... | 8 |
| Figure 2.5: Myostatin Protein Sequence..... | 9 |
| Figure 2.6: Myostatin Activation..... | 10 |
| Figure 3.1: Epinephrine and Norepinephrine Structures..... | 14 |
| Figure 3.2: Cascade of β -AR Agonist Receptor Complex..... | 15 |
| Figure 3.3: Ractopamine Structure..... | 16 |
| Figure 3.4: Clenbuterol Structure..... | 17 |
| Figure 4.1: Viable, Apoptotic, and Necrotic Cells..... | 20 |
| Figure 5.1: Retroperitoneal Fat Pad Weight, Epididymal/Parametrial Fat Pad Weight and Intrascapular Brown Adipose Tissue Weight for Control, 200 ppm Clenbuterol, 200 ppm Ractopamine and 800 ppm Ractopamine Treated Mice..... | 29 |
| Figure 5.2: Percent DNA Fragmentation (Apoptosis) in Epididymal/Parametrial Fat Pads in Control, 200ppm Clenbuterol, 200 ppm Ractopamine and 800 ppm Ractopamine Treated Mice..... | 30 |
| Figure 6.1: Daily Weight Gain (g) and Feed Efficiency in Male and Female Mice Fed 0 or 200ppm Clenbuterol for 21 Days..... | 44 |

Figure 6.2: Effects of Gender, Genotype and Treatment on Weight (mg/g Body Weight) of Individual Fat Pads, Skeletal Muscles and Heart.....46

Figure 6.3: Epididymal/Parametrial Apoptosis (% DNA fragmentation) in Female and Male Wild Type and GDF-8 Knockout Mice Fed 0 or 200 ppm Clenbuterol for 21 Days.....47

LIST OF TABLES

| | Page |
|--|------|
| Table 5.1: Effects of 21 Day Oral Treatment with Control, 200ppm Clenbuterol, 200ppm Ractopamine and 800ppm Ractopamine on Body Weight, Food Intake, Feed Efficiency, Body Temperature and Body Composition in Mice..... | 27 |
| Table 5.2: Effects of 21 Day Oral Treatment With Control, 200ppm Clenbuterol, 200ppm Ractopamine and 800ppm Ractopamine on Selected Tissue Weights in Male and Female Mice..... | 28 |
| Table 5.3: Effects of 21 Day Oral Treatment with Control, 200ppm Clenbuterol, 200ppm Ractopamine and 800ppm Ractopamine on Epididymal and Parametrial Weights in Male and Female..... | 29 |
| Table 6.1: Final Body Weight, Daily Weight Gain and Daily Food Intake in Female and Male Wild Type and GDF-8 Knockout Mice Fed 0 or 200ppm Clenbuterol for 21 Days..... | 43 |
| Table 6.2: Body Composition Analysis of Female and Male Wild Type and GDF-8 Knockout Mice fed 0 or 200ppm Clenbuterol for 21 Days by PIXImus Densitometry..... | 45 |
| Table 6.3: Epididymal/Parametrial and Retroperitoneal Fat Pad Apoptosis in Female and Male Wild Type and GDF-8 Knockout Mice Fed 0 or 200 ppm Clenbuterol for 21 Days..... | 47 |
| Table 6.4: Serum Leptin Concentration (ng/ml) in Female and Male Wild Type and GDF-8 Knockout Mice Fed 0 or 200 ppm Clenbuterol for 20 Days..... | 48 |

CHAPTER 1

INTRODUCTION

Since the time of Gregor Mendel, genetic manipulation and enhancement of various species of organisms has taken place. Currently, our scientific knowledge has brought us to a point where genetically altering organisms is a prime target for commercial production and biomedical research. In 1997, the gene for growth and differentiation factor 8 (GDF-8), or myostatin, was discovered by Lee and McPherron who were looking at genes in the transforming growth factor beta (TGF- β) family. GDF-8 is a member of the TGF- β superfamily of growth factors and acts to inhibit muscle growth. By genetically deleting the GDF-8 gene in mice, the researchers produced a knockout model by homologous recombination that has a “double muscled” phenotype. This unique model has opened many doors for muscle and adipose research and can be applied to many different areas of science, including muscle wasting disorders, diabetes, and obesity.

In the livestock industry, selection for better genetics has been a key in enhancing meat production. Two unique cattle breeds, the Belgian Blue and the Piedmontese, have been affected by genetic changes via natural mutations in the GDF-8 gene. Like the knockout mice, the cattle also have a double muscled appearance. When natural mutations do not occur and genetic selection has been exhausted, exogenous administration of partitioning agents is a way to further enhance muscle growth. One class of partitioning agents is beta adrenergic receptor (β -AR) agonists. There are currently three classes of β -AR agonists, β 1, β 2, and β 3. The receptors are located on all mammalian cells in different quantities and distribution varies between species. Certain agonists, therefore, work to enhance muscle and decrease fat better in certain species.

The focus of the work presented here was to study the effects of β -AR agonists on muscle and adipose tissue in GDF-8 knockout mice. If manipulation of the myostatin gene and oral administration of β -AR agonist can act together to further enhance the muscling in livestock then this could further advance the livestock industry, and the knowledge could also be beneficial to the biomedical industry. Chapter 5 of this thesis focuses on the effects of oral administration of ractopamine, a β 1-AR agonist, and clenbuterol, a β 2-AR agonist, in control mice. Chapter 6 then focuses on the effects of clenbuterol in GDF-8 knockout mice. Because adipocyte apoptosis was detected in all animals treated with clenbuterol, an in vitro study was conducted to determine if clenbuterol was acting directly, and is discussed in Chapter 4. Although lack of myostatin does not alter sensitivity to β -AR stimulation, the results from these studies show that further research should be done to better understand the complexities behind β -AR stimulation and that genetic manipulation of a model organism is a novel research tool.

CHAPTER 2

MYOSTATIN

Myostatin is a negative growth regulator expressed primarily in muscle and partially in fat tissue. This gene has evoked curiosity in individuals in both the livestock industry and the biomedical industry. Myostatin is a member of the TGF- β superfamily of growth factors, which regulates tissue growth. Myostatin is a 376-nucleotide protein that acts to inhibit muscle growth. During embryogenesis, myostatin is expressed specifically in the myotome layer of developing somites giving rise to muscle cells.

This gene has had a great impact on the Belgian Blue and the Piedmontese cattle breed of animals, due to unique mutations that occur in these breeds. These animals have 20-30% more muscle mass than other cattle breeds. The mutation that these animals experience is not harmful to the animals' health except that the organ size is slightly smaller and the fertility in the females is slightly decreased.

Once these double muscled animals became a phenomenon in the livestock industry, more emphasis was placed on how this natural mutation could be used to further enhance the industry in not only cattle, but in other species as well. The "double-muscling" effect could change the course of meat production, provided genetic engineering could manipulate this gene in other species. In other livestock breeds besides cattle, the myostatin deletion has not been very functional; however, in mice the story is different.

In 1997 genetic engineering was used to produce myostatin knockout mice. These mice, which were crossed from the SvJ/CJ7BL line, have 200-300% greater muscle mass than control

animals, and have significantly less adipose tissue mass. They are reproductively viable, have normal organ size, and have normal metabolic functions compared to wild type mice (Lee and McPherron, 1997). Because myostatin expression is increased in individuals with muscle wasting disorders such as HIV or muscular dystrophy, blocking myostatin may have practical implications for preventing muscle loss. Thus this novel gene could potentially affect both the livestock and biomedical industry.

History

The “double-muscled” phenotype was first observed several hundred years ago in various cattle breeds, most notably the Belgian Blue cattle breed as well as the Piedmontese cattle breed. This phenotype was first noticed in shorthorn cattle in the late 1700’s and in the Belgian Blue breed, specifically, in the mid 1800’s (Arnold 2001). Cattle and other livestock breeders were especially interested in this phenomenon because of the possibility of greater meat production.

The mh (muscular hypertrophy) locus associated with the “double muscling” phenotype, was localized to bovine chromosome 2 in 1995 (Charlier et al., 1995). This localization suggested that there was a single autosomal gene that caused the mutation in cattle, thus reinforcing the genetic homogeneity of the double muscled breeds. Because myostatin normally acts to inhibit muscle growth, the double muscled phenotype results from the hyperplastic effects of the mutation on muscle cells. In addition, animals with a myostatin gene mutation also have less fat mass compared to those without the mutation (McPherron and Lee, 1997).

The myostatin mutation in Belgian Blue cattle is a result of an 11 base pair deletion in the coding region of the myostatin gene, causing a frameship that is believed to produce a truncated protein terminating 14 codons from the mutation site (Grobet, et. al. 1997; Lee, and McPherron 2001). The mutation in the Piedmontese breed is the result of a missense mutation in exon 3,

which substitutes a cysteine with a tyrosine.



Figure 2.1: Belgian Blue Cow

<http://www.belgianblue.co.uk/breed/index.html>

In 1997 this mutation was produced in a murine model (McPherron et al., 1997b). To create this model, the entire C-terminal region of GDF-8 was deleted and the mutated gene was inserted into stem cells. Targeted clones were injected into blastocysts, and chimeras were obtained from independently derived ES clones that came from heterozygous offspring when crossed to C57BL females (McPherron et. al, 1997). The knockout mice produced have hypertrophic and hyperplastic muscles with body weights that are two to three times greater than wild-type mice (McPherron et. al, 1997). The animals have a slightly lower resting metabolic rate, and fat accumulation decreases with age even with normal food intake (McPherron and Lee, 2002). The mice have been affectionately deemed “mighty mice” (Westhusin, 1997).

The myostatin knockout mice also have a lower serum leptin level, which corresponds to their decreased fat mass, and normal uncoupling protein expression compared to control. (McPherron and Lee, 2002). Since leptin is produced by adipocytes, it would be expected that mice with less fat would have lower serum leptin levels. To determine the effect of myostatin gene knockout in animals with increased levels of body fat, McPherron and Lee used two models of genetically obese mice. The models used were the Agouti (Ay/a) model, which is characterized by an increase in food intake and food efficiency resulting in obesity, and the obese ($lep^{ob/ob}$) model,

characterized by deficient leptin signaling. In both models, myostatin gene knockout resulted in an increase in muscle mass, and over time, a decrease in fat pad mass. Genetically obese mice also have impaired glucose metabolism often leading to hyperglycemia, and the deletion of the myostatin gene prevented the development of the hyperglycemia. The results of the study suggested that a myostatin-blocking agent could be beneficial in the treatment of metabolic disorders, in addition to enhancing muscle growth (McPherron and Lee, 2002).



Figure 2.2: GDF-8 knockout mouse on left and control mouse on right.

<http://www.hopkinsmedicine.org/press/1997/MAY/199701.HTM>

When comparing the natural mutation found in the Belgian Blue and Piedmontese cattle breeds to the complete sequence in myostatin knockout mice, there is a great deal of similarity due to the extent of the frame shift at the active site of the gene in the cattle breeds (McPherron et al., 1997). However, the mutation in cattle causes a decrease in internal organ size, an increase in muscling of 25-30%, and a decrease in female fertility. In myostatin knockout mice, internal organs are normal, the increase in muscling is 200-300%, and fertility is normal. It is suggested that the difference in muscling in the cattle may be due to selective breeding such that the muscle size may be near the maximal limit for the species (McPherron et al., 1997a; McPherron and Lee, 2002). Conservation of this gene is great between species. At the C-terminus following the

putative proteolytic processing site, there is a 100% identical region in human, rat, murine, porcine, chicken, and turkey. The sequence conservation also suggests function conservation, and that this genetic manipulation could possibly be applied in other species (McPherron and Lee, 1997).

Structure

Transforming growth factor- β (TGF- β) superfamily members are proteolytically processed in the Golgi apparatus of the cell as large precursor molecules (Piek et al., 1999).

Latency-associated protein (LAP) and mature TGF- β are precursor molecules that are initially bound together to form latent complexes that are directed toward either the extra cellular matrix or the cell surface for activation. Activation is caused when LAP and mature TGF- β are cleaved by furin, which is a member of the convertase family of endoproteases (Grobet et al., 1997) (Figure 2.3).

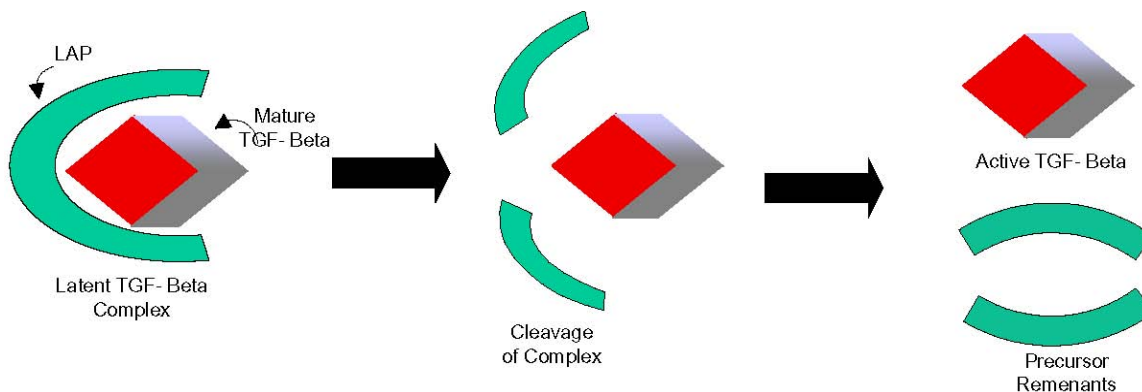


Figure 2.3: TGF- β activation

Myostatin, a member of the TGF- β superfamily, is a 376 amino acid propeptide that is produced during embryogenesis in the myotome layer of somites, and later in life in all skeletal muscle. Like other TGF- β members, it is proteolytically processed to give rise to its biologically active protein form (Thomas et al., 2000). It consists of 36 and 12.5 kDa propeptides that are bound to a disulfide-linked C-terminal dimer (Lee and McPherron, 2001). Binding to Act RIIB

triggers the signaling pathway for secreted myostatin. This signal can be inhibited by the myostatin propeptide as well as the activin-binding protein follistatin. Consequently, this inhibition causes an increase in muscle mass (Lee and McPherron, 2001).

The propeptide inhibition is also found in other TGF- β super family members. Other shared structural characteristics with the TGF- β superfamily members include a hydrophobic core near the N-terminus consisting of amino acids that code for its secretory function, a “cysteine knot”. The knot consists of nine cysteine residues in the C-terminal region, and a conserved proteolytic processing signal in the C-terminal region of the protein (Thomas et al., 2000). When examined stepwise, however, the C-terminal region of the myostatin protein does not fall into any of the closely related TGF- β subfamilies including TGF- β s, inhibins, and bone morphogenic proteins (BMPs), thus putting it into its own subcategory. In the C-terminal region myostatin is most closely related to Vgr-1 which is only a 45% amino-acid relatedness (McPherron et al., 1997b).



Figure 2.4: Myostatin protein (green) compared to TGF- β , BMP, and related proteins (gold)

The secretion of the mature myostatin protein is controlled by Titan-Cap (T-Cap). T-Cap is a 19kDa sarcomeric protein that contributes to the maintenance of the sarcomeric structure. The mature myostatin protein is then targeted by an amino acid sequence consisting of a core hydrophobic area close to the N-terminal area and the Arg-Ser-Arg-Arg (RSRR) proteolytic processing signal is located close to the C-terminal end of the protein (Thomas et al., 2000).

A nullifying mutation that contributes to the structure and function of the protein is C313Y.

This mutation is caused by a G to A base pair substitution that eventually causes a cysteine to tyrosine substitution during translation (Grobet et al., 1998)(Figure 2.5).

```
1 mmqklqmyvy iyflmliaag pvdlnegser eenvekeglc nacawrqnr ysrieaikiq
61 ilsklrleta pniskdairq llrapplre lidqydvqrd dssdgsledd dyhattetii
121 tmptesdfml qadgkpkccf fkfsskiqyn kvvkaqlwiw lrpvktpttv fvqilrlikp
181 mkdgtrytgi rslkldmspg tgiwqsidvk tvlqnwlkqp esnlgieika ldenghdlav
241 tfpgpgedgl npflevkvtd tpkrrrdfg ldcdehstes rccrypltvd feafgwdwii
301 apkrykanyc sgecefvflq kypthlvhq anprgsagpc ctptkmspin mlyfngkeqi
361 iygkipamvv drcgcs
```

Figure 2.5: Normal myostatin protein sequence. The red C (cystein) is changed to a Y (tyrosine) in the C313Y mutation.

Physiology and Function

Myostatin is a member of the transforming growth factor- β (TGF- β) super family of growth factors that regulate skeletal muscle growth. During embryogenesis, myostatin is expressed specifically in the myotome layer of developing somites, which gives rise to skeletal muscle (Lee and McPherron, 1999). In the adult, myostatin is expressed at different levels in muscle and is detected in other tissues including adipose (McPherron et al., 1997). Kim, et al.(2001) found that, in vitro, myostatin inhibits differentiation of 3T3-L1 preadipocytes, thus having a direct effect on adipogenesis and also an indirect effect due to the ratio change of muscle to fat tissue. Expression of myostatin is down-regulated in regenerating muscle (Sakuma et al., 2000) and is up-regulated after cardiac damage in cardiomyocytes (Sharma, 1999).

TGF- β superfamily members are positive or negative regulators that act via cell-surface receptors to determine the pathway for undifferentiated precursor cells. For example muscle precursor cells are committed to the mesoderm, and TGF- β acts to block their differentiation into myoblasts (Kelvin et al., 1989). Proliferation and withdrawal from the cell cycle of myoblasts

occurs during myogenesis at the first gap phase (G₁). Myoblasts then form myotubes by committing to a differentiation pathway in which cyclin dependent kinases (Cdk) and cyclin dependent kinase inhibitors (CKIs) determine cell cycle withdrawal and differentiation. Myostatin up-regulates a specific cyclin dependent inhibitor (CDI), p21, which inhibits Cyclin dependent kinase 2 (Cdk2). Cdk2 acts to regulate G₁ to S transitions. The inhibition then causes retinoblastoma (Rb) deactivation, which causes arrest of the cell in the G₁ stage and prevents the cell from entering the S stage. In C2C12 muscles cells, myostatin protein inhibits cell proliferation, DNA synthesis, and protein synthesis (Taylor et al., 2001). Therefore, in the absence of myostatin, p21 is no longer up regulated and the cascade is no longer inhibited thus causing increased myoblast proliferation (Thomas et. al, 2000).

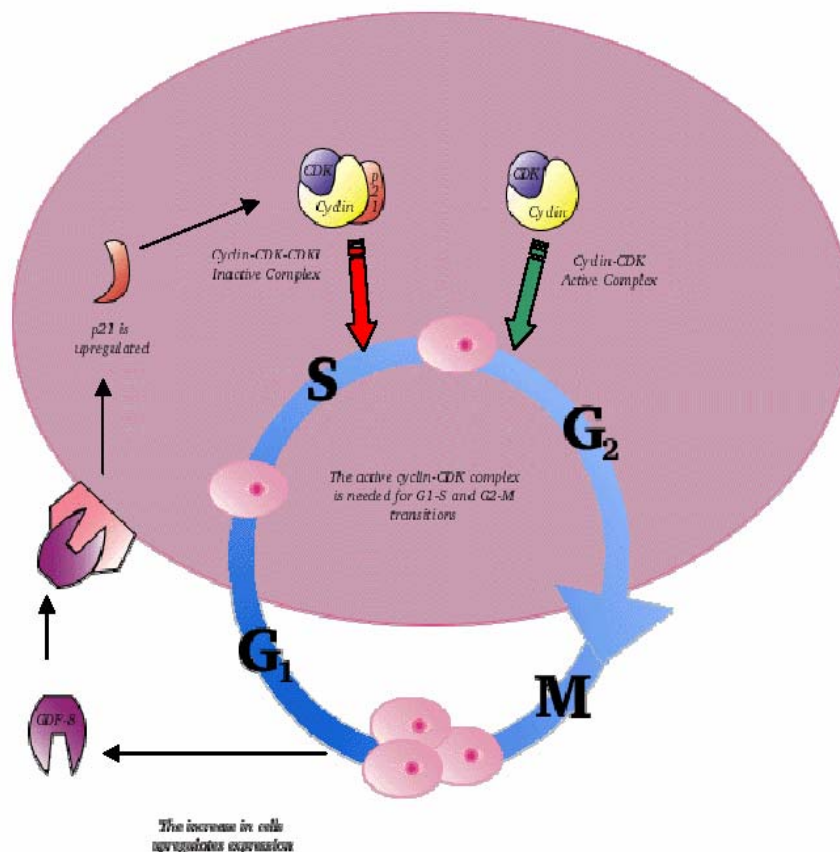


Figure 2.6: Myostatin Activation (Arnold, 2001)

Implications

In recent history, many advances have been made in biotechnology to improve both the biomedical and livestock industries. One unique gene, growth differentiation factor-8 (GDF-8) or myostatin, may be used to further improvements with the help of these new technologies. GDF-8 is a member of the transforming growth factor- β (TGF- β) family of growth factors. Myostatin inhibits muscle growth and is expressed primarily in muscle, but is also expressed to a smaller degree in adipose tissue.

Natural mutations in the GDF-8 gene occur in cattle result in muscle hypertrophy, resulting in a double muscled phenotype. Although the animals have smaller organ sizes, some cardiac myopathies, and decreased fertility, the amount and quality of the meat outweighs these flaws. Genetically modifying other livestock species could result in similar phenotypes, thus enhancing meat production.

Myostatin also has implications in the biomedical industry. In 1997, Lee and McPherron genetically modified mice by deleting, or knocking out, the GDF-8 gene. The 200-300% increase in the muscle mass of these mice makes for a unique model for various medical conditions. Over-expression of myostatin results in muscle atrophy (Zimmers et al., 2002); therefore, blocking myostatin may be of benefit in disorders that result in muscular atrophy. For example, myostatin is over-expressed in both men and women who are infected with HIV due to muscle wasting (Bogdanovich et al., 2002; Gonzalez-Cadavid et al., 1998; Sinha-Hikim et al., 1999). By blocking myostatin in those suffering from muscle cachexia due to HIV, cancer, and old age, a reversal or inhibition of muscle degeneration may result.

Muscular dystrophy (MD) is a disease involving a defective gene that alters protein expression, which results in faulty muscular development, therefore, myostatin blockage may be

of therapeutic use. When Duchenne muscular dystrophic (*mdx*) mice were injected with a neutralizing antibody, a reduction in necrosis and in serum creatine kinase was demonstrated compared to untreated *mdx* mice (Bogdanovich et al., 2002). In another study in which *mdx* mice were crossed with myostatin knockout mice (Wagner et al., 2002), the animals lacking myostatin showed an increase in muscle mass and a decrease in fibrosis and fatty replacement, but did not show a difference in muscle necrosis. Therefore, with further research, the myostatin antibody approach may be beneficial to those suffering from MD.

Myostatin inhibition may also be beneficial in the treatment of obesity or diabetes. McPherron and Li (2002) found that myostatin gene knockout increased muscle mass and decreased adipose tissue mass in genetically obese mice, as well as improving insulin sensitivity. An additional benefit from the deletion of the myostatin gene is an improvement in bone mineral density and content. In the femur of myostatin deficient mice, bone mineral density (BMD) is increased and in the humerus both BMD and bone mineral content (BMC) are increased (Hamrick et al., 2002a; Hamrick et al., 2002b). The spines of the myostatin deficient mice are also stronger than the spines of wild type mice. Myostatin deficient mice have 50% greater trabecular BMD and have an increase in cortical BMC, however there is some degeneration in the intervertebral disc between lumbar four and five (Hamrick et al., 2003). Because the mice have less fat, they produce less leptin. Leptin has been shown to increase chondrocyte production therefore with a decrease in leptin, as seen in myostatin deficient mice, there may be an inhibition in chondrocyte production or cartilage repair (Hamrick et al., 2003). Nevertheless, even with the small amount of intervertebral degeneration, blockage of myostatin may be a beneficial therapy for those suffering from osteoarthritis.

Increasing knowledge of myostatin function is allowing researchers to expand on a naturally occurring mutation that was first seen almost 200 years ago. By applying new technologies to interrupt the myostatin signaling pathway in novel ways, investigators will not only be able to provide improved livestock, but may also develop potentially life saving therapies. The potential for helping HIV patients, the elderly, the obese or those with muscular dystrophy is almost unlimited. The technologies that will arise from this genetic manipulation have the potential to leave a lasting mark in the scientific world.

CHAPTER 3

BETA-ADRENERGIC RECEPTORS AND AGONISTS

Beta adrenergic receptors (β -AR) are located on the surface of nearly all cell types in mammalian species. A physiological response occurs when a β -AR agonist binds to a β -AR. While there are many synthetic β -AR agonists, there are two physiological agonists, the catecholamines, norepinephrine, a sympathetic nervous system neurotransmitter molecule, and epinephrine.

Norepinephrine (figure 3.1) is biosynthesized from tyrosine while epinephrine is produced in the adrenal medulla as the methylation product of norepinephrine. Norepinephrine is typically circulated in higher concentrations except during stress responses where there is then a shift to higher concentrations of epinephrine.

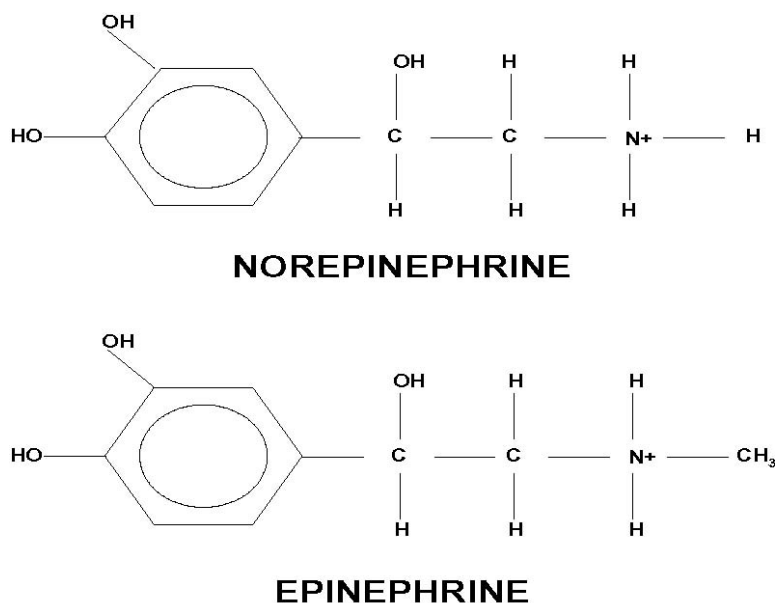


Figure 3.1: Chemical structures of the physiological β -AR agonists norepinephrine and epinephrine.

A complex is formed when epinephrine, norepinephrine, or a synthetic β -AR agonist bind to the B-AR which causes the G_s protein to be activated. In the case of synthetic β -AR antagonists the G_s protein is not activated. However, if the protein is activated by an agonist, the α -subunit then activates adenylyl cyclase. Adenylyl cyclase is the enzyme that produces cyclic adenosine monophosphate (cAMP). Cyclic AMP then binds to the regulatory subunit protein kinases A, which then releases its catalytic subunit to phosphorylate several intracellular proteins.

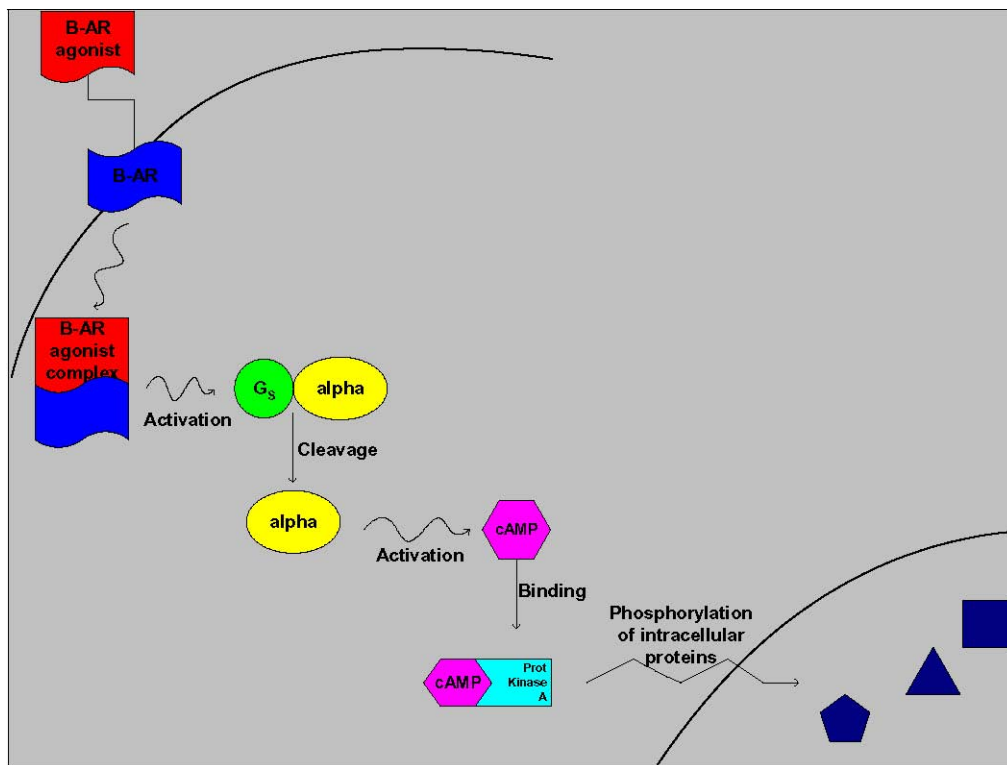


Figure 3.2: Cascade of β -AR agonist receptor complex for intracellular signaling.

Interest in beta-adrenergic receptors was first directed at creating synthetic agonists or antagonists specific for bronchial dilation or relaxation or for cardiovascular function. To turn off the action of the bound complex, monoamine oxidase, a ligand that deaminates, is used to break the complex (Mersmann, 1998). Other ways that the complex may be inactivated is by phosphorylation of specific kinases, like protein kinase A, that are localized in certain intracellular

loops of the β -AR. In addition, the receptor can be removed from the plasma membrane during chronic stimulation by agonists to reduce sensitivity (Mersmann, 1998).

Each mammalian species has a variety of β -ARs. In the 1960's, three basic subtypes, β 1, β 2, and β 3 of receptors were classified. Each species of animal and each tissue within species responds differently to various agonists and antagonists. With the many different combinations and complexities that occur with this physiology, research has been time consuming and not always conclusive. However, basic understandings have arisen and β -AR agonists have managed to work their way into therapies for various ailments and have the potential to enhance meat production in the livestock industry.

Beta 1 Adrenergic Receptor Agonists and Ractopamine

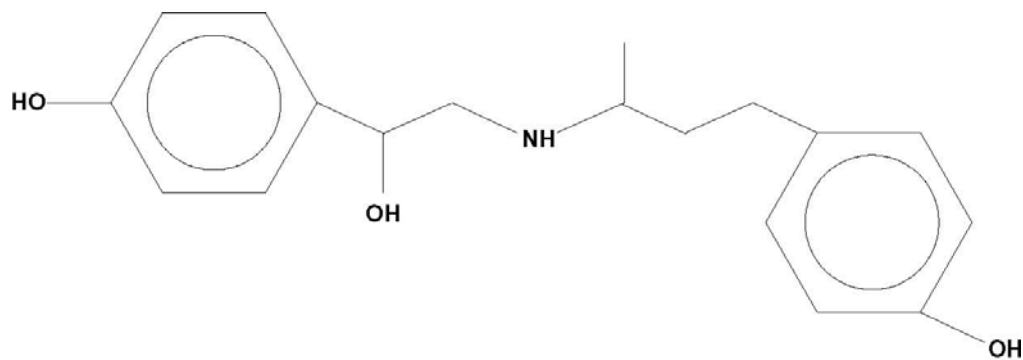


Figure 3.3: Ractopamine structure

Beta 2 Adrenergic Receptor Agonists and Clenbuterol

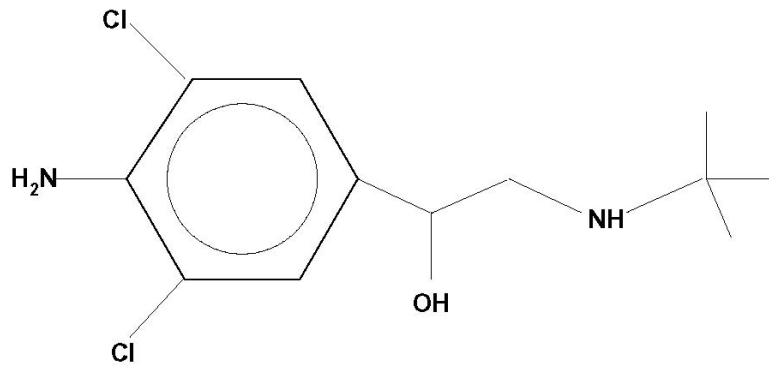


Figure 3.4: Clenbuterol structure

CHAPTER 4

CLENBUTEROL IN VITRO

Beta-adrenergic receptor (β -AR) agonists have been shown to reduce fat and increase muscle in both domestic animals and in rodents (Mersmann, 1998). Clenbuterol is a β 2-AR agonist that has been shown to induce adipocyte apoptosis in the mouse (Page et al., 2004). β 2-AR agonists are also associated with anti-apoptotic pathways in both brain and liver (Andre et al., 1999; Zhu et al., 1998; Zhu et al., 1999), as well as in ventricular myocytes, *in vitro* (Andre et al., 1999; Shizukuda and Buttrick, 2002; Zhu et al., 1998; Zhu et al., 1999). Stimulation of β -AR also protects against adipocyte apoptosis in brown adipose tissue (Lindquist and Rehnmark, 1998). Since the induction of adipocyte apoptosis by β 2-AR agonist is unique, we proposed to determine if the apoptosis effect is direct or if it was being stimulated via an indirect effect. We tested various concentrations and incubation times of clenbuterol on 3T3-L1 cells, and apoptosis was detected using a Laser Scanning Cytometer (LSC). Concentrations were based on other studies with clenbuterol *in vitro* (Young et al., 2002).

3T3-L1 mouse embryo fibroblasts were obtained from American Type Culture Collection (ATCC, Manassas, VA). In brief, cells were grown in 10% FCS/DMEM medium. Once the cells reached confluence, the preadipocytes were induced. Cells were cultured with 10% FBS/DMEM culture medium, supplemented with 1 mM insulin, 0.5 mM isobutylmethylxanthine (IBMX) and 1 mM dexamethasone for two days (Day 2). For two additional days cells were then maintained in culture medium with 1 mM insulin (Day 4), followed by culturing with 10% FBS/DMEM medium for additional 4 days. Once 90% of the cells appeared to be matured adipocytes, they were then

tested. Cells were cultured at 37C in a humidified 5% CO₂ atmosphere. All media contained 100 U/ml of penicillin, 100 µg/ml of streptomycin, and 292 µg of L-glutamine/ml (Invitrogen, Carlsbad, CA).

All treatments were tested in triplicate over two blocks. The 0, 250, 500, or 100 nM clenbuterol (Sigma) and rat recombinant 0.9 nM TNF- α (Sigma, in PBS/0.1% bovine serum albumin) was added to the culture medium (in DMEM/F12 for rat adipocyte culture and 10%FBS/DMEM for 3T3-L1) for either 0, 24, 48, 60, or 72 hours and then stained and scanned. Monolayer cells were washed twice with cold PBS and once in binding buffer, then incubated for 10 minutes with 5 µl Annexin V (AV)-FITC and 5 µl Propidium Iodide (PI) in 400 µl binding buffer (BD Biosciences, San Diego, CA) at room temperature on a slow rocker.

Laser Scanning Cytometry uses lasers to determine both morphological and quantitative data. LSC excites fluorochromes in cellular specimens and detects the fluorescence in discrete wavelengths with multiple photomultiplier tubes (PMT's). LSC also creates temporary digital images of the specimens on microscope slides for further analysis of the "events" or individual cells. LSC can additionally find and quantitate events by multiple filter settings, for example, making it possible to distinguish cytoplasmic fluorescence from nuclear fluorescence. LSC also generates high-resolution images for later analysis of physical characteristics employed by the individual cells.

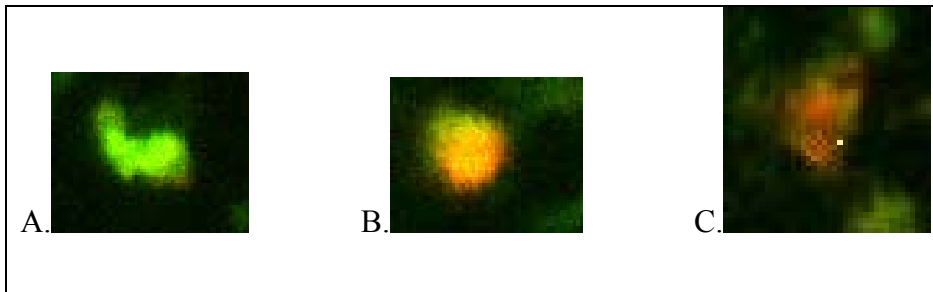


Figure 4.1: 3T3-L1 cells stained with AV/PI. A. Viable cell. B. Apoptotic cell. C. Necrotic cell.

The findings of the study showed no significant differences between treatments or times. Many possible factors could have produced this outcome. One possible factor is that the cells were not as viable as other cultured cells. This is the most likely explanation because of the amount of necrotic and apoptosis cells found in the dishes containing control media. Moreover, TNF- α did not induce apoptosis in this experiment, whereas TNF- α has been shown to induce adipocyte apoptosis in previous studies with 3T3-L1 cells (Lin et al., 2004). However, the dose was lower than that used in previous studies (15 nM versus 0.9 nM). The clenbuterol dosages may also have been too low. Although there did not appear to be a direct effect by clenbuterol, the replication of this experiment may be beneficial to determine if a direct effect is occurring and simply was not detected in this experiment due to cell conditions or because of dosage levels. Another possible outcome that would result from the duplication of this experiment would be that clenbuterol does not directly induce apoptosis. Once this determination has finally been made, future experiments can then be expedited to better understand this β -AR agonist's mechanisms.

CHAPTER 5

β -ADRENERGIC RECEPTOR AGONISTS INCREASE APOPTOSIS OF ADIPOSE TISSUE IN MICE¹

¹ Page, K. A., D. L. Hartzell, C. L. Li, A. L. Westby, M. A. Della-Fera, M. J. Azain, T. D. Pringle, C. A. Baile. β -adrenergic Receptor Agonists on Adipose Tissue Growth and Apoptosis in Mice. *Domestic Animal Endocrinology* 26 (1):23-31, 2004.

Abstract

β -adrenergic receptor (β -AR) agonists increase muscle mass and decrease body fat in rodents and livestock. With oral administration, however, the effects of β 1-AR and β 2-AR can be different, depending on the species tested. We tested the effects of clenbuterol, a β 2-AR agonist, and ractopamine, a β 1/ β 2-AR agonist, on growth, adiposity and adipose tissue apoptosis in male and female mice by feeding diets containing control, 200ppm clenbuterol, or 200 or 800ppm ractopamine. Food intake (FI) was measured daily; body weight (BW) and temperatures (BT) were measured on days 0, 3, 7, 10, 14, 17, and 20. On day 21 mice were sacrificed, body composition was determined using PIXImus densitometry, and muscle and adipose tissues were collected. There were no treatment effects on BT, FI, BW, feed efficiency or body composition. Retroperitoneal (Rp) and epididymal/parametrial (Epi/Par) fat pad masses were reduced in both 800ppm ractopamine (40 ± 3 and 207 ± 20 mg, respectively) and clenbuterol (35 ± 7 and 211 ± 22 mg) treated mice compared to control (66 ± 8 and 319 ± 30 mg, $p < .05$). Brown adipose tissue (BAT) mass was greater ($p < .05$) in clenbuterol treated mice compared to other treatments. Adipose tissue apoptosis (% DNA fragmentation) was increased in Epi/Par fat pads in clenbuterol ($5.2 \pm 1.1\%$) and 800ppm ractopamine ($4.1 \pm 0.8\%$) treated mice compared to control ($1.7 \pm 0.4\%$, $p < .05$). These findings show that WAT apoptosis can be induced by activation of β AR in mice, although the mechanism is unknown.

Introduction

A number of β -adrenergic receptor (β -AR) agonists have been shown to decrease body fat and increase muscle mass with oral administration in rodents, cattle, swine and sheep, although there appear to be species differences in responsiveness to different β -AR agonists (Anderson et al., 1991; Mersmann 1998; Yen et al., 1989). The mechanism for the decreased body fat in β -AR agonist treated animals is not fully understood. Although increased lipolysis has been demonstrated after β -AR agonist treatment of adipocytes in vitro, studies carried out in vivo have not consistently demonstrated increased lipolysis, even with a reduction in carcass fat (Mersmann 1998).

The effects of clenbuterol have been previously demonstrated in mice (Hinkle et al., 2002), while the effects of ractopamine have not. Since it has been suggested that these compounds target different β -AR subtypes and may have different mechanisms whereby they decrease adipose tissue mass, we wished to establish whether both were effective decreasing adipose tissue mass and whether increased adipose tissue apoptosis contributed to the decrease in adipose tissue mass in normal mice.

Materials and Methods

Animals

Five week old male (n=20) and female (n=20) ICR mice (Harlan Research Laboratories, Indianapolis, IN) were allowed to acclimate for one week prior to the experiment start date. Animals were housed singly in suspended wire cages and were provided ground rodent chow (ProLab[®] RMH 2500; Purina Mills, St. Louis, MO) and water *ad libitum*. Ambient room temperature was maintained and the light/dark cycle was 0600/1800 hours, respectively. Animals were cared for in accordance with the Guide for the Care and Use of Laboratory Animals (National

Academy of Science, 1996). Prior to the start of the study, animals were briefly anesthetized with isofluorane and an IPPT-200 transponder (programmable ID and temperature, BMDS, Seaford, DE) was implanted subcutaneously between the scapulae.

Materials

Test articles included clenbuterol (Sigma Chemical Company, St. Louis, MO, item# C5423) and ractopamine hydrochloride - Paylean[®] 9 (Elanco Animal Health, Indianapolis, IN). Clenbuterol is available as a pure product, and ractopamine is readily available as a type A medicated article. Paylean[®] 9 contains 20g ractopamine hydrochloride per kilogram in a ground corncob base. In order to achieve doses of 200 and 800 ppm it was necessary to add 20 and 80g of product per kilogram of diet. Control and clenbuterol diets were prepared with 80g of alphacel, which is a diluent used to mimic the effect of the corncob in the ractopamine product. The dose of clenbuterol used in this experiment was similar to those used in previous experiments with mice (Agbenyega and Wareham, 1992; Dupont-Versteegden, 1996; Hayes and Williams, 1994; Hyltander et al., 1993; Rothwell and Stock, 1985).

Daily observations

Food intake was measured daily, while body weight and body temperatures were measured on days 0, 3, 7, 10, 14, 17, and 20 at approximately the same time of day (1300h) during the treatment period. At 9 weeks of age (day 21), a final body weight measurement was obtained approximately one hour prior to euthanasia, and animals were sacrificed by decapitation following CO₂ asphyxiation.

Body composition analysis was performed after the mice had been decapitated, using a PIXImus[®] densitometer (GE Lunar Corporation; Waukesha, WI), which uses dual-energy x-ray

absorptiometry to measure whole body (subcranial) bone mineral density, bone mineral content, percent lean tissue and percent fat tissue (Brommage, 2003; Nagy and Clair, 2000). Brown intrascapular adipose tissue (BAT), inguinal (Ing), retroperitoneal (Rp), and epididymal (Epi) or parametrial (Par) white adipose tissues were harvested. Heart, liver, and kidney, as well as the right-side gastrocnemius (GC), semitendinosus, biceps femoris, triceps brachii, and longissimus dorsi muscles were removed, weighed individually, flash frozen in liquid nitrogen and then stored at -80°C. Tissue weights were recorded for statistical analysis.

DNA isolation and apoptosis assay

Only the Epi and Par fat pads had sufficient tissue for the apoptosis assay. Apoptosis was assayed in two ways: DNA isolated from fat tissue was separated into two fractions: fragmented and genomic DNA. First, the fragmented DNA was run on an agarose gel in order to identify a ladder pattern of internucleosomal DNA degradation that is characteristic of apoptosis (Gullicksen et al., 2003; Qian et al., 1998). Second, apoptosis was quantified as the ratio of fragmented- to total-DNA, multiplied by 100 (Shimabukuro et al., 1998). Briefly, approximately 50 mg of the Epi or Par white adipose tissue was homogenized in lysis buffer (10 mM Tris-HCL, pH 8.0; 10 mM EDTA, pH 8.0; 0.5% Triton X-100) and centrifuged at 14,000 x g for 15 min to separate fragmented DNA from genomic DNA. The supernatant, containing fragmented DNA, was extracted with phenol-chloroform-isoamyl alcohol (25:24:1), and the DNA was precipitated by adding polyacryl carrier (Molecular Research Center, Inc., Cincinnati, OH) and ethanol. Genomic (non-fragmented) DNA was extracted from the pellet with DNAzol and the polyacryl carrier. DNA in each fraction was quantified by the PicoGreen method (Molecular Probes, Inc., Eugene, OR) and fluorescence was measured using a SpectroMax Gemini (Molecular Devices).

Statistical Analysis

Analysis of variance (SAS) was used to determine significance of treatment and gender effects. Significance among means was determined by Tukey's test. Statistically significant differences are defined at the 95% confidence interval.

Results

Food Intake, Body Weight, Body Composition and Body Temperature

There were no significant gender, treatment or gender x treatment effects on body weight, weight gain, food intake, feed efficiency or body temperature. Densitometry indicated no significant gender, treatment or gender x treatment differences in body composition (Table 5.1).

Tissue Weights

There were significant gender effects for weights of Rp adipose tissue, biceps brachialis muscle, heart, kidney and liver, and significant treatment effects for Rp and Epi/Par adipose tissue and BAT (Table 5.2 and Figure 5.1). There was a significant gender x treatment interaction for the Epi/Par fat pad ($p < .05$; Table 5.3). Overall, Rp and Epi/Par fat pad weights were reduced in both 800ppm ractopamine and clenbuterol treated mice compared to control ($p < 0.05$; Figure 5.1), but for the Epi/Par fat pads, the effect occurred only in females (Table 5.3). BAT mass was significantly increased ($p < 0.05$) in the clenbuterol-treated group compared to control (Figure 5.1).

| | Control | Clenbuterol 200ppm | Ractopamine 200ppm | Ractopamine 800ppm | T_{SE} |
|-------------------------------|----------------|-------------------------------|-------------------------------|-------------------------------|-----------------------|
| Initial Body Weight (g) | 23.4 | 22.3 | 23.4 | 23.2 | 0.6 |
| Weight Gain (g) | 7.44 | 8.90 | 8.25 | 8.32 | 0.79 |
| Final Body Weight (g) | 30.75 | 32.1 | 31.4 | 31.5 | 0.70 |
| Body Temp (°C) | 37.2 | 36.2 | 37.0 | 36.8 | 0.60 |
| Cumulative Feed Intake (g) | 5.79 | 6.10 | 5.92 | 6.39 | 0.19 |
| Feed Efficiency | 16.4 | 14.4 | 15.8 | 16.6 | 1.17 |
| Densitometry | | | | | |
| Lean (g) | 25.68 | 26.80 | 25.63 | 27.42 | 0.8 |
| Fat (g) | 3.10 | 2.81 | 3.00 | 3.01 | 0.20 |
| Bone Mineral Content (g) | 0.67 | 0.65 | 0.67 | 0.67 | 0.004 |

Table 5.1. Effects of 21 Day Oral Treatment With Control, 200ppm Clenbuterol, 200ppm Ractopamine and 800ppm Ractopamine on Body Weight, Food Intake, Feed Efficiency, Body Temperature and Body Composition in Mice. There were no significant differences among treatment means. Data Shown Are Treatment Means. T_{SE}: Treatment Standard Error

| Gender | | Rp | Epi/Par | Inguinal | BAT | biceps | heart | kidney | liver |
|----------------|----------|----------------|----------------|-----------------|------------|---------------|----------------|----------------|----------------|
| Males | Mean | .058 | .272 | .2 | .106 | .154 | .164 | .672 | 2.41 |
| | N | 20 | 20 | 20 | 20 | 18 | 20 | 20 | 20 |
| | SEM | .006 | .02 | .01 | .008 | .005 | .005 | .014 | .05 |
| Females | Mean | .041 | .245 | .180 | .092 | .133 | .145 | .523 | 1.98 |
| | N | 20 | 20 | 20 | 20 | 20 | 20 | 20 | 20 |
| | SEM | .005 | .922 | .016 | .005 | .008 | .004 | .014 | .061 |
| Gender | P | <.05 | <.05 | <.01 | NS | NS | <.01 | <.01 | <.01 |

| Treatment | | Rp | Epi/Par | Ing | BAT | Biceps | Heart | Kidney | Liver |
|--------------------|----------|----------------|----------------|------------|----------------|---------------|--------------|---------------|--------------|
| Control | Mean | .065 | .319 | .207 | .081 | .141 | .151 | .595 | 2.20 |
| | SEM | .008 | .03 | .02 | .005 | .004 | .006 | .032 | .105 |
| Clenbuterol | Mean | .035 | .211 | .150 | .124 | .145 | .164 | .582 | 2.14 |
| | SEM | .007 | .021 | .022 | .014 | .009 | .008 | .026 | .072 |
| Rac200 | Mean | .058 | .295 | .230 | .096 | .128 | .147 | .586 | 2.16 |
| | SEM | .009 | .039 | .025 | .005 | .008 | .005 | .032 | .118 |
| Rac800 | Mean | .039 | .207 | .176 | .095 | .158 | .153 | .612 | 2.23 |
| | SEM | .003 | .019 | .020 | .007 | .015 | .008 | .034 | .033 |
| Treatment | P | <.05 | <.01 | NS | <.01 | NS | NS | NS | NS |

Table 5.2. Effects of 21 Day Oral Treatment With Control, 200ppm Clenbuterol, 200ppm Ractopamine and 800ppm Ractopamine on Selected Tissue Weights in Male and Female Mice (N=10). Data Shown Are Treatment Means. SEM: Standard Error of the Mean

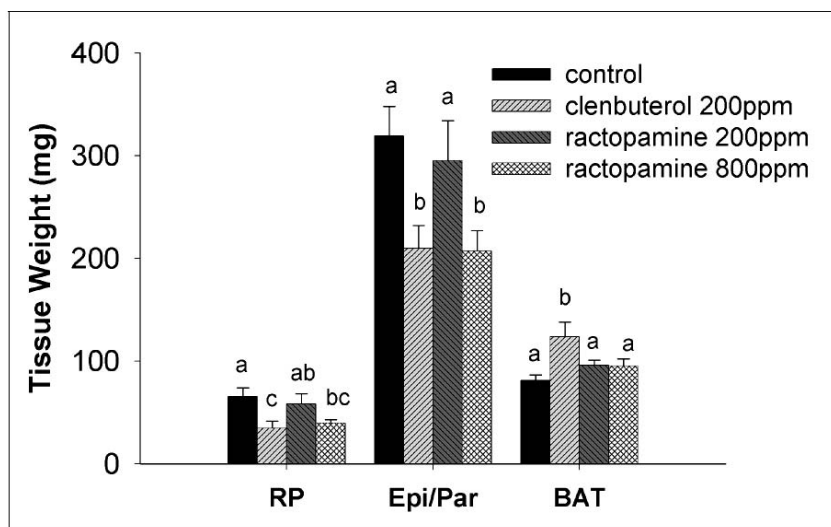


Figure 5.1. Retroperitoneal fat pad (Rp) weight, Epididymal/Parametrial fat pad (Epi/Par) weight and intrascapular brown adipose tissue (BAT) weight for control, 200 ppm clenbuterol, 200 ppm ractopamine and 800 ppm ractopamine treated mice. Data are means \pm SEM. **a,b,c**: Means with different letters are different, $p < 0.05$.

| Males | | | Females | | |
|-----------|-------------------|------|-----------|------------------|------|
| Treatment | Mean | SEM | Treatment | Mean | SEM |
| Control | .27 ^{ab} | .031 | Control | .36 ^a | .045 |
| Clen | .24 ^{ab} | .022 | Clen | .18 ^b | .034 |
| Rac200 | .36 ^a | .062 | Rac200 | .22 ^b | .023 |
| Rac800 | .19 ^b | .018 | Rac800 | .22 ^b | .032 |

Table 5.3. Effects of 21 Day Oral Treatment With Control, 200ppm Clenbuterol, 200ppm Ractopamine and 800ppm Ractopamine on Epi and Par Weights in Male and Female Mice (N=5). ^{a,b}: Means with different superscripts are different, $p < .05$

Adipose tissue apoptosis

There was no significant gender effect on % DNA fragmentation in the Epi/Par fat pad, but there was a significant treatment effect ($F(3,30)=4.0$; $p=.017$). Percent DNA fragmentation in the Epi/Par fat pad in the 200ppm clenbuterol-treated group was increased compared to control and 200ppm ractopamine-treated groups ($p<0.05$; Figure 2). There was also a significant increase in %DNA fragmentation in the 800ppm ractopamine treatment group compared to control ($p<0.05$; Figure 2). Neither clenbuterol nor ractopamine treatments increased DNA fragmentation in retroperitoneal or inguinal fat pads.

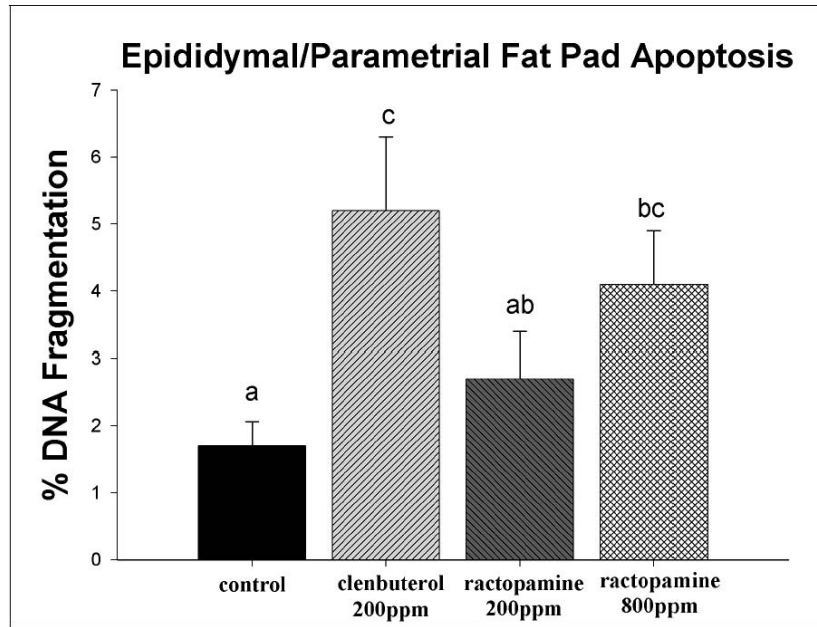


Figure 5.2. Percent DNA fragmentation (apoptosis) in Epididymal/Parametrial fat pads in control, 200ppm clenbuterol, 200 ppm ractopamine and 800 ppm ractopamine treated mice. Data are means \pm SEM. **a,b,c**: Means with different letters are different, $p<0.05$.

Discussion

Treatment of male and female mice with either 200 ppm clenbuterol or 800 ppm ractopamine in the diet resulted in a significant increase in apoptosis in the epididymal and parametrial adipose tissues, a finding that has not been previously reported. This finding suggests that activation of β -adrenergic receptors can trigger the apoptotic process in adipose tissue. Although we did not specifically identify the cell type involved, these results are similar to those in previous experiments in which leptin administration was shown to increase apoptosis of adipocytes (Qian et al., 1998) and decrease the number of adipocytes in fat pads in which apoptosis was found (Gullicksen et al., 2002). Clenbuterol has been shown to have direct effects on mouse adipocytes in previous studies. For example, clenbuterol stimulated lipolysis and inhibited insulin-induced lipolysis in mouse adipocytes in vitro (Orcutt et al., 1989), and clenbuterol decreased insulin binding to mouse adipocytes in vitro (Dubrovin et al., 1990). These findings suggest that the effects of clenbuterol and ractopamine on adipocyte apoptosis may also be direct effects.

Clenbuterol treatment also resulted in increased BAT mass in both males and females and decreased mass of Rp and Epi/Par fat pads in females only, findings that are similar to those of a previous study with mice (Eisen et al., 1988). We also found that 800ppm ractopamine resulted in decreased Rp and Epi/Par fat pad mass. The increase in BAT mass in clenbuterol treated mice is consistent with the increase that occurs as a result of increased sympathetic nervous system (SNS) stimulation during cold exposure (Lindquist and Rehnmark, 1998) and after exogenous administration of specific β -AR agonists (Nagase et al., 1994). Phosphorylation of the mitogen-activated protein kinase ERK1/2 has been shown to be involved in the hyperplastic effect of β -AR stimulation of BAT (Lindquist and Rehnmark, 1998).

Body composition, food intake, feed efficiency, body weight, and body temperature were not significantly affected by either ractopamine or clenbuterol in our study. Likewise, neither β -AR agonist increased muscle mass, although this was a prominent effect in other studies in mice (Orcutt et al., 1989) and rats (Emery et al., 1984). In rats, oral administration of ractopamine also had little effect on body weight, while intraperitoneal administration caused an increase (Smith and Paulson, 1994). Studies with pigs, however, have shown increased body weight and food intake following administration of ractopamine (Uttaro et al., 1993; Crome et al., 1996). Whether these differences are a result of differences in mouse strain or species used is not known. It is possible that the use of densitometry to measure body composition did not provide sufficient sensitivity to detect differences. However, Nagy and Clair (Nagy and Clair, 2000) and Brommage (Brommage, 2003) both found a consistent linear relationship between densitometry-derived lean mass and fat mass and those obtained by chemical analysis. It is unlikely that these small differences would have affected the results of our study. Thus, it is unclear why we did not find differences in body composition in mice treated with clenbuterol or ractopamine.

The effect of clenbuterol and ractopamine on adipose apoptosis is interesting. Clenbuterol has been shown to protect against apoptosis in both brain and liver (Andre et al., 1999; Zhu et al., 1998; Ahu et al., 1999), and in BAT, β -AR stimulation also protects against adipocyte apoptosis (Lindquist and Rehnmark, 1998). In contrast, norepinephrine, a β -AR agonist, was found to induce apoptosis of cardiac myocytes via β 1-AR stimulation (Singh et al., 2001; Singh et al., 2000). However, the effect of β -AR agonists on apoptosis of white adipose tissue has not previously been reported.

Apoptosis of white adipose tissue can be induced by a variety of factors, some of which act directly on adipocytes, such as tumor necrosis factor- α (Prins et al., 1997), galectin-12 (Hotta et al.,

2001) and conjugated linoleic acids (Tsuboyama-Kasaoka et al., 2000). Adipose tissue apoptosis can also be induced by leptin, acting via central nervous system receptors (Qian et al., 1998; Della-Fera et al., 2001). The mechanisms and central pathways involved in leptin-induced adipose apoptosis have not yet been determined, but Neuropeptide Y (NPY) may be a negative downstream effector, because administration of an NPY receptor blocker resulted in increased adipose tissue apoptosis (Margaeto et al., 2000). Both NPY and leptin have been shown to influence SNS activity. Leptin acts centrally to increase SNS activity in brown and white adipose tissue (Shiraishi et al., 1999), while intracerebroventricular injection of NPY suppressed SNS stimulation of brown adipose tissue (Egawa et al., 1991). NPY is also co-localized with norepinephrine in sympathetic nerve terminals and can act prejunctionally to suppress the release of norepinephrine (Wahlestedt and Hakanson, 1986). The effects of these two peptides on SNS activity and adipose tissue apoptosis are interesting in light of our current findings of increased adipose apoptosis in response to β -AR stimulation. Our demonstration of adipose apoptosis induced by β -AR stimulation suggests a mechanism by which centrally active neuropeptides and neurotransmitters could affect adipose tissue cellularity.

Acknowledgements

This study was supported in part by the Georgia Research Alliance Eminent Scholar endowment held by CAB.

References

- Agbenyega ET, and Wareham AC. Effect of clenbuterol on skeletal muscle atrophy in mice induced by the glucocorticoid dexamethasone. *Comp Biochem Physiol Comp Physiol* 1992;102:141-145.
- Anderson DB, Veenhuizen EL, Jones DJ, Schroeder AL, and Hancock DL. The Use of Phenethanolamines to Reduce Fat and Increase Carcass Leanness in Meat Animals. In: *Fat and Cholesterol Reduced Foods: Technologies and Strategies*. Haberstroh C, and Morris CE, Ed. (^Eds.), Houston: Gulf Publishing Co., 1991.
- Mersmann HJ. Overview of the effects of beta-adrenergic receptor agonists on animal growth including mechanisms of action. *J Anim Sci* 1998;76:160-172.
- Andre C, Couton D, Gaston J, Erraji L, Renia L, Varlet P, Briand P, and Guillet JG. Beta2-adrenergic receptor-selective agonist clenbuterol prevents Fas-induced liver apoptosis and death in mice. *Am J Physiol* 1999;276:G647-654.
- Brommage R. Validation and calibration of DEXA body composition in mice. *Am J Physiol Endocrinol Metab* 2003.
- Crome PK, McKeith FK, Carr TR, Jones DJ, Mowrey DH, and Cannon JE. Effect of ractopamine on growth performance, carcass composition, and cutting yields of pigs slaughtered at 107 and 125 kilograms. *J Anim Sci* 1996;74:709-716.
- Della-Fera MA, Qian H, and Baile CA. Adipocyte apoptosis in the regulation of body fat mass by leptin. *Diabetes Obes Metab* 2001;3:299-310.
- Dubrovin LC, Liu CY, and Mills SE. Insulin binding to mouse adipocytes exposed to clenbuterol and ractopamine in vitro and in vivo. *Domest Anim Endocrinol* 1990;7:103-109.
- Dupont-Versteegden EE. Exercise and clenbuterol as strategies to decrease the progression of muscular dystrophy in mdx mice. *J Appl Physiol* 1996;80:734-741.
- Egawa M, Yoshimatsu H, and Bray GA. Neuropeptide Y suppresses sympathetic activity to interscapular brown adipose tissue in rats. *Am J Physiol* 1991;260:R328-334.
- Eisen EJ, Croom WJ, Jr., and Helton SW. Differential response to the beta-adrenergic agonist cimaterol in mice selected for rapid gain and unselected controls. *J Anim Sci* 1988;66:361-371.
- Emery PW, Rothwell NJ, Stock MJ, and Winter PD. Chronic effects of beta 2-adrenergic agonists on body composition and protein synthesis in the rat. *Biosci Rep* 1984;4:83-91.
- Gullicksen PS, Dean RG, and Baile CA. Detection of DNA fragmentation and apoptotic proteins, and quantification of uncoupling protein expression by real-time RT-PCR in Adipose Tissue. *J Biochem Biophys Methods* 2004;58(1):1-13.
- Gullicksen PS, Hausman DB, Dean RG, Hartzell DL, and Baile CA. Adipose tissue cellularity and apoptosis after intracerebroventricular injections of leptin and 21 days of recovery in rats. *International Journal of Obesity* 2003;27(3):302-312.
- Hayes A, and Williams DA. Long-term clenbuterol administration alters the isometric contractile properties of skeletal muscle from normal and dystrophin-deficient mdx mice. *Clin Exp*

- Pharmacol Physiol 1994;21:757-765.
- Hinkle RT, Hodge KM, Cody DB, Sheldon RJ, Kobilka BK, and Isfort RJ. Skeletal muscle hypertrophy and anti-atrophy effects of clenbuterol are mediated by the beta2-adrenergic receptor. *Muscle Nerve* 2002;25:729-734.
- Hotta K, Funahashi T, Matsukawa Y, Takahashi M, Nishizawa H, Kishida K, Matsuda M, Kuriyama H, Kihara S, Nakamura T, Tochino Y, Bodkin NL, Hansen BC, and Matsuzawa Y. Galectin-12, an adipose-expressed galectin-like molecule possessing apoptosis-inducing activity. *J Biol Chem* 2001;276:34089-34097.
- Hyltander A, Svaninger G, and Lundholm K. The effect of clenbuterol on body composition in spontaneously eating tumour-bearing mice. *Biosci Rep* 1993;13:325-331.
- Institute of Laboratory Animal Resources Commission on Life Sciences National Research Council. Guide for the Care and Use of Laboratory Animals. National Academy of Sciences, 1996.
- Lindquist JM, and Rehnmark S. Ambient temperature regulation of apoptosis in brown adipose tissue. Erk1/2 promotes norepinephrine-dependent cell survival. *J Biol Chem* 1998;273:30147-30156.
- Margareto J, Aguado M, Oses-Prieto JA, Rivero I, Monge A, Aldana I, Marti A, and Martinez JA. A new NPY-antagonist strongly stimulates apoptosis and lipolysis on white adipocytes in an obesity model. *Life Sci* 2000;68:99-107.
- Nagase I, Sasaki N, Tsukazaki K, Yoshida T, Morimatsu M, and Saito M. Hyperplasia of brown adipose tissue after chronic stimulation of beta 3- adrenergic receptor in rats. *Jpn J Vet Res* 1994;42:137-145.
- Nagy TR, and Clair AL. Precision and accuracy of dual-energy X-ray absorptiometry for determining in vivo body composition of mice. *Obes Res* 2000;8:392-398.
- Orcutt AL, Cline TR, and Mills SE. Influence of the beta 2-adrenergic agonist clenbuterol on insulin-stimulated lipogenesis in mouse adipocytes. *Domest Anim Endocrinol* 1989;6:59-69.
- Prins JB, Niesler CU, Winterford CM, Bright NA, Siddle K, O'Rahilly S, Walker NI, and Cameron DP. Tumor necrosis factor-alpha induces apoptosis of human adipose cells. *Diabetes* 1997;46:1939-1944.
- Qian H, Azain MJ, Compton MM, Hartzell DL, Hausman GJ, and Baile CA. Brain administration of leptin causes deletion of adipocytes by apoptosis. *Endocrinology* 1998;139:791-794.
- Rothwell NJ, and Stock MJ. Modification of body composition by clenbuterol in normal and dystrophic (mdx) mice. *Biosci Rep* 1985;5:755-760.
- Shimabukuro M, Zhou YT, Levi M, and Unger RH. Fatty acid-induced beta cell apoptosis: a link between obesity and diabetes. *Proc Natl Acad Sci U S A* 1998;95:2498-2502.
- Singh K, Xiao L, Remondino A, Sawyer DB, and Colucci WS. Adrenergic regulation of cardiac myocyte apoptosis. *J Cell Physiol* 2001;189:257-265.
- Singh K, Communal C, Sawyer DB, and Colucci WS. Adrenergic regulation of myocardial apoptosis. *Cardiovasc Res* 2000;45:713-719.

- Shiraishi T, Sasaki K, Nijima A, and Oomura Y. Leptin effects on feeding-related hypothalamic and peripheral neuronal activities in normal and obese rats. *Nutrition* 1999;15:576-579.
- Smith DJ, and Paulson GD. Growth characteristics of rats receiving ractopamine hydrochloride and the metabolic disposition of ractopamine hydrochloride after oral or intraperitoneal administration. *J Anim Sci* 1994;72:404-414.
- Tsuboyama-Kasaoka N, Takahashi M, Tanemura K, Kim HJ, Tange T, Okuyama H, Kasai M, Ikemoto S, and Ezaki O. Conjugated linoleic acid supplementation reduces adipose tissue by apoptosis and develops lipodystrophy in mice. *Diabetes* 2000;49:1534-1542.
- Uttaro BE, Ball RO, Dick P, Rae W, Vessie G, and Jeremiah LE. Effect of ractopamine and sex on growth, carcass characteristics, processing yield, and meat quality characteristics of crossbred swine. *J Anim Sci* 1993;71:2439-2449.
- Wahlestedt C, and Hakanson R. Effects of neuropeptide Y (NPY) at the sympathetic neuroeffector junction. Can pre- and postjunctional receptors be distinguished? *Med Biol* 1986;64:85-88.
- Yen TT, Anderson DB, and Veenhuizen EL. Phenethanolamine: Reduction of Fat and Increase of Muscle, from Mice to Pigs. In: *Hormones, Thermogenesis, & Obesity*. Lardy H, and Stratman F, Ed. (Eds.), Elsevier Science Publishing Co., Inc., 1989.
- Zhu Y, Culmsee C, Semkova I, and Krieglstein J. Stimulation of beta2-adrenoceptors inhibits apoptosis in rat brain after transient forebrain ischemia. *J Cereb Blood Flow Metab* 1998;18:1032-1039.
- Zhu Y, Prehn JH, Culmsee C, and Krieglstein J. The beta2-adrenoceptor agonist clenbuterol modulates Bcl-2, Bcl-xl and Bax protein expression following transient forebrain ischemia. *Neuroscience* 1999;90:1255-1263

CHAPTER 6

EFFECTS OF CLENBUTEROL ON MUSCLE, ADIPOSE TISSUE AND ADIPOCYTE

APOPTOSIS IN MYOSTATIN KNOCKOUT MICE²

²K.A. Page, M. A. Della-Fera, C-L Li, M.J. Azain, T.D. Pringle, D. L. Hartzell, and C. A. Baile. Submitted to *Journal of Animal Science*, 2/20/04.

Abstract

Clenbuterol, a β 2-adrenergic receptor (β 2-AR) agonist, increases muscle mass and decreases adipose tissue mass, in part, by increasing adipose apoptosis. Myostatin (growth and differentiation factor-8, GDF-8) is a member of the TGF- β family of growth factors and inhibits muscle growth. We tested the effects of clenbuterol on muscularity and adiposity in male and female GDF-8 knockout (GDF-8 KO) (n=20) and wild type (WT) mice (n=20) by feeding 0 or 200 ppm clenbuterol for 21 days. Analysis of main effects showed that clenbuterol treatment increased weight gain ($p < 0.05$), reduced epididymal/parametrial (EPI/PAR) fat pad weights ($p < 0.005$), increased heart weights ($p < 0.03$), and increased adipocyte apoptosis in EPI/PAR and retroperitoneal (RP) fat pads ($p < 0.001$). There was a trend for clenbuterol to increase feed efficiency ($p = 0.07$), and a significant gender x treatment interaction showed that clenbuterol more than doubled feed efficiency in males ($p < .01$), but had no effect in females. For all other variables, GDF-8 KO and WT mice responded similarly to clenbuterol. Comparison of genotypes showed that GDF-8 KO mice had greater bone mineral density, bone mineral content, and lean tissue than WT mice ($p < 0.04$), as determined by PIXImus densitometry. We conclude that the lack of GDF-8 does not alter sensitivity to β 2-AR stimulation.

Introduction

Development of methods to enhance muscle growth and improve body composition has long been a primary goal in animal production. For this reason, the phenomenon of “double muscling” in cattle has been of great interest to both livestock producers and scientists. It is only within the last seven years, however, that the physiological basis for this condition was finally identified (McPherron et al., 1997; McPherron and Lee, 1997). Myostatin, or growth and differentiation factor-8 (GDF-8), is a member of the transforming growth factor- β (TGF- β)

superfamily. It is expressed predominantly in skeletal muscle and acts to inhibit muscle growth. Natural mutations of the GDF-8 gene, such as those that occur in Belgian blue and Piedmontese cattle breeds, or GDF-8 gene knockout (GDF-8 KO) in mice result in dramatically increased skeletal muscle mass and decreased adipose tissue mass (Grobet et al., 1997; Kambadur et al., 1997; Lin et al., 2002; McPherron and Lee, 1997, 2002). GDF-8 has been shown to inhibit both proliferation and differentiation of myoblasts in vitro (Langley et al., 2002; Thomas et al., 2000). Thus, the absence of GDF-8 can result in both muscle hypertrophy and hyperplasia.

GDF-8 is also expressed in low levels in adipose tissue (Sharma et al., 1999), and like the myostatin mutant cattle, GDF-8 KO mice have significantly reduced adipose tissue mass (McPherron and Lee, 2002). It is not known, however, whether this is a direct effect of loss of myostatin in adipose tissue or due to metabolic changes resulting from the increase in muscle tissue. GDF-8 administration has actually been shown to cause body fat loss (Zimmers et al., 2002), and GDF-8 inhibited preadipocyte differentiation and adipogenesis in vitro (Kim et al., 2001; Rebbapragada et al., 2003); thus, the mechanisms involved in the effects of GDF-8 on adipose tissue are likely complex.

Beta-adrenergic receptor (β -AR) agonists have also been under investigation for their potential use as anabolic agents. Certain β -AR agonists have been shown to increase muscle and decrease adipose tissue mass in several species (Mersmann, 1998). Clenbuterol, a β 2-AR agonist, has been shown to increase muscle mass and decrease fat mass when fed to cattle, chickens, pigs, sheep, rats or mice (Anderson et al., 1991; Mersmann, 1998; Yen et al., 1989). Although clenbuterol and other β 2-AR agonists have been under investigation for two decades, their mechanisms of action on muscle and adipose tissue are still not well understood. This is due, at least in part, to the fact that β -AR are present in nearly every cell type in the body; additionally,

both the distribution of β -AR subtypes among tissues and the proportion of different β -AR subtypes within a tissue vary greatly among species. Much of the work on mechanism of β -AR agonists in muscle indicates that their primary effects may be to decrease protein degradation, although they may also increase protein synthesis and stimulate proliferation of myoblasts (Navegantes et al., 2003; Navegantes et al., 2000; Shappell et al., 2000; Zeman et al., 2000). Clenbuterol has been shown to cause skeletal muscle hypertrophy and to reduce muscle atrophy caused by denervation or a genetic form of muscular dystrophy in mice (Agbenyega et al., 1995; Hinkle et al., 2002; Rothwell and Stock, 1985).

In adipose tissue, β -AR agonists increase lipolysis and decrease insulin-induced lipogenesis (Orcutt et al., 1989). More recently, clenbuterol was shown to increase apoptosis of white adipose tissue when fed to mice (Page et al., 2004).

Because the mechanisms involved in the muscle anabolic and adipose tissue catabolic effects of GDF-8 absence and β 2-AR agonists appear to be different, it was of interest to determine whether clenbuterol treatment in GDF-8 KO mice could further increase muscle and reduce adipose tissue mass. We found that clenbuterol treatment increased weight gain but did not affect either muscle or adipose tissue mass in WT or GDF-8 KO mice. In both genotypes, clenbuterol decreased weights of specific fat pads and increased adipose tissue apoptosis.

Materials and Methods

Animals

Twelve-week old male (n=10) and female (n=10) GDF-8 (-/-) knockout mice and male (n=10) and female (n=10) GDF-8 (+/+) WT mice were used in the study. GDF-8 knockout mice, which were derived from the 129/SvJ mouse strain, were originally obtained from MetaMorphix Inc. and were bred in-house for the study. Mice were housed singly in suspended wire cages in a

room maintained at 22 ± 1 C and with a 12:12 hour light/dark cycle. Mice were provided ground rodent chow (ProLab[®] RMH 2500; Purina Mills, St. Louis, MO) and water *ad libitum*. Mice were cared for in accordance with the Guide for the Care and Use of Laboratory Animals. .

Materials

Clenbuterol (Sigma Chemical Company, St. Louis, MO, item# C5423), was thoroughly mixed into the ground rodent chow to provide a 200 ppm concentration.

Daily Observations

Food intake was measured daily, and body weight was measured on days 0, 3, 7, 10, 14, 17, 20, and 21 at approximately 1430 h during the treatment period. At 15 weeks of age (day 21), a final body weight measurement was obtained approximately one hour prior to euthanasia, and mice were sacrificed by decapitation following CO₂ asphyxiation.

Body composition analysis was performed using a dual-energy x-ray PIXImus[®] densitometer (GE Lunar Corporation; Waukesha, WI). The data obtained included bone mineral density (BMD), bone mineral content (BMC), body surface area (area, cm²) lean weight (g), fat weight (g) and fat percent. The x-ray instrument has moderately low energy and a high resolution (80/35kVp and 0.18x0.18 mm pixel size). The densitometer was calibrated using an aluminum and lucite phantom prior to scanning the mice. After scanning, brown intrascapular adipose tissue (BAT), inguinal (ING), retroperitoneal (RP), and epididymal (EPI) or parametrial (PAR) white adipose tissue, as well as heart (HT), liver, kidney, the right-side gastrocnemius (GC), semitendinosus (ST), biceps femoris (BF), and triceps brachii (TB) were harvested. After removal, each tissue was weighed individually; all tissues except adipose were flash frozen in liquid nitrogen and then stored at -80°C (within 15 min of death).

DNA isolation and apoptosis assay

DNA was isolated from fresh fat tissues and separated into two fractions: fragmented and genomic DNA. The samples were first run on an agarose gel to identify a ladder pattern of internucleosomal DNA degradation, which is characteristic of apoptosis (Qian et al., 1998). Apoptosis was then quantified as the ratio of fragmented- to total-DNA as previously described (Gullicksen et al., 2003). Briefly, approximately 50 mg of EPI/PAR or RP adipose tissue from each animal was homogenized in lysis buffer (10 mM Tris-HCL, pH 8.0; 10 mM EDTA, pH 8.0; 0.5% Triton X-100) and centrifuged at 14,000 x g for 15 minutes to separate fragmented DNA from genomic DNA. The supernatant, containing fragmented DNA, was extracted with phenol-chloroform-isoamyl alcohol (25:24:1) and precipitated by adding polyacryl carrier (Molecular Research Center, Inc., Cincinnati, OH) and ethanol. Genomic (non-fragmented) DNA was extracted from the pellet with DNAzol (Molecular Research Center, Inc.) and the polyacryl carrier. DNA content was measured using PicoGreen (Molecular Probes, Inc., Eugene, OR) on a SpectraMax Gemini Spectrofluorometer (Molecular Devices, Sunnyvale, CA). Normalized by fat depot weight, both fragmented and genomic DNA from each sample were loaded on 1.5% agarose gel (pre-stained with 1:10,000 SYBR Green, Molecular Probes, Eugene, OR) for electrophoresis. Apoptosis was verified by the presence of a DNA ladder pattern, which was visualized by a FluorChem 8000 fluorescence imaging system (Alpha Innotech, San Leandro, CA).

Statistical Analysis

The study was analyzed as a 2 x 2 x 2 factorial design (N=5/cell). Analysis of variance (SAS) was used to determine significance of main effects of gender, genotype (WT vs GDF-8 KO) and clenbuterol (0 vs 200 ppm) and interactions. Statistically significant differences are defined at the 95% confidence interval.

Results

Food Intake, Body Weight, Weight Gain and Feed Efficiency

There were no significant differences in food intake between genotypes or treatments, but there was a significant difference between females and males in food intake, with females eating less than males ($p < 0.001$; Table 6.1). There was a significant difference in final body weight (FBW) ($P < 0.01$), but not in weight gain, between females and males (Table 6.1). There was a difference in both FBW ($p < 0.05$) and weight gain ($p < 0.05$) between WT and GDF-8 KO genotypes.

Compared to control, clenbuterol treatment increased weight gain ($p < 0.05$), but did not significantly affect FBW (Table 6.1). There was a significant gender x treatment interaction for weight gain, showing that clenbuterol significantly increased weight gain in males, but not in females (Figure 6.1).

Feed efficiency was calculated as the total food intake (g)/cumulative weight gain (g). There was a trend ($p = 0.07$) for clenbuterol to improve feed efficiency (g feed/g weight gain) (Table 6.1).

| | Final Body Wt (g) | Wt Gain (g/d) | Food Intake (g/d) | Feed Efficiency (g feed/g wt gain) |
|--------------------|--------------------------|----------------------|------------------------------|---|
| Female | 26.0 ± 0.5** | 0.14 ± 0.01 | 4.48 ± 0.085** | 40.4 ± 4.1 |
| Male | 33.3 ± 0.8 | 0.15 ± 0.015 | 5.14 ± 0.14 | 40.3 ± 5.8 |
| WT | 28.6 ± 0.9 | 0.16 ± 0.015 | 4.89 ± 0.12 | 36.2 ± 3.8 |
| GDF-8 KO | 30.6 ± 1.2* | 0.13 ± 0.01* | 4.74 ± 0.15 | 44.4 ± 5.8 |
| Control | 29.4 ± 0.9 | 0.03 ± 0.01 | 4.83 ± 0.12 | 46.3 ± 5.2 |
| Clenbuterol | 29.9 ± 1.2 | 0.165 ± 0.01* | 4.78 ± 0.16 | 34.4 ± 4.4† |

Table 6.1. Final body weight, daily weight gain and daily food intake in female and male WT and GDF-8 KO mice fed 0 or 200 ppm clenbuterol for 21 days (Mean ± SEM).

* $p < 0.05$; ** $p < 0.01$; † $p = 0.07$

There was also a significant gender x treatment interaction for feed efficiency ($p < .001$), showing that clenbuterol significantly improved feed efficiency in males ($p = 0.002$), but not in females (Figure 6.1).

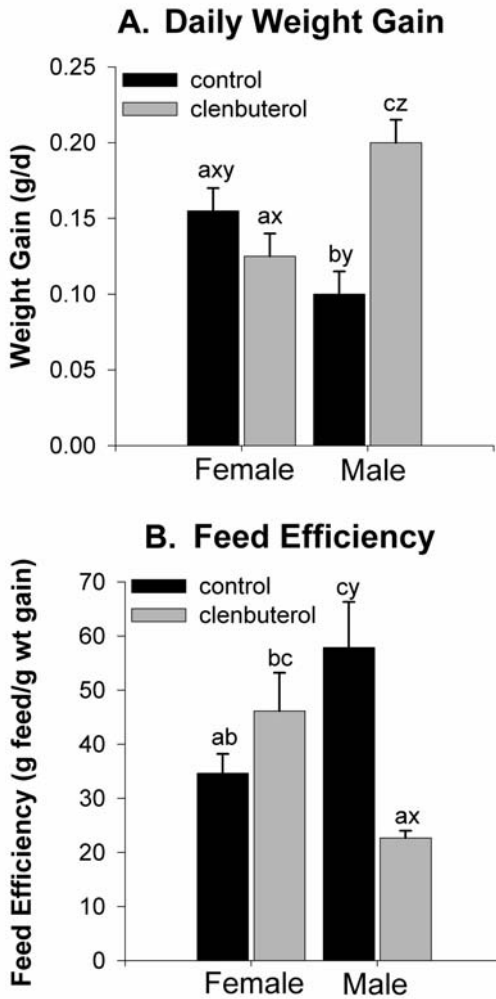


Figure 6.1: A. Daily weight gain (g) and B. feed efficiency in male and female mice fed 0 or 200 ppm clenbuterol for 21 days. Columns with different letters are different, a,b,c: $p < 0.05$; x,y,z: $p < 0.01$.

Body Composition and Tissue Weights

Analysis of main effects for body composition (Table 6.2) showed that clenbuterol had no effect on BMD, BMC, body area, lean weight, fat weight, or fat %. Compared to WT mice, GDF-8 KO mice had higher BMD ($p < 0.05$), BMC ($p < 0.001$), area ($p < 0.001$) and lean weight ($p < 0.01$)

and lower fat weight and fat % ($p < 0.01$). Compared to females, males had higher BMD ($p < 0.001$), BMC ($p < 0.001$), area ($p < 0.01$) and lean weight ($p < 0.001$) and had lower fat % ($p < 0.05$). There were no significant interactions.

| | Control | Clenbuterol | WT | GDF-8 KO | Female | Male |
|------------------------------|-------------|--------------|-------------|--------------|------------|---------------|
| Bone Mineral Density | 0.06 ± | 0.06 ± 0.001 | 0.056 ± | 0.06 ± 0.01 | 0.05 | 0.06 |
| (g) | 0.001 | | 0.01 | | ± .001 | ± .001*** |
| Bone Mineral Content | 0.53 ± 0.02 | 0.52 ± 0.02 | 0.48 ± 0.02 | 0.56 ± | 0.47 ± | 0.58 ± |
| (g) | | | | 0.02** | 0.01 | 0.01*** |
| Area (cm²) | 9.0 ± 0.2 | 9.2 ± 0.2 | 8.6 ± .0.2 | 9.6 ± 0.2** | 8.6 ± 0.2 | 9.6 ± 0.2** |
| Lean (g) | 22.2 ± 0.9 | 22.7 ± 1.1 | 21.0 ± 0.8 | 23.9 ± 1.1** | 19.1 ± 0.6 | 25.7 ± 0.6*** |
| Fat (g) | 4.5 ± 0.3 | 4.1 ± 0.2 | 4.9 ± 0.3 | 3.7 ± 0.2** | 4.2 ± 0.3 | 4.4 ± 0.2 |
| % Fat | 17.0 ± 1.2 | 15.7 ± 1.0 | 19.2 ± 1.1 | 13.5 ± | 18.0 ± 1.3 | 14.7 ± 0.8* |
| | | | | 0.7*** | | |

Table 6.2. Body Composition Analysis of female and male WT and GDF-8 KO mice fed 0 or 200 ppm clenbuterol for 21 days by PIXImus Densitometry (Mean ± SEM). Main effect differences: * $p < .05$; ** $p < .01$; *** $p < .001$

Figure 6.2 shows the main effects for adipose and muscle tissue weights expressed per unit body weight. The PAR fat pad in females was larger than the EPI fat pad in males ($p < 0.05$), but there were no differences between males and females in muscle weights when corrected for body weight. In GDF-8 KO mice both the actual weights (not shown) and weights per g body weight of all three white adipose tissues and BAT were lower than in WT mice ($p < 0.01$ and $p < 0.05$ respectively). The actual weights (not shown) and weight per g body weight of all dissected muscles and of the heart were higher in GDF-8 KO mice ($p < 0.01$). Clenbuterol did not affect the actual weights or weight per g body weight of any of the dissected muscles, but mice treated with clenbuterol had smaller RPI and EPI/PAR ($p < 0.05$) fat pads when corrected for body weight.

Heart weight was significantly increased in clenbuterol treated mice ($p < 0.01$). There were no significant interactions.

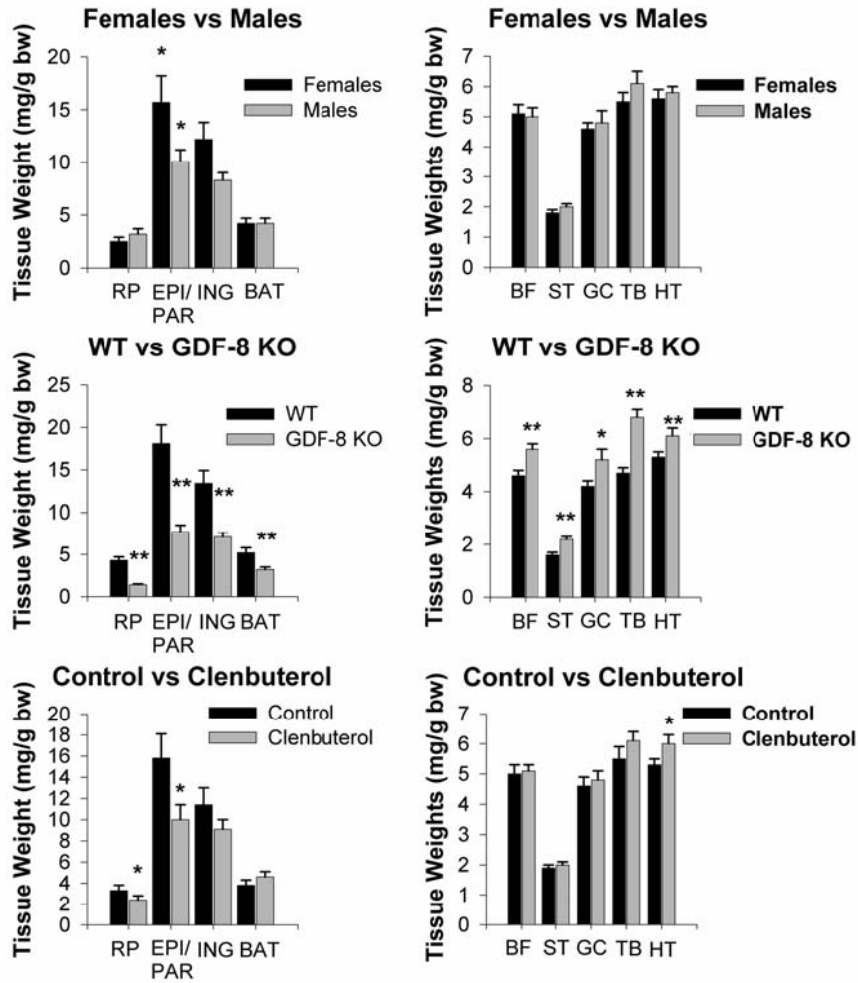


Figure 6.2. Effects of gender, genotype and treatment on weight (mg/g body wgt) of individual fat pads, skeletal muscles and heart. (RP, retroperitoneal fat pad; EPI/PAR, epididymal/parametrial fat pad; ING, inguinal fat pad; BAT, intrascapular brown adipose tissue; BF, biceps femoris; ST, semitendinosus; GC, gastrocnemius; TB, triceps brachii; HT, heart). * $p < 0.05$, ** $p < 0.01$

Adipose Tissue Apoptosis

Adipose tissue apoptosis (percent DNA fragmentation) was measured in the EPI/PAR and RP white fat pads. In both tissues clenbuterol treatment increased apoptosis compared to control ($p < 0.01$, Table 6.3).

| Treatment | % DNA Fragmentation | | Genotype | % DNA Fragmentation | | Sex | % DNA Fragmentation | |
|-------------|---------------------|-------------|----------|---------------------|-----------|-----|---------------------|-----------|
| | EPI/PAR | RP | | EPI/PAR | RP | | EPI/PAR | RP |
| Control | 0.9 ± 0.1 | 0.9 ± 0.2 | WT | 1.5 ± 0.2 | 1.6 ± 0.3 | F | 1.8 ± 0.3 | 1.4 ± 0.3 |
| Clenbuterol | 2.5 ± 0.2** | 2.5 ± 0.2** | GDF-8 KO | 1.8 ± 0.3 | 1.8 ± 0.4 | M | 1.5 ± 0.2 | 2.0 ± 0.4 |

Table 6.3. EPI/PAR and RP fat pad apoptosis in female and male WT and GDF-8 KO mice fed 0 or 200 ppm clenbuterol for 21 days (Mean ± SEM). ** Column means are different, p<0.01

There were no genotype or gender effects on apoptosis, but there was a significant gender x genotype x treatment interaction. The gender x genotype x treatment interaction resulted in a clenbuterol-induced increase in apoptosis that was significant only in females, however, the clenbuterol-treated males had similar increases in apoptosis (Figure 6.3).

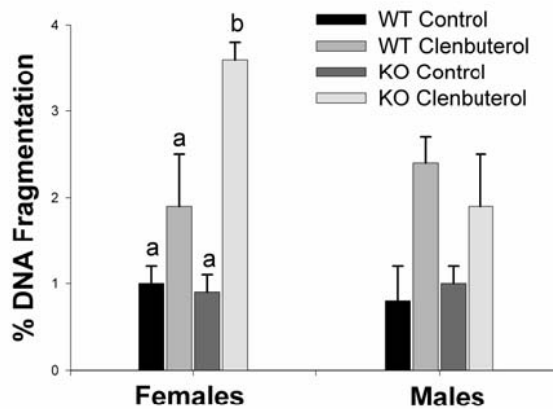


Figure 6.3. EPI/PAR apoptosis (% DNA fragmentation) in female and male WT and GDF-8 KO mice fed 0 or 200 ppm clenbuterol for 21 days. a,b: Columns with different letters are different, p<0.05.

Serum Leptin Concentrations

Serum leptin concentrations were lower in the GDF-8 KO mice compared to WT mice ($p < 0.03$); however, clenbuterol did not significantly affect leptin concentrations (Table 6.4).

Leptin concentrations were also lower in the males compared to females ($p < 0.02$).

| Treatment | Leptin (ng/ml) | Genotype | Leptin (ng/ml) | Sex | Leptin (ng/ml) |
|-------------|----------------|----------|----------------|-----|----------------|
| Control | 5.31 ± 1.10 | WT | 5.97 ± 0.85 | F | 5.94 ± 1.06 |
| Clenbuterol | 3.98 ± 0.49 | GDF-8 KO | 3.50 ± 0.73* | M | 3.27 ± 0.28* |

Table 6.4. Serum Leptin Concentration (ng/ml) in female and male WT and GDF-8 KO mice fed 0 or 200 ppm clenbuterol for 20 days (Mean ± SEM). * Column means are different, $p < 0.05$

Discussion

Clenbuterol did not affect food intake, body weight or body composition in either WT or GDF-8 KO mice, although it did increase cumulative weight gain and improve feed efficiency in a gender-specific manner. Male mice fed the clenbuterol-containing diet gained twice as much weight and were more than 250% more efficient compared to males fed control diet, whereas there were no differences in female mice. Clenbuterol also had no effect on weights of specific skeletal muscles, but it decreased weight of the EPI/PAR fat pad and increased heart weight. Adipocyte apoptosis was also detected in clenbuterol treated animals.

Clenbuterol has been shown to increase muscle mass and reduce adipose mass in cattle, chicken, pigs and sheep (Ricks et al., 1984). Others have shown that clenbuterol induces muscle hypertrophy in wild type mice (Hayes and Williams, 1994; Hinkle et al., 2002; Lynch et al., 1999), and it reduces muscle degeneration and increases total body protein in mdx dystrophic mice (Agbenyega et al., 1995; Zeman et al., 2000). In a previous study, however, we found no effect of either clenbuterol or ractopamine on muscle weight or on body protein or total body fat content in

ICR mice (Page et al., 2004). Since we now have shown the same lack of effect in a different strain of mice, it is less likely that our previous findings were simply due to strain-related differences.

As in our previous study (Page et al., 2004), clenbuterol increased apoptosis in both the EPI/PAR and RP fat pads. Although there appeared to be a difference in sensitivity between males and females, this was likely due to the higher variability in samples from males compared to females, since there were increases in apoptosis in clenbuterol-treated males that were similar to those in females.

The differences between GDF-8 KO and WT mice in body weight, weight gain, body composition and tissue weights are typical of animals with GDF-8 gene knockout or mutation (Hamrick, 2003; McPherron et al., 1997; McPherron and Lee, 2002). Serum leptin concentrations were not affected by clenbuterol treatment; however, GDF-8 KO mice had lower leptin levels compared to WT mice. This corresponds to a previous study in which serum leptin concentrations were lower in GDF-8 KO mice, a finding that is likely due to the reduced amount of adipose tissue mass in GDF-8 KO mice (McPherron and Lee, 2002).

The reason for the lack of effect of clenbuterol on muscle mass in WT or GDF-8 KO mice is not known. It is possible that including both gender and genotype variables in the study made it difficult to measure significance of small changes in muscle weights caused by clenbuterol. In a similar study with cimaterol, Eisen et al (1988) showed that a dose of 200 ppm in the feed actually reduced weight gain in mice selected for high growth rate, and had no effect on body weight in normal male ICR mice. Our dose of 200 ppm corresponds to approximately 35 mg/kg body weight/day, which is 5-10 times higher than doses used parenterally in mice or rats in previous studies (Cartana et al., 1994; Hinkle et al., 2002; Lynch et al., 1999). Whether the dose of clenbuterol used in our study might have been responsible for the lack of effect on muscle growth

is not known.

GDF-8 has been shown to act directly on myoblasts to inhibit proliferation by controlling the G1- to S-phase and G2- to M-phase transition (Thomas et al., 2000). GDF-8 also inhibits myoblast differentiation by down-regulating the expression of MyoD, a basic helix-loop-helix transcription factor that has the ability to convert non-muscle cell types into myogenic cells capable of undergoing terminal differentiation (Langley et al., 2002). Thus, loss of GDF-8 results in disinhibition of myoblast proliferation and differentiation leading to hypertrophy and hyperplasia of skeletal muscle. In contrast to GDF-8, the molecular mechanisms responsible for muscular hypertrophy caused by β -AR agonists have not been well studied. There is some evidence that ractopamine, a β 1/ β 2-AR agonist, acts directly on myoblasts to increase cell number, protein and DNA content (Shappell et al., 2000), and clenbuterol has been shown to reduce protein degradation in muscle in vitro (Navegantes et al., 2003). Because β -AR agonists can have widespread effects on glucose utilization, blood flow and other endocrine systems, how much of the muscle hypertrophy effect is a result of direct action on muscle cells is not known. This limited information, therefore, makes it difficult to speculate on possible reasons for the lack of response to clenbuterol. Morton et al. (1995) showed that clenbuterol actually decreased body weight and muscle weight in suckling rat pups; thus, it is clear that β -AR agonists can have complex effects on growth.

The increased muscle mass in GDF-8 KO mice is due to both hypertrophy and hyperplasia (McPherron et al., 1997). Although it is conceivable that adult GDF-8 KO mice have reached their maximum physiological potential for increased muscle mass, identifying a molecular mechanism that defines that potential could have important implications for livestock production.

References

- Agbenyega, E. T., R. H. Morton, P. A. Hatton, and A. C. Wareham. 1995. Effect of the beta 2-adrenergic agonist clenbuterol on the growth of fast- and slow-twitch skeletal muscle of the dystrophic (c57bl6j dy2j/dy2j) mouse. *Comp Biochem Physiol C Pharmacol Toxicol Endocrinol* 111: 397-403.
- Anderson, D. B., E. L. Veenhuizen, D. J. Jones, A. L. Schroeder, and D. L. Hancock. 1991. The use of phenethanolamines to reduce fat and increase carcass leanness in meat animals. In: C. Haberstroh and C. E. Morris (eds.) *Fat and cholesterol reduced foods: Technologies and strategies*. Gulf Publishing Co., Houston.
- Cartana, J., T. Segues, M. Yebras, N. J. Rothwell, and M. J. Stock. 1994. Anabolic effects of clenbuterol after long-term treatment and withdrawal in the rat. *Metabolism* 43: 1086-1092.
- Eisen, E. J., W. J. Croom, Jr., and S. W. Helton. 1988. Differential response to the beta-adrenergic agonist cimaterol in mice selected for rapid gain and unselected controls. *J Anim Sci* 66: 361-371.
- Grobet, L., L. J. Martin, D. Poncelet, D. Pirottin, B. Brouwers, J. Riquet, A. Schoeberlein, S. Dunner, F. Menissier, J. Massabanda, R. Fries, R. Hanset, M. Georges. 1997. A deletion in the bovine myostatin gene causes the double-musled phenotype in cattle. *Nat Genet* 17: 71-74.
- Gullicksen, P. S., D. B. Hausman, R. G. Dean, D. L. Hartzell, and C. A. Baile. 2003. Adipose tissue cellularity and apoptosis after intracerebroventricular injections of leptin and 21 days of recovery in rats. *International Journal of Obesity* 27: 302-312.
- Hamrick, M. W. 2003. Increased bone mineral density in the femora of *gdf8* knockout mice. *Anat Rec* 272A: 388-391.
- Hayes, A., and D. A. Williams. 1994. Long-term clenbuterol administration alters the isometric contractile properties of skeletal muscle from normal and dystrophin-deficient *mdx* mice. *Clin Exp Pharmacol Physiol* 21: 757-765.
- Hinkle, R. T., K. M. Hodge, D. B. Cody, R. J. Sheldon, B. K. Kobilka, and R. J. Isfort. 2002. Skeletal muscle hypertrophy and anti-atrophy effects of clenbuterol are mediated by the beta2-adrenergic receptor. *Muscle Nerve* 25: 729-734.
- Kambadur, R., M. Sharma, T. P. Smith, and J. J. Bass. 1997. Mutations in myostatin (*gdf8*) in double-musled belgian blue and piedmontese cattle. *Genome Res* 7: 910-916.
- Kim, H. S., L. Liang, R. G. Dean, D. B. Hausman, D. L. Hartzell, and C. A. Baile. 2001. Inhibition of preadipocyte differentiation by myostatin treatment in 3T3-L1 cultures. *Biophys Biochem Res Commun* 281: 902-906.
- Langley, B., M. Thomas, A. Bishop, M. Sharma, S. Gilmour, and R. Kambadur. 2002. Myostatin inhibits myoblast differentiation by down-regulating myo-D expression. *J Biol Chem* 277: 49831-49840.
- Lin, J., H. B. Arnold, D. L. Hartzell, and C. A. Baile. 2002. Myostatin knockout in mice increases myogenesis and decreases adipogenesis. *Biochem Biophys Res Commun* 291: 701-706.

- Lynch, G. S., R. T. Hinkle, and J. A. Faulkner. 1999. Year-long clenbuterol treatment of mice increases mass, but not specific force or normalized power, of skeletal muscles. *Clin Exp Pharmacol Physiol* 26: 117-120.
- McPherron, A. C., A. M. Lawler, and S. J. Lee. 1997. Regulation of skeletal muscle mass in mice by a new *tgf-beta* superfamily member. *Nature* 387: 83-90.
- McPherron, A. C., and S. J. Lee. 1997. Double muscling in cattle due to mutations in the myostatin gene. *Proc Natl Acad Sci U S A* 94: 12457-12461.
- McPherron, A. C., and S. J. Lee. 2002. Suppression of body fat accumulation in myostatin-deficient mice. *J Clin Invest* 109: 595-601.
- Mersmann, H. J. 1998. Overview of the effects of beta-adrenergic receptor agonists on animal growth including mechanisms of action. *J Anim Sci* 76: 160-172.
- Morton, R. H., E. T. Agbenyega, P. A. Hatton, and A. C. Wareham. 1995. Effects of clenbuterol and icil18551, a selective beta 2-antagonist, on the growth of skeletal muscle of suckling rats. *Pflugers Arch* 431: 237-243.
- Navegantes, L. C., C. R. Machado, N. M. Resano, R. H. Migliorini, and I. C. Kettelhut. 2003. Beta2-agonists and camp inhibit protein degradation in isolated chick (*gallus domesticus*) skeletal muscle. *Br Poult Sci* 44: 149-154.
- Navegantes, L. C., N. M. Resano, R. H. Migliorini, and I. C. Kettelhut. 2000. Role of adrenoceptors and camp on the catecholamine-induced inhibition of proteolysis in rat skeletal muscle. *Am J Physiol Endocrinol Metab* 279: E663-668.
- Orcutt, A. L., T. R. Cline, and S. E. Mills. 1989. Influence of the beta 2-adrenergic agonist clenbuterol on insulin-stimulated lipogenesis in mouse adipocytes. *Domest Anim Endocrinol* 6: 59-69.
- Page, K. A., D. L. Hartzell, C. Li, A. L. Westby, M. A. Della-Fera, M. J. Azain, T. D. Pringle, and C. A. Baile. 2004. Beta-adrenergic receptor agonists increase apoptosis of adipose tissue in mice. *Domest Anim Endocrinol* 26: 23-31.
- Qian, H., M. J. Azain, M. M. Compton, D. L. Hartzell, G. J. Hausman, and C. A. Baile. 1998. Brain administration of leptin causes deletion of adipocytes by apoptosis. *Endocrinology* 139: 791-794.
- Rebbapragada, A., H. Benchabane, J. L. Wrana, A. J. Celeste, and L. Attisano. 2003. Myostatin signals through a transforming growth factor beta-like signaling pathway to block adipogenesis. *Mol Cell Biol* 23: 7230-7242.
- Ricks, C. A., P. K. Baker, and R. H. Dalrymple. 1984. Use of repartitioning agents to improve performance and body composition of meat animals. *Reciprocal Meat Conf. Proc.* 37: 5-11.
- Rothwell, N. J., and M. J. Stock. 1985. Modification of body composition by clenbuterol in normal and dystrophic (*mdx*) mice. *Biosci Rep* 5: 755-760.
- Shappell, N. W., V. J. Feil, D. J. Smith, G. L. Larsen, and D. C. McFarland. 2000. Response of *c2c12* mouse and turkey skeletal muscle cells to the beta-adrenergic agonist ractopamine. *J Anim Sci* 78: 699-708.

- Sharma, M., R. Kambadur, K. G. Matthews, N. G. Somers, G. P. Devlin, J. V. Conaglen, P. J. Fowke, J. J. Bass. 1999. Myostatin, a transforming growth factor-beta superfamily member, is expressed in heart muscle and is upregulated in cardiomyocytes after infarct. *J Cell Physiol* 180: 1-9.
- Thomas, M., B. Langley, C. Berry, M. Sharma, S. Kirk, J. Bass, R. Kambadur. 2000. Myostatin, a negative regulator of muscle growth, functions by inhibiting myoblast proliferation. *J Biol Chem* 275: 40235-40243.
- Yen, T. T., D. B. Anderson, and E. L. Veenhuizen. 1989. Phenethanolamine: Reduction of fat and increase of muscle, from mice to pigs. In: H. Lardy and F. Stratman (eds.) *Hormones, thermogenesis, & obesity*. Elsevier Science Publishing Co., Inc.
- Zeman, R. J., H. Peng, M. J. Danon, and J. D. Etlinger. 2000. Clenbuterol reduces degeneration of exercised or aged dystrophic (mdx) muscle. *Muscle Nerve* 23: 521-528.
- Zimmers, T. A., M. V. Davies, L. G. Koniaris, P. Haynes, A. F. Esquel, K. N. Tomkinson, A. C. McPherron, N. M. Wolfman, S. J. Lee. 2002. Induction of cachexia in mice by systemically administered myostatin. *Science* 296: 1486-1488.

CHAPTER 7

CONCLUSIONS

The review of the literature shows the uniqueness of the myostatin protein and the complexities of beta adrenergic receptor agonists. Blockage of the protein may provide novel new technologies that will be beneficial for both the biomedical and livestock industries, while beta agonists have already been put to use in both of these industries. Although the combination of myostatin deletion and β -AR agonist treatment in Chapter 6 did not result in increased skeletal muscle mass, the detection of apoptosis is still an exciting finding.

We first discovered that both 200ppm clenbuterol and 800ppm ractopamine increased DNA fragmentation in the epididymal/parametrial (Epi/Par) white fat pads and reduced the mass of both Epi/Par and the retroperitoneal (Rp) fat pads. An additional finding was that clenbuterol increased brown adipose tissue mass. Our overall findings suggest that the adipose tissue apoptosis can be induced by β -AR agonist treatment.

Because the differences between 800ppm ractopamine and clenbuterol did not differ significantly in their effects in the ICR control mice, we tested the only the clenbuterol in the next experiment. In the second experiment clenbuterol increased weight gain, feed efficiency, cardiac muscle weight, and adipocyte apoptosis of Epi/Par and Rp adipose tissue. Treatment showed a decrease in the Epi/Par fat pads. Genotype differences included increased skeletal muscle, bone mineral density, and bone mineral content. When looking at the results of this study loss of myostatin function does not effect β -AR agonist treatment.

Although this myostatin deficient model did not effect the action of β -AR agonist treatment, the model continues to be one that can potentially lead to treatments for people suffering from muscle wasting disorders, obesity, and diabetes. With better understandings of cell cycle control and how to manipulate the gene in other model species, the field for myostatin research is rather vast.

Due to the increase in adipocyte apoptosis in both experiments, clenbuterol was tested on 3T3 cells in vitro and tumor necrosis factor alpha (TNF- α). The detection of adipocyte apoptosis was determined using Laser Scanning Cytometry. Adipocyte apoptosis was not detected in this experiment. This would suggest that β -AR agonist stimulation does not have a direct effect on adipocytes.

The discoveries from these experiments reinforces that there is still a great deal of work that needs to be conducted in order to better understand the pathways involved with β -AR agonists on growth. Clearly there are species differences and perhaps strain differences within species particularly in regards to muscle growth. The work that lies ahead in the biomedical and livestock industries may be expansive and exhausting. However, the new technologies that have arisen and continue to evolve will allow for continuous better understandings of the portions of the mechanisms that will enhance the livestock industry and those with muscle wasting disorders.

REFERENCES

- Andre, C., D. Couton, J. Gaston, L. Erraji, L. Renia, P. Varlet, P. Briand, and J. G. Guillet. 1999. beta 2-Adrenergic receptor-selective agonist clenbuterol prevents Fas-induced liver apoptosis and death in mice. *Am J Physiol Gastrointest Liver Physiol* 276:G647.
- Arnold, H. B., Exploring Myostatin. Master's Thesis. The University of Georgia. 2001.
- Bogdanovich, S., T. O. B. Krag, E. R. Barton, L. D. Morris, R. S. Ahima, and T. S. Khurana. 2002. Myostatin (GDF-8) blockage improves muscle function in MDX mouse. *Journal of the Neurological Sciences* 199:402.
- Charlier, C., W. Coppeters, F. Farnir, L. Grobet, P. L. Leroy, C. Michaux, M. Mni, A. Schwers, P. Vanmanshoven, R. Hanset, and M. Georges. 1995. The mh gene causing double-muscling in cattle maps to bovine chromosome-2. *Mammalian Genome* 6:788-792.
- Gonzalez-Cadavid, N. F., W. E. Taylor, K. Yarasheski, I. Sinha-Hikim, K. Ma, S. Ezzat, R. Q. Shen, R. Lalani, S. Asa, M. Mamita, G. Nair, S. Arver, and S. Bhasin. 1998. Organization of the human myostatin gene and expression in healthy men and HIV-infected men with muscle wasting. *Proceedings of the National Academy of Sciences of the United States of America* 95:14938-14943.
- Grobet, L., D. Poncelet, L. J. Royo, B. Brouwers, D. Pirottin, C. Michaux, F. Menissier, M. Zanotti, S. Dunner, and M. Georges. 1998. Molecular definition of an allelic series of mutations disrupting the myostatin function and causing double-muscling in cattle. *Mammalian Genome* 9:210-213.
- Hamrick, M., G. Njus, and D. Ducharme. 2002a. Femora of mice lacking myostatin show increased trabecular bone density. *Journal of Bone and Mineral Research* 17:SU177.
- Hamrick, M. W., A. C. McPherron, and C. O. Lovejoy. 2002b. Bone mineral content and density in the humerus of adult myostatin-deficient mice. *Calcified Tissue International* 71:63-68.
- Hamrick, M. W., C. Pennington, and C. D. Byron. 2003. Bone architecture and disc degeneration in the lumbar spine of mice lacking GDF-8 (myostatin). *Journal of Orthopaedic Research*

21:1025-1032.

- Lee, S. J. and A. C. McPherron. 2001. Regulation of myostatin activity and muscle growth. *Proceedings of the National Academy of Sciences of the United States of America* 98:9306-9311.
- Lindquist, J. M. and S. Rehnmark. 1998. Ambient temperature regulation of apoptosis in brown adipose tissue - Erk1/2 promotes norepinephrine-dependent cell survival. *J. Biol. Chem.* 273:30147-30156.
- McPherron, A. C., A. M. Lawler, and S. J. Lee. 1997a. Regulation of skeletal muscle mass in mice by a new TGF- β superfamily member. *Nature* 387:83-90.
- McPherron, A. C., A. M. Lawler, and S. J. Lee. 1997b. Regulation of skeletal muscle mass in mice by a new TGF- β superfamily member. *Nature* 387:83-90.
- McPherron, A. C. and S. J. Lee. 1997. Double muscling in cattle due to mutations in the myostatin gene. *Proceedings of the National Academy of Sciences of the United States of America* 94:12457-12461.
- McPherron, A. C. and S. J. Lee. 2002. Suppression of body fat accumulation in myostatin-deficient mice. *Journal of Clinical Investigation* 109:595-601.
- Mersmann, H. J. 1998. Overview of the effects of beta-adrenergic receptor agonists on animal growth including mechanisms of action. *J. Anim Sci.* 76:160.
- Page, K. A., D. L. Hartzell, C. Li, A. L. Westby, M. A. Della-Fera, M. J. Azain, T. D. Pringle, and C. A. Baile. 2004. β -Adrenergic receptor agonists increase apoptosis of adipose tissue in mice. *Domestic Animal Endocrinology* 26:23-31.
- Piek, E., C. H. Heldin, and P. Ten Dijke. 1999. Specificity, diversity, and regulation in TGF- β superfamily signaling. *FASEB J.* 13:2105-2124.
- Shizukuda, Y. and P. M. Buttrick. 2002. Subtype Specific Roles of β -Adrenergic Receptors in Apoptosis of Adult Rat Ventricular Myocytes. *Journal of Molecular and Cellular Cardiology* 34:823-831.
- Sinha-Hikim, I., N. Gonzalez-Cadavid, K. Yarasheski, R. Shen, R. Shivji, W. E. Taylor, K. Ma,

- and S. Bhasin. 1999. Serum myostatin levels are higher in HIV-infected women, and older women compared to young, menstruating women. *Journal of Investigative Medicine* 47:22A.
- Thomas, M., B. Langley, C. Berry, M. Sharma, S. Kirk, J. Bass, and R. Kambadur. 2000. Myostatin, a negative regulator of muscle growth, functions by inhibiting myoblast proliferation. *Journal of Biological Chemistry* 275:40235-40243.
- Wagner, K. R., A. C. McPherron, N. Winik, and S. J. Lee. 2002. Loss of myostatin attenuates severity of muscular dystrophy in mdx mice. *Annals of Neurology* 52:832-836.
- Westhusin, M. From mighty mice to mighty cows. *Nature Genetics* 17, 4-5. 1997.
- Young, R. B., K. Y. Bridge, A. J. Wuethrich and D. L. Hancock. 2002. Effect of serum from chickens treated with clenbuterol on myosin accumulation, β -adrenergic receptor population and cyclic AMP synthesis in embryonic chicken skeletal muscle cell cultures. *In Vitro Cellular & Developmental Biology - Animal* 38:102-110.
- Zhu, Y., C. Culmsee, I. Semkova, and J. Krieglstein. 1998. Stimulation of $\beta(2)$ -adrenoceptors inhibits apoptosis in rat brain after transient forebrain ischemia. *Journal of Cerebral Blood Flow and Metabolism* 18:1032-1039.
- Zhu, Y., J. H. M. Prehn, C. Culmsee, and J. Krieglstein. 1999. The $\beta(2)$ -adrenoceptor agonist clenbuterol modulates Bcl-2, Bcl-xl and Bax protein expression following transient forebrain ischemia. *Neuroscience* 90:1255-1263.
- Zimmers, T. A., M. V. Davies, L. G. Koniaris, P. Haynes, A. F. Esquela, K. N. Tomkinson, A. C. McPherron, N. M. Wolfman, and S. J. Lee. 2002. Induction of cachexia in mice by systemically administered myostatin. *Science* 296:1486-1488.

APPENDIX A

P27 KNOCKOUT MICE; REDUCED MYOSTATIN IN MUSCLE AND ALTERED
ADIPOGENESIS³

³Lin, J., M. A. Della-Fera, C. Li, K. Page, Y. H. Choi, D. L. Hartzell, and C. A. Baile.
Biochemical and Biophysical Research Communications 300 (2003) 938-942.

Abstract

Knockout of the P27kip gene, which encodes a cyclin-dependent kinase inhibitor involved in cell proliferation regulation, results in growth enhancement in mice. To investigate how p27 deficiency affected adipogenesis and myogenesis, levels of PPAR γ , C/EBP α and the myogenesis inhibitor, myostatin, were measured in p27^{-/-} (n=14), p27^{+/-} (n=18) and p27^{+/+} mice (n=11). Body weight and gastrocnemius muscle (GC) mass were increased in p27^{-/-} mice (P<0.05), but there were no differences in fat depot weights, percent body fat or serum leptin concentrations among genotypes. PPAR γ , but not C/EBP α , was markedly increased in p27^{-/-} mice (P<0.05). There also was a higher incidence of inguinal fat apoptosis (P<0.01) in p27^{-/-} mice. Myostatin levels were reduced in GC muscle of p27^{-/-} mice (P<0.05). These findings suggest that in p27 deficient mice, increased skeletal muscle mass is mediated in part through decreased myostatin. Although total adiposity was not changed, increased PPAR γ levels suggest an alteration in adipogenesis.

Introduction

In mammals cell cycle progression is regulated by the orderly activation of cyclin-dependent kinases (Cdks) and several cyclin-dependent kinase inhibitors (CKI). There are two families of CKIs: ink and kip/cip. The ink family includes p15^{ink}, p16^{ink}, p18^{ink} and p19^{ink}. The kip/cip family includes p21^{cip}, p27^{kip} and p57^{kip}. During cell differentiation, CKIs play important roles in maintaining growth arrest, and in some cases, terminating cell differentiation (Johnson and Walker, 1999). P27^{kip} seems most likely involved in cell cycle control including the Cyclin D–Cdk4/Cdk6 regulation of G1 progression (Phelps and Xiong, 1998; Toyoshima and Hunter, 1994). Knockout of the p27^{kip} gene in mice results in growth enhancement due to hyperplasia (Fero et al., 1996; Kiyokowa et al., 1996; Nakayama et al., 1996). In adult animals,

terminal differentiation and growth arrest in adipocytes and myocytes occurs with cessation of cell proliferation at the G1 phase. Consequently, we were interested in determining whether p27 knockout would affect both myogenesis and adipogenesis.

Myostatin (growth differentiation factor 8, GDF-8), a recent discovered gene that belongs to the TGF- β superfamily, acts as a negative regulator of skeletal muscle development (McPherron et al., 1996). Natural mutations of myostatin result in significantly increased muscle mass in cattle. Thomas et al. (Thomas et al., 2000) reported that in muscle precursor cell culture, myostatin induced p21 expression. However, it is not known whether there is an association between p27 and myostatin, especially since the muscle hyperplasia that results from p27 knockout may, in itself, affect myostatin levels.

Adipogenesis is a complex process, beginning with pre-adipocyte differentiation and progressing through lipogenesis to mature adipocyte (Rosen and Spiegelman, 2000). It is known that preadipocyte differentiation is mainly controlled by two families of transcription factors: the CCAAT/enhancer binding proteins (C/EBPs) and peroxisome proliferator-activated receptors (PPARs). Among them, PPAR γ and C/EBP α are two important factors that induce growth arrest during pre-differentiation and stimulate adipocyte specific gene expression that begins the process of terminal differentiation (Gregoire et al., 1998; Fajas et al., 2001). Leptin, one of adipocyte specific genes, begins to be expressed and secreted during the late stage of adipogenesis (lipogenesis) (Chen et al., 2000). It is believed to serve as a hormone signaling “adipostat”, playing an important role in regulation of food intake and energy homeostasis (Zhang et al., 1994).

We investigated in this study the effects of p27 knockout on the growth and development, body composition, myostatin, leptin, PPAR γ and C/EBP α production in 12 weeks old mice.

Materials and Methods

Animals

P27 knockout mice were kindly provided by Dr. Fero (Fred Hutchinson Cancer Research Center, Seattle, Washington) and bred in our lab. Mouse colonies were maintained in a pathogen-free environment and fed a normal mouse diet (PMI 5020 diet; Purina Test Diets, Richmond, IN) ad libitum. Animal care and experiments were conducted in accordance with guidelines and under protocols approved by the Animal Care Use Committee at the University of Georgia.

Three founders of forty-three mice were used in this experiment. At 6 weeks of age, DNA was isolated from tail tissues using DNAeasy kit (Qiagen, Valencia, CA). DNA (100 ng) was used for PCR reaction to differentiate the genotype using the primer set shown in Table 1. Based on PCR results, mice were separated into three groups by genotypes: $p27^{kip-/-}$ (n=14), $p27^{kip+/-}$ (n=18) or $p27^{kip+/+}$ (n=11). Body weights were measured every week from 7 to 12 weeks of age. All mice were sacrificed at 12 weeks of age. Blood was collected for serum leptin assay; gastrocnemius muscle (GC) and inguinal, parametrial/epididymal, and retroperitoneal fat pads were collected, weighed and stored at -80°C until use.

Body Composition Measurement

The LUNAR PIXI system (Lunar Corporation, Madison, WI) was used for the body composition measurement. Mice ($p27^{+/+}$, n=8 and $p27^{-/-}$, n=7) were analyzed at week 8 and week 12 of age. The mice were anesthetized with a mixture of ketamine, acepromizine and xylazine (3:2:1;v/v/v) at the ratio of 50 μl /40g body weight. They were then placed on a tray, the region of interest was selected, and data acquisition was completed. After analysis, total fat mass as

percentage of whole body weight was calculated.

Serum leptin assay

Serum leptin concentrations were measured by radioimmunoassay (Linco Research, St. Charles, MO). Serum (50 μ l) was used to perform the assay according to the manufacture's protocol. The inter-assay variation was 2.8%.

DNA isolation and Apoptosis Assay

Approximately 50 mg inguinal fat from 17 samples (p27^{+/+}, n=4, p27^{-/-}, n=9 and p27^{+/-}, n=4) were homogenized in lysis buffer (10 mM Tris-HCL, pH 8.0; 10 mM EDTA, pH 8.0; 0.5% Triton X-100) and centrifuged at 14,000 x g for 15 min to separate fragmented DNA from genomic DNA. The supernatant, containing fragmented DNA, was extracted with phenol-chloroform-isoamyl alcohol (25:24:1) and precipitated by adding polyacryl carrier (Molecular Research Center, Inc., Cincinnati, OH) and ethanol. Genomic (non-fragmented) DNA was extracted from the pellet with DNAzol (Molecular Research Center, Inc.) and the polyacryl carrier. DNA content was measured by PicoGreen (Molecular Probes, Inc., Eugene, OR), using SpectroMax Gemini (Molecular Devices, Sunnyvale, CA). Normalized by fat depot weight, both fragmental and genomic DNA from each sample were loaded on 1.5% agarose gel (pre-stained with 1:10,000 SYBR Green, Molecular Probes, Eugene, OR) for electrophoresis. Apoptosis was identified as the DNA ladder pattern visualized by FluorChem 8000 (Alpha Innotech, San Leandro, CA).

Western Blot

PPAR γ and C/EBP α protein levels in inguinal fat pads were determined as previously described (12). Thirty micrograms of total protein isolated from GC muscle per sample was

separated by SDS–PAGE. SyproRuby staining (Molecular Probes, Eugene, OR) was used to confirm the equal loading of protein in each lane. After transfer to PDVF membrane, protein was detected by incubation with specific primary antibodies (Santa Cruz Biotechnology, San Diego, CA), followed by incubation with horseradish peroxidase-conjugated second antibody. The immunoreactive polypeptides were visualized by the ECL-plus detection system (Amersham Pharmacia Biotech, Buckinghamshire, England), following the procedures recommended by the supplier. Data were recorded as band densities (integrated density value/area, IDV/area) by FluorChem 8000(Alpha Innotech Corporation, San Leandro, CA).

RT-PCR

Myostatin mRNA expression was determined by semi-quantitative RT-PCR as a ratio to 18s rRNA, which served as an internal control. Total RNA from each sample was extracted with RNAeasy kit (Qiagen, Valencia, CA) with one additional step of on-column treatment of DNase digestion. RNA content was quantified with RiboGreen (Molecular Probes, Eugene, OR). The first-strand cDNA was generated using 1 µg of total RNA with the combination of random primer and oligo (dT) primer at about 1:50 ratio with the Superscript II reverse transcriptase (Invitrogen, Carlsbad, CA). Two microliters of the reverse transcription reaction mix was amplified with primers specific for myostatin by 28 cycles at 94°C for 30 s, 54°C for 1 min, and 70°C for 1 min. 18s was co-amplified as an internal control. Primers used are listed in Table 1. The PCR products were electrophoresed on agarose gel and signal intensity was quantitated by ChemiImage system (Alpha Innotech Corporation, San Leandro, CA). Data were recorded as band densities (IDV/area) and transformed as square root ratio of myostatin to 18s.

Statistical Analysis

Data were expressed as mean \pm SEM. The Mann Whitney U test was used to determine significance of differences between genotypes in adipose tissue apoptosis. All other data were analyzed by one way ANOVA to determine significance of genotype effect. $P < 0.05$ was considered significant.

Results

Compared to $p27^{+/-}$ and $p27^{+/+}$ groups, the $p27^{-/-}$ mice showed increased growth rate and body weight from the age of 7 weeks to 12 weeks ($p < 0.05$). There was no difference between hemizygous ($p27^{+/-}$) and wildtype controls ($p27^{+/+}$) (Figure 1). At 12 weeks of age, there was increased GC muscle mass in the $p27^{-/-}$ group ($p < 0.05$) (Figure 2).

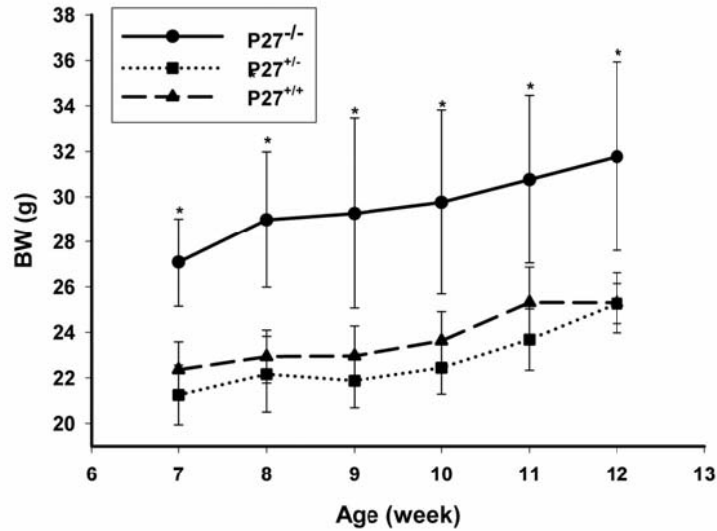


Fig 1. Body weights of $p27^{-/-}$, $p27^{+/-}$ and $p27^{+/+}$ mice from week 7 to week 12. * Means are significantly different from other groups ($p < 0.05$).

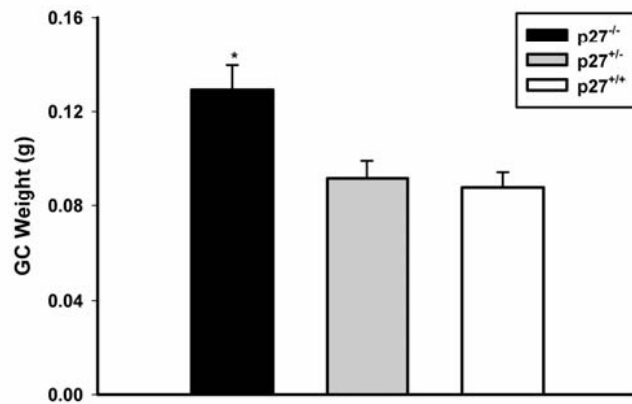


Fig 2. GC muscle mass (g) at 12 weeks of age in p27^{-/-}, p27^{+/-} and p27^{+/+} mice. * Means are significantly different from other groups (p<0.05).

There was no difference between p27^{-/-} and wildtype controls (p27^{+/+}) in total fat percentage at both 8 and 12 weeks of age. There were also no significant differences in weight of any of the fat pads among genotypes. Serum leptin concentrations did not differ significantly among genotypes (Table 2).

| | P27^{-/-} | P27^{+/-} | P27^{+/+} |
|-----------------------------|--------------------------|--------------------------|--------------------------|
| Ing (g) | 0.46±0.16 | 0.37±0.12 | 0.38±0.03 |
| Epi/Par (g) | 0.93±0.23 | 0.76±0.13 | 0.68±0.10 |
| Rp (g) | 0.28±0.03 | 0.27±0.04 | 0.21±0.10 |
| Fat percent | 22.10±2.11 (8 wk) | -- | 24.3±2.63 (8 wk) |
| | 25.03±3.13 (12 wk) | -- | 25.46±0.45 (12 wk) |
| Serum Leptin (ng/ml) | 9.96±1.72 | 10.23±1.23 | 8.49±1.28 |

Table 2. Mean fat depot weights, serum leptin concentrations and fat ratio

Apoptosis assay showed DNA fragmentation in inguinal fat tissue of 6 out of 9 $p27^{-/-}$ mice, in 1 out of 4 wild type control and 0 out of 4 hemizygous mice (Figure 3). The $p27^{-/-}$ group had a higher incidence of apoptosis (Mann Whitney U test; $z = -2.2$, $p < 0.05$) compared to the combined group of wildtype and hemizygous mice.

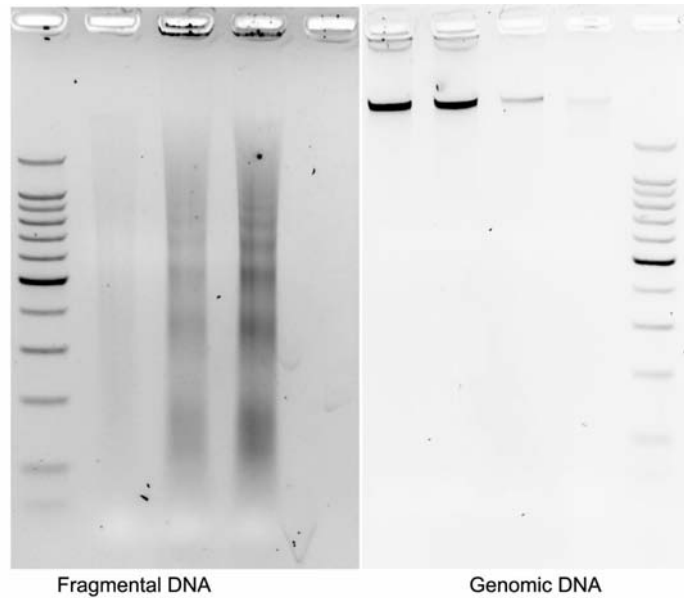


Fig 3. Apoptosis assay (DNA laddering stained with SYBR Green I). $P27^{-/-}$ group had higher rate of apoptosis ($P < 0.05$) compared to control group (Mann Whitney U test). Fragmental DNA was separated from genomic DNA to increase the sensitivity. To ensure the uniformity, all DNA sample was normalized by its fat mass weight and when loading on gel; genomic DNA was diluted to 1% volume of fragmental DNA so image could be acquired under similar conditions.

In inguinal fat pads, there were no differences among genotypes in C/EBP α levels (Figure 4), but PPAR γ level was markedly higher in $P27^{-/-}$ group ($P < 0.05$) compared to the $p27^{+/-}$ or $p27^{+/+}$ group (Figure 5). RT-PCR results indicated that in GC muscle, myostatin mRNA levels were decreased in the $p27^{-/-}$ group ($p < 0.01$) as compared to other groups (Figure 6); in addition, myostatin protein level was lower ($p < 0.05$) in $p27^{-/-}$ mice (Figure 7).

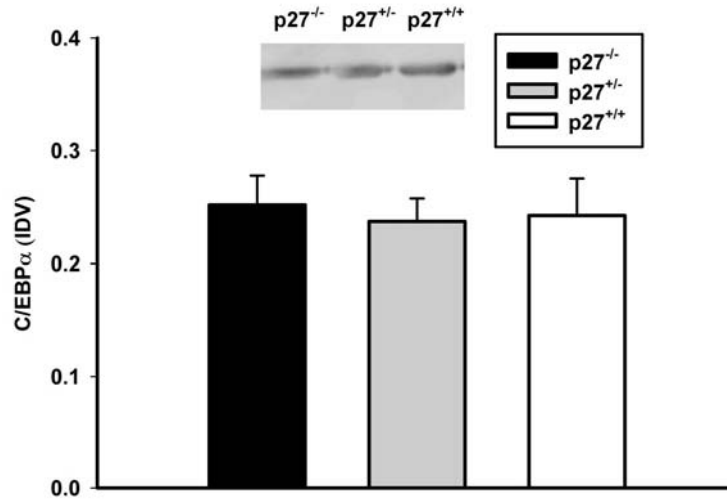


Fig 4. C/EBP α protein levels in inguinal adipose tissue of p27^{-/-}, p27^{+/-} and p27^{+/+} mice quantitated by Western blot (IDV, integrated density value).

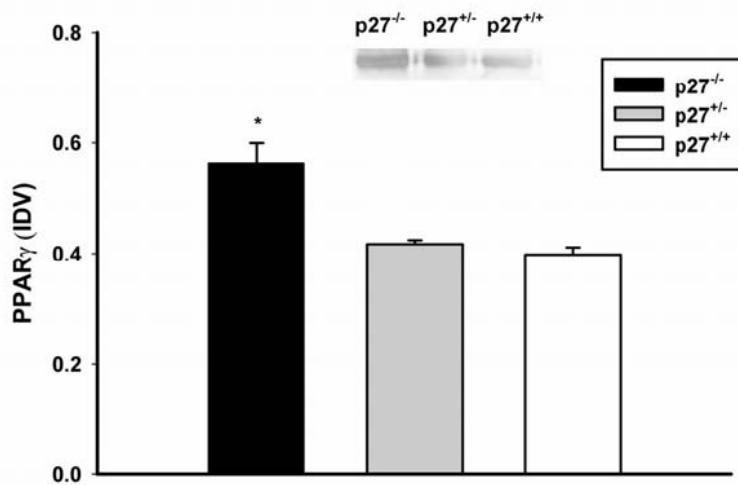


Fig 5. PPAR γ protein levels in inguinal adipose tissue of p27^{-/-}, p27^{+/-} and p27^{+/+} mice quantitated by Western blot (IDV, integrated density value). * Means are significantly different from other groups (p<0.05).

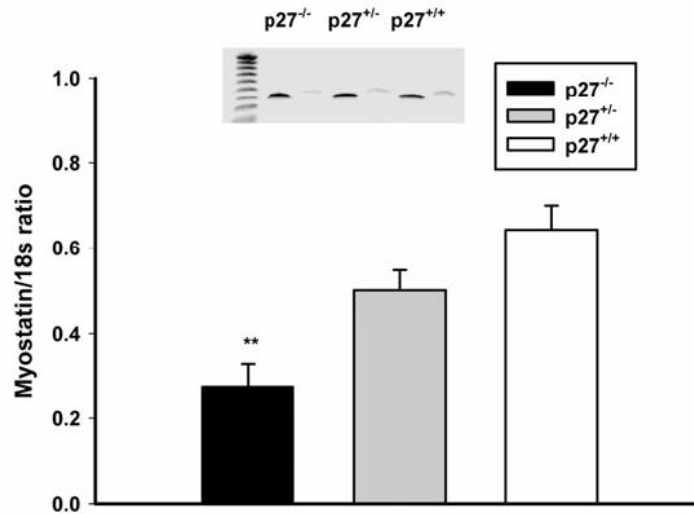


Fig 6. Semi-quantitative RT-PCR result of myostatin mRNA expression in GC muscle as a ratio of 18s rRNA. ** Means are significantly different from other groups (P <0.01).

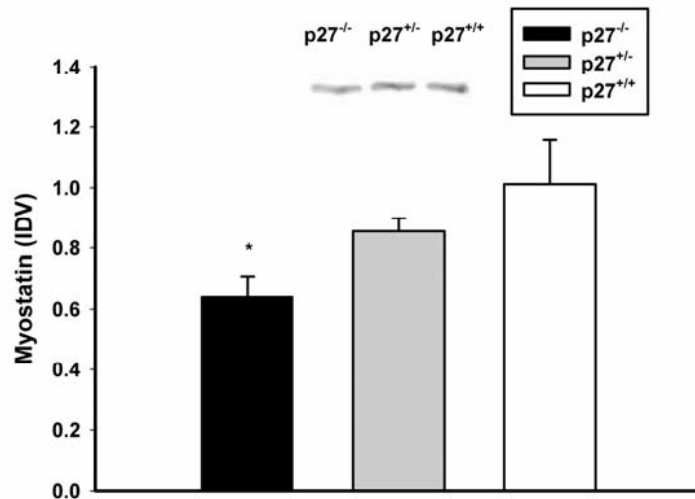


Fig 7. Myostatin protein levels in GC muscle of p27^{-/-}, p27^{+/-} and p27^{+/+} mice quantitated by Western blot (IDV, integrated density value). * Means are significantly different from other groups (p<0.05).

Discussion

P27 plays an important role in maintaining growth arrest. Cells lacking p27 have a shortened G1 phase (Coats et al., 1999). Earlier reports on p27 deficient mice showed multiple organ hyperplasia caused by hypercellularity (Fero et al., 1996; Kiyokowa et al., 1996; Nakayama et al., 1996). In this study, p27 knockout mice showed increased growth rate: beginning at 7 weeks of age, average body weight of p27 knockout mice was significantly greater than other groups, and this trend lasted to the end of this study at 12 weeks of age.

Myostatin (growth differentiation factor 8, GDF-8) belongs to the transforming growth factor- β (TGF- β) superfamily and acts as a negative regulator of skeletal muscle growth. In cattle such as the Belgian Blue, mutations of the myostatin gene result in enlarged muscles, primarily due to a marked increase in the number of muscle fibers. McPherron et al. (McPherron et al., 1997) showed that mice with targeted deletion of myostatin had a two to three-fold increase in muscle mass as a result of muscle cell hyperplasia and hypertrophy. Conversely, Gonzalez-Cadavid (Gonzalez-Cadavid et al., 1998) reported that in HIV patients, muscle wasting was associated with increased myostatin expression. In addition, muscle regeneration is related to myostatin changes (Yamanouchi et al., 2000). In our study, both myostatin mRNA and protein levels were decreased in p27 knockout mice. Together with the finding of increased GC muscle mass, this data suggests that in p27 knockout mice, increased myogenesis is a result of decreased myostatin level.

During adipogenesis, the transcription factors C/EBP α and PPAR γ are two key factors involved in inducing growth arrest and differentiation of preadipocytes, and promoting lipid storage and stimulating adipocyte specific gene production. For example, Morrison and Farmer (Morrison and Farmer, 1999) showed in an *in vitro* study that ectopic expression of PPAR γ in

non-precursor fibroblastic cell lines resulted in conversion to adipocytes. Our study showed that at 12 weeks of age, p27 knockout mice had no change in C/EBP α level, but they did have increased PPAR γ level, which may suggest that p27 deficiency results in altered adipogenic activity. This finding is consistent with an earlier report (Kim et al., 2001) showing that treatment of preadipocytes with myostatin in vitro resulted in decreased PPAR γ levels and inhibition of differentiation. In our study, the decrease in myostatin production in p27 knockout mice may have been responsible for the increased PPAR γ levels in adipose tissue.

Although p27 deficient mice have relative larger body size and body weight, percent body fat and fat depot weights were not significantly different from wild type mice. In addition, plasma leptin concentrations, which reflect adipose tissue mass, were not affected by p27 knockout in our study. Recent reports have indicated that activation of PPAR γ can induce apoptosis in a variety of tumor cell types (Houseknecht et al., 2002; Fajas et al., 2001). Our data showed that apoptosis in inguinal fat pads was present in a greater number of p27 deficient mice (p27^{-/-}) than in non-p27 deficient mice (p27^{+/+} and p27^{+/-}). This finding suggests that p27 deficiency results in adipocyte apoptosis, possibly due to increased PPAR γ levels. Thus, PPAR γ could affect both adipogenesis and adipocyte apoptosis, with the net effect being a lack of change in adipose depot weight.

In summary, this study showed that p27 deficient mice had an increased growth rate, increased body weight and increased GC muscle mass. Although p27 gene knockout alone may not alter the total adiposity and muscularity, it may have altered adipogenesis and myogenesis via increased adipose tissue PPAR γ levels and decreased muscle tissue myostatin levels. Additional studies involving the regulation of cellular mechanisms of proliferation and apoptosis in muscle and adipose tissue may provide mechanisms for producing animals with increased growth rate and increased percent of lean tissue but not increased fat tissue, which will benefit the domestic animal

industry.

Acknowledgement

This study was supported in part by the Georgia Research Alliance Eminent Scholar endowment held by C. A. Baile.

References

- Chen, X., Lin, J., Hausman, D.B., Martin, R.J., Dean, R.G., and Hausman, G.J., Alterations in fetal adipose tissue leptin expression correlate with the development of adipose tissue, *Biol Neonate* 78 (2000) 41-47.
- Coats, S., Whyte, P., Fero, M.L., Lacy, S., Chung, G., Randel, E., Firpo, E., and Roberts, J.M., A new pathway for mitogen-dependent cdk2 regulation uncovered in p27(Kip1)-deficient cells, *Curr Biol* 9 (1999) 163-173.
- Fajas, L., Debril, M.B., and Auwerx, J., Peroxisome proliferator-activated receptor-gamma: from adipogenesis to carcinogenesis, *J Mol Endocrinol* 27 (2001) 1-9.
- Fajas, L., Debril, M.B., and Auwerx, J., PPAR gamma: an essential role in metabolic control, *Nutr Metab Cardiovasc Dis* 11 (2001) 64-69.
- Fero, M.L., Rivkin, M., Tasch, M., Porter, P., Carow, C.E., Firpo, E., Polyak, K., Tsai, L.H., Broudy, V., Perlmutter, R.M., Kaushansky, K., and Roberts, J.M., A syndrome of multiorgan hyperplasia with features of gigantism, tumorigenesis, and female sterility in p27(Kip1)-deficient mice, *Cell* 85 (1996) 733-744.
- Gregoire, F.M., Smas, C.M., and Sul, H.S., Understanding adipocyte differentiation, *Physiol Rev* 78 (1998) 783-809.
- Gonzalez-Cadavid, N.F., Taylor, W.E., Yarasheski, K., Sinha-Hikim, I., Ma, K., Ezzat, S., Shen, R., Lalani, R., Asa, S., Mamita, M., Nair, G., Arver, S., and Bhasin, S., Organization of the human myostatin gene and expression in healthy men and HIV-infected men with muscle wasting, *Proc Natl Acad Sci U S A* 95 (1998) 14938-14943.
- Houseknecht, K.L., Cole, B.M., and Steele, P.J., Peroxisome proliferator-activated receptor gamma (PPARgamma) and its ligands: A review, *Domest Anim Endocrinol* 22 (2002) 1-23.
- Johnson, D.G., and Walker, C.L., Cyclins and cell cycle checkpoints, *Annu Rev Pharmacol Toxicol* 39 (1999) 295-312.
- Kim, H.S., Liang, L., Dean, R.G., Hausman, D.B., Hartzell, D.L., and Baile, C.A., Inhibition of preadipocyte differentiation by myostatin treatment in 3T3-L1 cultures, *Biochem Biophys Res Commun* 281 (2001) 902-906.
- Kiyokawa, H., Kineman, R.D., Manova-Todorova, K.O., Soares, V.C., Hoffman, E.S., Ono, M., Khanam, D., Hayday, A.C., Frohman, L.A., and Koff, A., Enhanced growth of mice lacking the cyclin-dependent kinase inhibitor function of p27(Kip1), *Cell* 85 (1996) 721-732.
- Morrison, R.F., and Farmer, S.R., Role of PPARgamma in regulating a cascade expression of

- cyclin-dependent kinase inhibitors, p18(INK4c) and p21(Waf1/Cip1), during adipogenesis, *J Biol Chem* 274 (1999) 17088-17097.
- Nakayama, K., Ishida, N., Shirane, M., Inomata, A., Inoue, T., Shishido, N., Horii, I., and Loh, D.Y., Mice lacking p27(Kip1) display increased body size, multiple organ hyperplasia, retinal dysplasia, and pituitary tumors, *Cell* 85 (1996) 707-720.
- McPherron, A.C., Lawler, A.M., and Lee, S.J., Regulation of skeletal muscle mass in mice by a new TGF-beta superfamily member, *Nature* 387 (1997) 83-90.
- Phelps, D.E., and Xiong, Y., Regulation of cyclin-dependent kinase 4 during adipogenesis involves switching of cyclin D subunits and concurrent binding of p18INK4c and p27Kip1, *Cell Growth Differ* 9 (1998) 595-610.
- Rosen, E.D., and Spiegelman, B.M., Molecular regulation of adipogenesis, *Annu Rev Cell Dev Biol* 16 (2000) 145-171.
- Toyoshima, H., and Hunter, T., p27, a novel inhibitor of G1 cyclin-Cdk protein kinase activity, is related to p21, *Cell* 78 (1994) 67-74.
- Thomas, M., Langley, B., Berry, C., Sharma, M., Kirk, S., Bass, J., and Kambadur, R., Myostatin, a negative regulator of muscle growth, functions by inhibiting myoblast proliferation, *J Biol Chem* 275 (2000) 40235-40243.
- Yamanouchi, K., Soeta, C., Naito, K., and Tojo, H., Expression of myostatin gene in regenerating skeletal muscle of the rat and its localization, *Biochem Biophys Res Commun* 270 (2000) 510-516.
- Zhang, Y., Proenca, R., Maffei, M., Barone, M., Leopold, L., and Friedman, J.M., Positional cloning of the mouse obese gene and its human homologue, *Nature* 372 (1994) 425-432.

APPENDIX B

MELANOCORTIN RECEPTORS MEDIATE LEPTIN EFFECTS ON FEEDING AND BODY WEIGHT BUT NOT ADIPOSE APOPTOSIS⁴

⁴ Choi, Y. H., C. L. Li, K. A. Page, A. L. Westby, M. A. Della-Fera, J. Lin, D. L. Hartzell, and C. A. Baile. Melanocortin Receptors Mediate Leptin Effects on Feeding and Body Weight, But Not Adipose Apoptosis. *Physiology and Behavior* 79 (2003) 795-801.

Abstract

Melanocortin receptors mediate leptin effects on feeding and body weight, but not adipose apoptosis. The melanocortin (MC) system is a known downstream mediator of leptin signaling in the brain; thus, activation of MC receptors by melanotan II (MTII), a MC3/4 receptor agonist, was hypothesized to increase adipose apoptosis, a phenomenon seen after leptin treatments. To test this hypothesis, male Sprague-Dawley rats received pretreatments of intracerebroventricular (ICV) injections of artificial cerebrospinal fluid (aCSF, 5 μ l) or SHU9119 (1.0 nmol/5 μ l), an MC3/4 receptor antagonist. One hour later, aCSF (5 μ l), leptin (10 μ g/5 μ l) or MTII (0.1 nmol/5 μ l) was injected ICV in the aCSF-pretreated groups, and either leptin (10 μ g/5 μ l) or MTII (0.1 nmol/5 μ l) was injected ICV in SHU9119-pretreated groups. Each pair of treatments was given once daily for 4 successive days. Body weight (BW), food intake (FI) and body temperature (BT) were measured daily at 4 and 24-h intervals. SHU9119 completely prevented the decrease in FI and BW caused by either MTII or leptin. Muscle mass remained unchanged regardless of treatment, but both leptin and MTII significantly reduced mass of inguinal (iWAT), retroperitoneal (rWAT) and epididymal (eWAT) white adipose tissues ($p < 0.05$). SHU9119 prevented the decrease in mass of intrascapular brown fat, iWAT and rWAT ($p < 0.05$). Leptin, but not MTII, increased DNA fragmentation in eWAT ($p < 0.05$), but SHU9119 pretreatment had no effect on leptin-induced apoptosis. Thus, although the MC receptors in the brain are involved in mediating actions of leptin on FI, fat mass and BW, leptin-induced adipose apoptosis is regulated independently of MC receptors.

Introduction

Alpha-melanocyte-stimulating hormone (α -MSH), a product of the pro-opiomelanocortin (POMC) gene, plays an important role in eating behavior and energy homeostasis (Yeo et al.,

2000). The effects of α -MSH on food intake and body weight are mediated in the brain via two of the five known melanocortin (MC) receptors (R), MC3-R and MC4-R (Raffin-Sanson and Bertherat, 2001). The MC3-R are densely localized in the arcuate nucleus of the CNS but are found only in low levels peripherally, in the pancreas and stomach. MC4-R are localized primarily in the CNS (Harrold et al., 1999). Functional mutations of MC4-R, either inherited or induced, are associated with hyperphagia and obesity (Huszar et al., 1997), and in contrast to normal animals, MC4-R-deficient mice do not respond to the food intake inhibitory effect of the MC-R agonist, melanotan II (MTII), administered intracerebroventricularly (ICV), thus demonstrating the importance of these MC receptors in the control of food intake (Ludwig et al., 2001; Marsh et al., 1999; Hwa et al., 2001).

Treatments with MTII cause a variety of endocrine and metabolic effects (Fan et al., 1997; Hamilton et al., 2002; Pierroz et al., 2002). MTII reduced concentrations of leptin and insulin in serum and increased oxygen consumption in rats fed a highly palatable diet (Hamilton et al., 2002), as well as in diet-induced obese mice (Pierroz et al., 2002). MTII dose-dependently suppressed food intake, body weight and respiratory quotient in both Zucker obese and lean rats and increased utilization of fat as energy substrate, but obese rats were more sensitive to MTII's inhibitory effect on body weight (Hwa et al., 2001). In contrast, ICV injection of SHU9119, an MC3/4-R antagonist, for 11 days increased daily food intake, body weight and total fat mass (Adage et al., 2001).

There is much similarity in the actions of leptin and MTII (Cettour-Rose and Rohner-Jeanrenaud, 2002), and there is evidence that melanocortins act as downstream effectors for at least some of leptin's CNS effects (Elmquist, 2001). One of the most distinctive actions of leptin is its stimulatory effect on apoptosis in adipose tissues (Qian et al., 1998; Della-Fera et al.,

2001); however the role of the MC system in regulation of adipose tissue apoptosis has only begun to be studied. We recently found that rats injected IP with MTII at a dose of 2 mg/kg once a day for 4 days showed a substantial reduction in food intake, body weight gain and fat mass; however, no increase in apoptosis was observed in the epididymal, inguinal or retroperitoneal white adipose tissue (WAT) (Choi et al., 2003). MTII is much more potent when administered centrally, rather than peripherally (Pierroz et al., 2002; Cettour-Rose and Rohner-Jeanrenaud, 2002; Cowley et al., 1999; Grill et al., 1998), and it is likely that MTII primarily acts through the central nervous system. Therefore, the present study was carried out to determine whether MTII injected ICV induced adipose tissue apoptosis and whether blocking MC3/4 receptors with SHU9119 could prevent leptin- or MTII-induced adipose tissue apoptosis in rats.

Material and Methods

Animals

Fifty-two male Sprague-Dawley rats (250 – 274 g), purchased from Harlan, Inc. (Indianapolis, IN), were individually housed in suspended polycarbonate cages in a room with controlled lighting (on 2400 h – 1200 h and off 1200 – 2400 h), 22 ± 1 °C ambient temperature, and 50 % humidity. Rats were fed pelleted standard lab chow (LabDiet 5001, PMI Nutritional International, LLC., Brentwood, MO) and had ad libitum access to water throughout the study, unless otherwise noted. Water was supplied via water taps until the rats were transferred to hanging stainless steel wire-mesh-cages with a water bottle on each, two days before the initiation of angiotensin II tests. The Animal Care and Use Committee for the University of Georgia approved all procedures used in this study.

Materials

Artificial cerebrospinal fluid (aCSF) (Alzet, 2001). All peptides were solubilized based on net protein content in the container. Rat leptin was purchased from R&D Systems (Minneapolis, MN) and both SHU9119 and MTII from Phoenix Pharmaceuticals, Inc. (Belmont, CA). They were solubilized in aCSF at concentrations of 2.0 µg/µl for leptin, 1.0 nmol/5 µl (or 215.2 ng/µl) for SHU9119, and 0.1 nmol/5 µl (or 20.5 ng/µl) for MTII, and stored as aliquots at -80 C (Grill et al., 1998) for daily use.

Implantation of guide cannulas and transponders

Rats were anesthetized with a 3:2:1 (V:V:V) mixture (1 ml/kg, IP) of ketamine HCl (Ketaset®, Fort Dodge Laboratories, Inc., Fort Dodge, IA; 100 mg/ml), acepromazine maleate (PromAce®, Fort Dodge; 10 mg/ml), and xylazine (Rompun, Miles Inc., Shawnee Mission, KS; 20 mg/ml), and the hair in the dorsum of the head as well as the area behind scapular bones was removed. Each rat was then placed in the stereotaxic instrument (Stoelting Co., Wood Dale, IL) and the skin disinfected with chlorhexidine (Nolvasan®, Fort Dodge Laboratories). A 22-gauge guide cannula (C313G, Plastics One, Inc., Roanoke, VA), which was cut 13.2 mm long, was aseptically implanted into the right lateral ventricle of each rat, with the coordinates of 0.8 mm posterior to the bregma, 1.5 mm lateral to the midline and 3.2 mm ventral to the surface of the skull based on the atlas of the rat brain (Paxinos and Watson, 1998). The cannula was held in place with four stainless steel machine screws and cranioplastic cement (Plastics One, Roanoke, VA) attached to the skull. A 28-gauge stylet (C313DC, Plastics One) was installed into the guide cannula when the rat did not receive an injection. A programmable transponder (IPTT-200TM, BioMedic Data Systems, Inc., Seaford, DE) for telemetry was implanted under the skin using a needle-syringe type injector. To control post-surgery pain, flunixin meglumine (Banamine,

Schering Plough Animal Health) was given subcutaneously at a dose of 1.1 mg/kg. The rats were returned to their home cage and were allowed to recover for at least one week before angiotensin II tests began.

Verification of cannula placement

Water intake in response to ICV angiotensin II was tested at the end of the recovery period. In the morning of the test, food was removed from their cages, and rats were injected with angiotensin II (Sigma, St. Louis, MO) at a concentration of 100 ng/10 μ l sterile aCSF. Those consuming more than 5 ml of water in 30 min were used in the study.

Experimental Design

Fifty rats were randomly assigned to five treatment groups (N = 10). Treatments were administered at 24-h intervals for 4 days as two bolus ICV injections. The first injections (pretreatments) were either aCSF (5 μ l), given to 3 groups, or SHU9119 (1.0 nmol/5 μ l), given to 2 groups at t = -1 h. One hour later (t = 0 h), the three aCSF-pretreated groups were injected with either aCSF (5 μ l), leptin (10 μ g/5 μ l) or MTII (0.1 nmol/5 μ l), and the two SHU9119-pretreated groups were injected with either leptin (10 μ g/5 μ l) or MTII (0.1 nmol/5 μ l).

Treatment administration

Each rat was transferred from its home cage to a stainless steel bowl so they could freely move about during the injection procedure. They were gently held while both inserting and removing the injector. The injections were carried out using an injector cannula (C313I, Plastics One) that protruded 1.1 mm below the tip of the guide cannula and was connected to a Gilmont micrometer syringe by way of a 92-cm length of polyethylene tubing. Two separate injections, 1 h apart, were given once daily to the five treatment groups of rats. Each injection was administered into the lateral ventricle over 30 sec between 0900–1200 h each day, and the injector was left in

place for additional 30 sec to allow the CSF to diffuse the drug, followed by removal of the injector and replacement of the stylet into the guide cannula. The rats were returned to their home cages following each injection.

Body weight (BW), food intake (FI) adjusted for spillage, and body temperature (BT) were measured daily on the four experimental days between 0900 – 1000 h (T = -1 h), and FI and BT were additionally recorded at 4 h after the second injections (T = 4 h).

Tissue and blood collection

On day 5 the final data for BT, FI and BW were recorded, and the rats were euthanized in a CO₂ chamber and decapitated by a guillotine for blood and tissue collections between 0900 and 1300 h. Blood from the trunk was allowed to clot on ice for several hours before centrifuging at 2,400 rpm at 4°C for 20 min and resultant serum was stored at –20 °C until assay. Serum concentrations of insulin and leptin were determined by RIA according to the manufacturer's instruction (Linco Research, Inc., St. Charles, MO).

Intrascapular brown adipose tissue (iBAT), epididymal white adipose tissue (eWAT), inguinal WAT (iWAT), retroperitoneal WAT (rWAT) and gastrocnemius (GC) muscle were collected and weighed. Adipose tissue samples (approx 150 mg) were immediately placed in tubes containing lysis buffer for apoptosis assay. The remainder of the adipose tissue was frozen in liquid nitrogen and stored at –80°C.

Gel electrophoresis apoptosis assay. Apoptosis was determined following DNA isolation from fresh fat tissues by separating it into two fractions: fragmented and genomic DNA. The samples were first run on an agarose gel to identify a ladder pattern of internucleosomal DNA degradation of the fat tissue, which is characteristic of apoptosis (Qian et al., 1998). Apoptosis was then quantified as the ratio of fragmented- to total-DNA, multiplied by 100 (Shimabukuro et

al., 1998). Briefly, approximately 150 mg of fresh eWAT, iWAT and rWAT were homogenized in lysis buffer (10 mM Tris-HCL, pH 8.0; 10 mM EDTA, pH 8.0; 0.5% Triton X-100) and centrifuged at 14,000 x g for 15 min to separate fragmented DNA from genomic DNA. The supernatant, containing fragmented DNA, was extracted with phenol-chloroform-isoamyl alcohol (25:24:1) and the DNA was precipitated by adding polyacryl carrier (Molecular Research Center, Inc., Cincinnati, OH) and ethanol. Genomic (non-fragmented) DNA was extracted from the pellet with DNAzol and the polyacryl carrier. DNA in each fraction was quantified by the PicoGreen method (Molecular Probes, Inc., Eugene, OR) and fluorescence was measured using SpectroMax Gemini (Molecular Devices).

Statistical Analysis

Analysis of Variance followed by Duncan's multiple range test was used to determine significance of differences among treatments. In addition, a direct test of the effects of SHU9119 and leptin or MTII on the various parameters measured in this experiment was tested using a 2 X 2 factorial analysis. Data were considered significant when $P < 0.05$ and are expressed as mean \pm SEM.

Results

There were both significant treatment ($F(4,41) = 5.30, P = 0.0016$) and day ($F(4,164) = 30.74, P = 0.0001$) effects on BW (Figure 1). Both leptin and MTII decreased BW, and SHU9119 reversed their effects, even increasing BW above control level. Despite gradual recovery of FI in the aCSF/MTII group (Figure 1), BW remained significantly lower compared with control (aCSF/aCSF), resulting in a significant interaction of treatment and day ($F(16,164) = 19.75, P = 0.0001$).

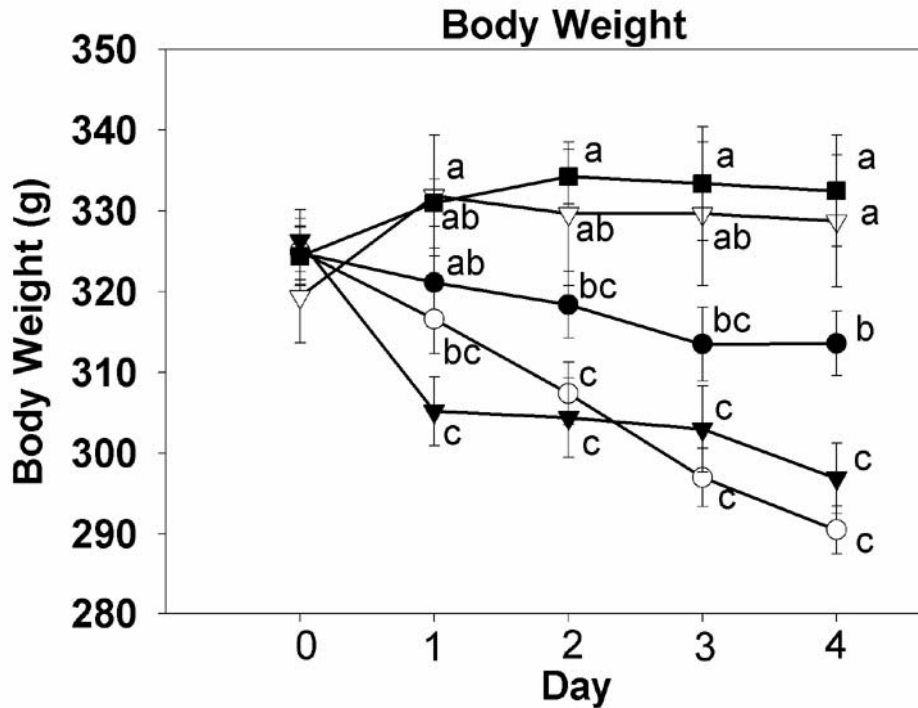


Figure 1. Body weight (g) of rats pre-injected ICV once a day for 4 days with either artificial cerebrospinal fluid (aCSF, 5 μ g) or SHU9119 (SHU, 1 nmol/5 μ g) followed one hour later with either aCSF (5 μ g), leptin (10 μ g/5 μ l) or MTII (0.1 nmol/5 μ g) ICV. Food was removed for 1 h between injections. Means with different letters at a given day are significantly different at $P < 0.05$. Data are means \pm SEM ($n = 8-10$).

-- aCSF/aCSF; -o- aCSF/leptin; -- aCSF/MTII; -- SHU9119/leptin; -- SHU9119/MTII

Daily FI was reduced in both aCSF/leptin and aCSF/MTII groups (Figure 2). One way ANOVA revealed significant effects of both treatment ($F(4,41) = 36.72$, $P = 0.0001$) and day ($F(4,164) = 13.88$, $P = 0.0001$) as well as interaction of treatment \times day ($F(16,164) = 10.24$, $P = 0.0001$). Food intake continued to decline during the treatment period in the aCSF/leptin group, whereas in the aCSF/MTII group, both 4 h and 24 h FI had returned to control level by day 3 (Figures 2, 3). In both SHU9119/leptin and SHU9119/MTII groups, FI was consistently above control level (Figure 2). The anorexigenic effects of both leptin and MTII were completely blocked by pretreatments with SHU9119, resulting in increased FI (Figures 2, 3).

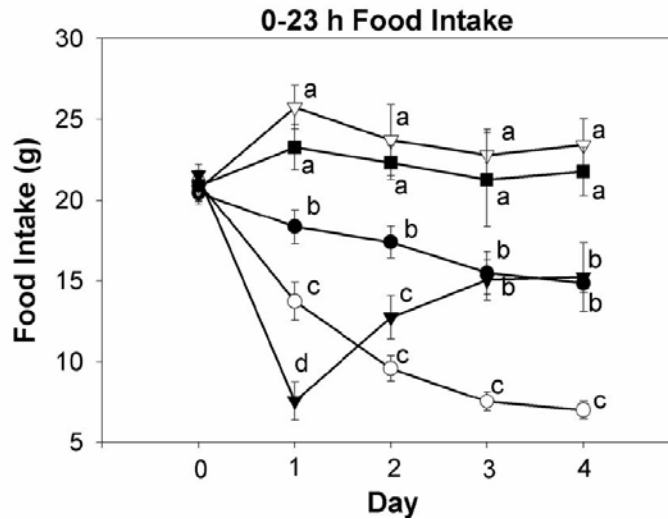


Figure 2. Twenty four hour food intake (g) of rats pre-injected ICV once a day for 4 days with either artificial cerebrospinal fluid (aCSF, 5 μ g) or SHU9119 (SHU, 1 nmol/5 μ g) followed one hour later with either aCSF (5 μ g), leptin (10 μ g/5 μ l) or MTII (0.1 nmol/5 μ g) ICV. Food was removed for 1 h between injections. Means with different letters at a given day are significantly different at $P < 0.05$. Data are means \pm SEM (n = 8–10).
 --●-- aCSF/aCSF; --○-- aCSF/leptin; --▼-- aCSF/MTII; --■-- SHU9119/leptin; --△-- SHU9119/MTII

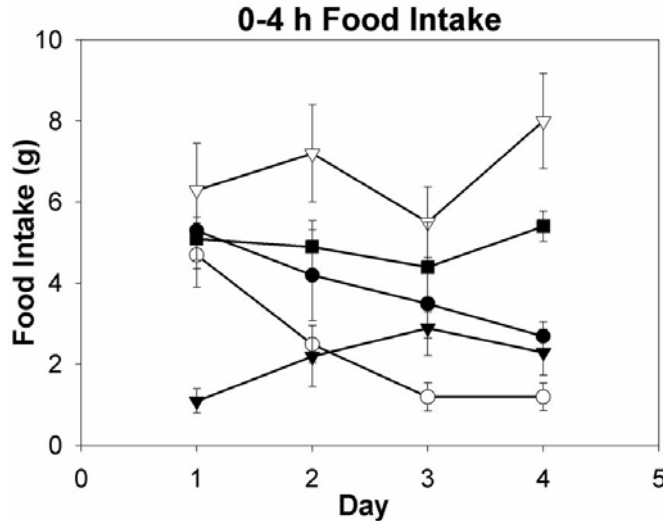


Figure 3. Four hour food intake (g) of rats pre-injected ICV once a day for 4 days with either artificial cerebrospinal fluid (aCSF, 5 μ g) or SHU9119 (SHU, 1 nmol/5 μ g) followed one hour later with either aCSF (5 μ g), leptin (10 μ g/5 μ l) or MTII (0.1 nmol/5 μ g) ICV. Food was removed for 1 h between injections. Means with different letters at a given day are significantly different at $P < 0.05$. Data are means \pm SEM (n = 8–10).
 --●-- aCSF/aCSF; --○-- aCSF/leptin; --▼-- aCSF/MTII; --■-- SHU9119/leptin; --△-- SHU9119/MTII

There were significant treatment ($F(4,164)=18.4$; $P<.0001$) and day ($F(3,164)=3.0$; $P<.05$) effects on 4 h body temperature, but no significant treatment x day interaction. By day 2, 4 h BT was significantly lower in the SHU9119/MTII group, and this decrease was maintained through the end of the study (Table 1). In rats treated with either aCSF/MTII or SHU9119/leptin, mean BT for the 4 treatment days was lower than either the control (aCSF/aCSF) or leptin alone (aCSF/leptin) groups, but for each of these treatments, there was only one day during which BT was significantly lower than control. Leptin alone (aCSF/leptin) had no effect on BT.

| Treatments | n | Day 1 | Day 2 | Day 3 | Day 4 | Overall |
|----------------|----|--------------|--------------|---------------|---------------|--------------|
| aCSF/aCSF | 10 | 38.9 ± 0.14a | 39.0 ± 0.13a | 39.3 ± 0.24a | 39.1 ± 0.25ab | 39.1 ± 0.01a |
| aCSF/Leptin | 10 | 38.6 ± 0.13a | 39.1 ± 0.01a | 39.0 ± 0.19ab | 39.4 ± 0.18a | 39.0 ± 0.01a |
| aCSF/MTII | 10 | 38.2 ± 0.12b | 38.8 ± 0.01a | 38.9 ± 0.25ab | 38.9 ± 0.20ab | 38.7 ± 0.01b |
| SHU9119/Leptin | 8 | 38.6 ± 0.23a | 38.7 ± 0.18a | 38.5 ± 0.19bc | 38.6 ± 0.15bc | 38.6 ± 0.01b |
| SHU9119/MTII | 8 | 38.0 ± 0.17b | 38.2 ± 0.28b | 37.8 ± 0.12c | 38.0 ± 0.22c | 38.0 ± 0.10c |

Table 1. Body Temperature of Rats 4 h After Second ICV Injections*

*Treatment means with different letters within a column are different at $P < 0.05$

ICV leptin, but not MTII, treatment decreased insulin concentrations in serum, (Table 2). SHU9119 treatment blocked the leptin treatment induced decrease and increased insulin concentrations more than 8 times. Treatment with SHU9119 and MTII also resulted in increased insulin concentrations but to a slightly less extent than that observed with treatment with SHU9119 and leptin. Serum leptin concentrations in leptin-treated rats were below the detection limit of 0.5 ng/ml. The mean concentrations of leptin of the control, leptin and MTII treated rats were not different. Pretreatment with SHU9119 prior to either injections of leptin or MTII resulted in

increased leptin serum concentrations by about ten fold ($P < 0.0001$).

| Treatments | n | Insulin (ng/ml) | Leptin (ng/ml) |
|----------------|----|-----------------|----------------|
| aCSF/aCSF | 10 | 1.51 ± 0.18c | 0.57 ± 0.17b |
| aCSF/Leptin | 10 | 0.48 ± 0.08d | ND**b |
| aCSF/MTII | 10 | 1.12 ± 0.17cd | 0.39 ± 0.32b |
| SHU9119/Leptin | 8 | 3.96 ± 0.63a | 6.50 ± 1.17a |
| SHU9119/MTII | 8 | 2.80 ± 0.42b | 5.54 ± 1.26a |

Table 2. Serum Insulin and Leptin Concentrations of Rats 24 h After the Last ICV Injection*

*Treatment means with different letters within a column are different at $P < 0.05$.

**ND: below the detection limit (0.5 ng/ml).

Both leptin and MTII treatments resulted in a significant reduction in eWAT mass that was completely prevented by prior injections of SHU9119 ($F(4,41) = 16.18$, $P = 0.0001$) (Figure 4). SHU9119 pretreatment also abolished the reduction in iWAT mass induced by leptin, and even increased it significantly compared with those treated with either aCSF or MTII ($F(4,41) = 15.94$, $P = 0.0001$) (Figure 4). The rWAT showed an 82 % reduction in the aCSF/leptin-treated group relative to aCSF control and, in fact, no rWAT was visibly detected in three rats of this group. The reduction in rWAT mass in response to leptin and MTII was blocked by SHU9119 pretreatment, and was actually increased above control level in the SHU9119/leptin group ($F(4,41) = 18.18$, $P = 0.0001$) (Figure 4). Neither leptin nor MTII altered iBAT mass, but prior treatments with SHU9119 approximately doubled the mass of the iBAT compared with control ($F(4,41) = 15.14$, $P = 0.0001$) (Figure 5). GC muscle mass was not changed by any of the treatments ($F(4,41) = 1.99$, $P = 0.115$) (Figure 5).

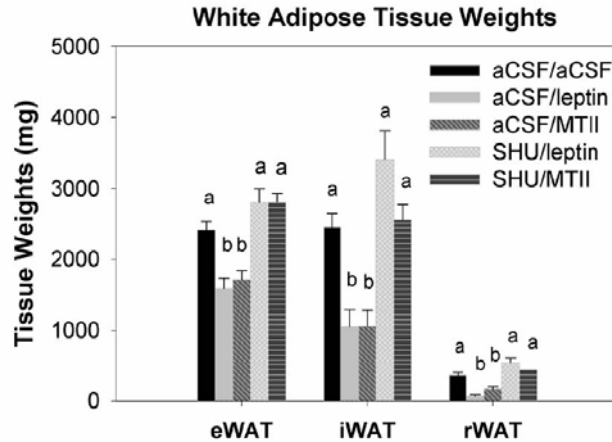


Figure 4. White adipose tissue weight of rats pre-injected ICV once a day for 4 days with either artificial cerebrospinal fluid (aCSF, 5 μ g) or SHU9119 (SHU, 1 nmol/5 μ g) followed one hour later with either aCSF (5 μ g), leptin (10 μ g/5 μ l) or MTII (0.1 nmol/5 μ g) ICV. Food was removed for 1 h between injections. Tissues were collected on day 5 between 24-28 h after the last injections. Epididymal white adipose tissue (eWAT); inguinal WAT (iWAT); retroperitoneal WAT (rWAT). Means with different letters are significantly different at $P < 0.05$. Data are means \pm SEM (n = 8–10).

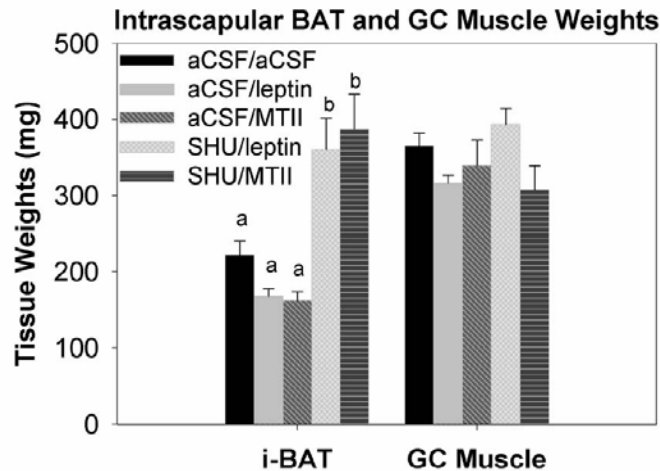


Figure 5. Intrascapular brown adipose tissue (iBAT) and gastrocnemius (GC) muscle weights of rats pre-injected ICV once a day for 4 days with either artificial cerebrospinal fluid (aCSF, 5 μ g) or SHU9119 (SHU, 1 nmol/5 μ g) followed one hour later with either aCSF (5 μ g), leptin (10 μ g/5 μ l) or MTII (0.1 nmol/5 μ g) ICV. Food was removed for 1 h between injections. Tissues were collected on day 5 between 24-28 h after the last injections. Means with different letters are significantly different at $P < 0.05$. Data are means \pm SEM (n = 8–10).

Apoptosis in the eWAT ($F(4,39) = 3.47, P = 0.016$), but not the iWAT ($F(4,40) = 1.42, P = 0.256$) or rWAT ($F(4,38) = 0.52, P = 0.723$), was significantly increased by leptin treatment, and SHU9119 had no effect on leptin-induced eWAT apoptosis (Figure 6). These results were supported by a subsequent analysis of the data using a planned factorial ANOVA revealing a significant treatment effect on apoptosis in eWAT ($F(1,26) = 10.5, P = 0.0033$), but with no SHU9119 pretreatment effect or interaction.

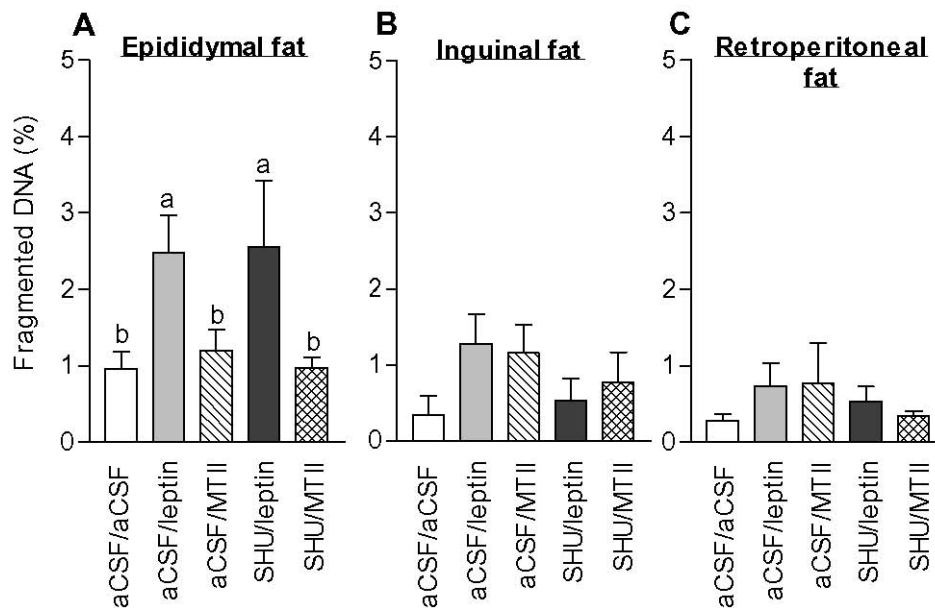


Figure 6. Fragmented-to-total DNA ratio (%) in fat tissues collected from rats pre-injected ICV once a day for 4 days with either artificial cerebrospinal fluid (aCSF, 5 μ g) or SHU9119 (SHU, 1 nmol/5 μ g) followed one hour later with either aCSF (5 μ g), leptin (10 μ g/5 μ l) or MTII (0.1 nmol/5 μ g) ICV. Food was removed for 1 h between injections. Fresh tissues, taken on day 5 between 24-28 h after the last injections, were immediately analyzed for DNA. A) Epididymal, B) inguinal and C) retroperitoneal fats. Means with different letters are significantly different at $P < 0.05$. Data are means \pm SEM ($n = 7-10$).

Discussion

A decrease in fat mass, along with reduction of FI and BW, was characteristic in rats treated with either leptin or MTII, and these decreases were completely abolished by prior administration of SHU9119. BAT mass was not modified in response to either leptin or MTII, but

was increased approximately 100 % by pretreatments with SHU9119. The lack of decrease in BAT mass in leptin-treated rats, despite the significant decrease in food intake, is likely a result of increased sympathetic nervous system output to BAT caused by leptin (Scarpace et al., 1997). The increase in BAT mass in rats that received SHU9119 pretreatment may have been a result of their increased food intake. In an earlier study, we found that BAT mass was greatly increased in hyperphagic rats after cessation of leptin treatments (Gullicksen et al., 2002).

SHU9119 has been shown to decrease BT after third ventricular injection in rats (Adage et al., 2001). In this study, we found a consistent decrease in BT 4 h after rats were treated with SHU9119/MTII. This effect was obviously not a result of inhibition of MTII, since MTII alone also decreased BT, although not as much as the combination of SHU9119 and MTII. The effect of MTII alone on BT may be consistent with studies showing an antipyretic effect of α -MSH (Feng et al., 1987; Villar et al., 1991) however, SHU9119 was shown to block the antipyretic effect of α -MSH (Haung et al., 1998). α -MSH and MTII have also been shown to have either no effect on normal thermoregulation or to increase body temperature at high doses (Villar et al., 1991; Murphy et al., 2000; Rezvani et al., 1986). Thus, the mechanism for the decrease in BT by SHU9119 is not clear. Although leptin alone had no effect on BT, in rats treated with the combination of SHU9119 and leptin, BT was higher than in rats treated with SHU9119 and MTII. This finding suggests that leptin was able to moderate the effect of SHU9119).

The insulin and leptin serum concentrations reflected the status of the fat pads and food intake at the end of the experimental period when the serum samples were collected. The treatments which included SHU9119 resulted in at least the maintenance of the mass of the fat pads as well as the daily food intake and thus account for both insulin and leptin serum concentrations being much greater than those of either the control, leptin or MTII treatments. In

contrast, the insulin and leptin serum concentrations were either similar or decreased by the MTII and leptin treatments without the prior treatment with SHU9119. The insulin concentrations of rats treated with MTII were similar to those of the control rats probably because the rats on these two treatments ate similar amounts on the day prior to the collection of the serum samples (Figure 2).

Because leptin and MTII have similar actions on body fat, body weight and food intake (Cettour-Rose and Rohner-Jeanrenaud, 2002), we hypothesized that MTII treatments might increase adipose tissue apoptosis, a phenomenon seen after leptin treatments (Qiqn et al., 1998). However, MTII administered ICV failed to induce adipose apoptosis in the present study, confirming our previous observations that IP injections of MTII accelerated lipid mobilization without apoptosis (Choi et al., 2003). These findings thus indicate that melanocortin receptors are not involved in leptin-induced adipose tissue apoptosis.

Although α -MSH has been suggested to be a downstream effector of leptin's central effects on food intake and body weight, recent studies have shown that some of leptin's actions may be independent of MC signaling. For example, Hohmann et al showed that SHU9119 attenuated leptin's effects on food intake and body weight in ob/ob mice, but had no effect on leptin's stimulatory effect on the reproductive axis. These findings, together with the results from our present and previous studies (Choi et al., 2003), indicate that not all leptin actions in the brain are mediated by MC receptor activation.

Reductions in FI and fat mass do not appear to be critical in determining apoptosis. A recent study showed that adipose apoptosis can occur without FI reduction [31]. In addition, we have previously shown that the reduction of fat mass following leptin treatments does not necessarily parallel the apoptotic response in fat tissues. For example, Gullicksen et al failed to

detect apoptosis in the eWAT of rats treated ICV with murine leptin, despite a significant reduction in fat pad weight (Gullicksen et al., 2002). In another study, leptin-induced apoptosis was detected in the rWAT but not iWAT, even though the two fat pads had similar reductions in mass in response to ICV leptin (Choi et al, unpublished data). In the present study, elevated apoptosis was detected in the eWAT, even though the other two fat pads had significant loss of mass without enhancing apoptosis. Fat tissues with a reduction in mass but no apoptosis in response to leptin treatments may be sensitive to lipolysis but resistant to apoptosis (Gullicksen et al., 2002).

As the present findings do not support a role of the MC3/4-Rs in the brain in mediation of leptin-induced fat depot apoptosis, what would be a potential mediator of the action of leptin on apoptosis? In a recent study, adipose tissue apoptosis was increased in rats treated with a neuropeptide Y (NPY) receptor blocker [31]. Because leptin has been shown to suppress NPY mRNA expression in the arcuate nucleus and decreases NPY secretion at nerve terminals in the PVN [32, 33] suppression of NPY signaling by leptin may result in adipose tissue apoptosis. We have also recently found that chronic oral administration of a β 2-adrenergic agonist resulted in increased adipose tissue apoptosis in mice [34]. Because leptin has been shown to increase sympathetic nervous system activity [35-37], it is possible that leptin-induced increased β 2-adrenergic receptor activation in specific fat depots could trigger adipocyte apoptosis.

In conclusion, these findings show that the MC receptors in the brain are involved in mediating actions of leptin on FI, fat mass and BW, however leptin-induced adipose apoptosis is regulated independently of the MC receptors.

References

- Adage T., Scheurink A. J., de Boer S. F., de Vries K., Kongsman J. P., Kuipers F., Adan R. A., Baskin D. G., Schwartz M. W. and van Dijk G. Hypothalamic, metabolic, and behavioral responses to pharmacological inhibition of CNS melanocortin signaling in rats. *J Neurosci.*21: 3639-3645; 2001.
- Alzet. (2001) Preparation of artificial CSF, Solution A.
- Cettour-Rose P. and Rohner-Jeanrenaud F. The leptin-like effects of 3-d peripheral administration of a melanocortin agonist are more marked in genetically obese Zucker (fa/fa) than in lean rats. *Endocrinology.*143: 2277-2283; 2002.
- Choi Y.-H., Li C., Page K. A., Westby A. L., Della-Fera M. A., Lin J., Hartzell D. L. and Baile C. A. Effect of MTII or leptin injected IP and ICV for 4 days on food intake, body weight, fat mass and adipose apoptosis in rats. *J Endocrinol.* in press; 2003.
- Cowley M. A., Pronchuk N., Fan W., Dinulescu D. M., Colmers W. F. and Cone R. D. Integration of NPY, AGRP, and melanocortin signals in the hypothalamic paraventricular nucleus: evidence of a cellular basis for the adipostat. *Neuron.*24: 155-163; 1999.
- Della-Fera M. A., Qian H. and Baile C. A. Adipocyte apoptosis in the regulation of body fat mass by leptin. *Diabetes Obes Metab.*3: 299-310; 2001.
- Elmqvist J. K. Hypothalamic pathways underlying the endocrine, autonomic, and behavioral effects of leptin. *Int J Obes Relat Metab Disord.*25 Suppl 5: S78-82; 2001.
- Fan W., Boston B. A., Kesterson R. A., Hruby V. J. and Cone R. D. Role of melanocortinergic neurons in feeding and the agouti obesity syndrome. *Nature.*385: 165-168; 1997.
- Feng J. D., Dao T. and Lipton J. M. Effects of preoptic microinjections of alpha-MSH on fever and normal temperature control in rabbits. *Brain Res Bull.*18: 473-477; 1987.
- Grill H. J., Ginsberg A. B., Seeley R. J. and Kaplan J. M. Brainstem application of melanocortin receptor ligands produces long-lasting effects on feeding and body weight. *J Neurosci.*18: 10128-10135; 1998.
- Gullicksen P. S., Hausman D. B., Dean R. G., Hartzell D. L. and Baile C. A. Adipose tissue cellularity and apoptosis after intracerebroventricular injections of leptin and 21 days of recovery in rats. *International Journal of Obesity* in press; 2002.
- Hamilton B. S. and Doods H. N. Chronic application of MTII in a rat model of obesity results in sustained weight loss. *Obes Res.*10: 182-187; 2002.
- Harrold J. A., Widdowson P. S. and Williams G. Altered energy balance causes selective changes in melanocortin-4(MC4-R), but not melanocortin-3 (MC3-R), receptors in specific

- hypothalamic regions: further evidence that activation of MC4-R is a physiological inhibitor of feeding. *Diabetes*.48: 267-271; 1999.
- Huang Q. H., Hruby V. J. and Tatro J. B. Systemic alpha-MSH suppresses LPS fever via central melanocortin receptors independently of its suppression of corticosterone and IL-6 release. *Am J Physiol*. 275: R524-530; 1998.
- Huszar D., Lynch C. A., Fairchild-Huntress V., Dunmore J. H., Fang Q., Berkemeier L. R., Gu W., Kesterson R. A., Boston B. A., Cone R. D., Smith F. J., Campfield L. A., Burn P. and Lee F. Targeted disruption of the melanocortin-4 receptor results in obesity in mice. *Cell*.88: 131-141; 1997.
- Hwa J. J., Ghibaudi L., Gao J. and Parker E. M. Central melanocortin system modulates energy intake and expenditure of obese and lean Zucker rats. *Am J Physiol Regul Integr Comp Physiol*. 281: R444-451; 2001.
- Ludwig D. S., Tritos N. A., Mastaitis J. W., Kulkarni R., Kokkotou E., Elmquist J., Lowell B., Flier J. S. and Maratos-Flier E. Melanin-concentrating hormone overexpression in transgenic mice leads to obesity and insulin resistance. *J Clin Invest*.107: 379-386; 2001.
- Marsh D. J., Hollopeter G., Huszar D., Laufer R., Yagaloff K. A., Fisher S. L., Burn P. and Palmiter R. D. Response of melanocortin-4 receptor-deficient mice to anorectic and orexigenic peptides. *Nat Genet*.21: 119-122; 1999.
- Murphy B., Nunes C. N., Ronan J. J., Hanaway M., Fairhurst A. M. and Mellin T. N. Centrally administered MTII affects feeding, drinking, temperature, and activity in the Sprague-Dawley rat. *J Appl Physiol*.89: 273-282; 2000.
- Paxinos G. and Watson C. (1986) *The Rat Brain in Stereotaxic Coordinates*. Academic Press, Sydney.
- Pierroz D. D., Ziotopoulou M., Ungsuan L., Moschos S., Flier J. S. and Mantzoros C. S. Effects of acute and chronic administration of the melanocortin agonist MTII in mice with diet-induced obesity. *Diabetes*.51: 1337-1345; 2002.
- Qian H., Azain M. J., Compton M. M., Hartzell D. L., Hausman G. J. and Baile C. A. Brain administration of leptin causes deletion of adipocytes by apoptosis. *Endocrinology*.139: 791-794; 1998.
- Raffin-Sanson M. L. and Bertherat J. Mc3 and Mc4 receptors: complementary role in weight control. *Eur J Endocrinol*.144: 207-208; 2001.
- Rezvani A. H., Denbow D. M. and Myers R. D. alpha-Melanocyte-stimulating hormone infused ICV fails to affect body temperature or endotoxin fever in the cat. *Brain Res Bull*.16: 99-105; 1986.

Scarpace P. J., Matheny M., Pollock B. H. and Tumer N. Leptin increases uncoupling protein expression and energy expenditure. *Am J Physiol.*273: E226-230; 1997.

Shimabukuro M., Zhou Y. T., Levi M. and Unger R. H. Fatty acid-induced beta cell apoptosis: a link between obesity and diabetes. *Proc Natl Acad Sci U S A.*95: 2498-2502; 1998.

Villar M., Perassi N. and Celis M. E. Central and peripheral actions of alpha-MSH in the thermoregulation of rats. *Peptides.*12: 1441-1443; 1991.

Yeo G. S., Farooqi I. S., Challis B. G., Jackson R. S. and O'Rahilly S. The role of melanocortin signaling in the control of body weight: evidence from human and murine genetic models. *Qjm.*93: 7-14; 2000.

APPENDIX C

EVALUATION OF ADIPOCYTE APOPTOSIS BY LASER SCANNING CYTOMETRY⁵

⁵ Lin, J., K. A. Page, M. A. Della-Fera, and C. A. Baile. Evaluation of Adipocyte Apoptosis by Laser Scanning Cytometry. *International Journal of Obesity*.

Abstract

Objective: Adipocyte apoptosis plays an important role in adipose tissue homeostasis and can be altered under a variety of physiological and pathological conditions. This study was carried out to determine whether laser scanning cytometry (LSC) can be used to measure changes in apoptosis of adipocytes over time.

Design: LSC was used to investigate adipocyte apoptosis induced by tumor necrosis factor-alpha (TNF- α), a cytokine that is associated with obesity and insulin resistance. LSC, a slide-based solid phase cytofluorometer, provides quantitative flow fluorescence data together with morphological information for apoptotic detection. Both 3T3-L1 cells and rat adipocytes from primary cell culture were incubated with 0 or 25 nM TNF- α for up to 24 hrs. Both the FITC-conjugated annexin V/propidium iodide assay and the TUNEL assay were used to distinguish cells with apoptotic characteristics from non-apoptotic cells.

Results: Apoptosis did not increase over time in the absence of TNF- α for both 3T3-L1 cells and rat primary adipocytes. For both 3T3-L1 cells and rat primary adipocytes, a significant increase in the percentage of apoptotic cells was observed by 3-4 h incubation with TNF- α ($P < 0.05$). By 24 h, more than 50% of cells incubated with TNF- α were apoptotic ($P < 0.001$). This process was also associated with morphological changes typical of adipocytes undergoing apoptosis. By estimating the percentage of cell subpopulations after different times of incubation with TNF- α , we were able to develop grading parameters, based on the adipose apoptotic measurements.

Conclusion: With morphological information, LSC can be a useful tool to evaluate adipocyte apoptosis.

Introduction

Adipose tissue is an important component of the body's energy balance regulatory system. Although in the past, energy storage was believed to be its only function (Ailhaud et al., 1992), it is now recognized that adipose tissue also plays an important role as an endocrine organ (Kim and Moustaid-Moussa, 2000; Ahima RS and Flier, 2000). Secreted proteins produced by adipocytes are involved in a variety of metabolic functions and serve as signals of peripheral energy balance to the central nervous system.

Because of the tremendous rise in the incidence of obesity and type II diabetes, diseases in which adipose tissue plays a central role, there is an even greater urgency today in understanding critical aspects in adipose tissue growth and physiology. The molecular regulation of adipogenesis, the development of fat cells from preadipocytes, has been intensively studied (Rosen and Spiegelman, 2000); however, there is relatively little known about the other end of the life cycle of adipocytes—apoptosis, or the regulated destruction of adipocytes.

Although it was once believed that adipocyte acquisition was permanent and that weight loss caused a decrease in cell size only (Ailhaud et al., 1992), it is now recognized that adipocyte acquisition is balanced by a process including cell deletion (Prins JB and O'Rahilly, 1997; Prins et al., 1997). One factor that is known to cause apoptosis of adipocytes is TNF- α , a cytokine that plays key roles in both proinflammatory processes and the development of insulin resistance (Prins et al., 1997; Hotamisligil et al., 1993). Apoptosis is a closely regulated event, occurring under both physiological and pathological conditions. Apoptosis can be triggered through either a mitochondria-dependent pathway or via cell surface death receptor-mediated pathway, both of which lead to the activation of a cascade of proteases, called caspases, resulting in cleavage of nuclear and cytoplasmic substrates, DNA fragmentation and condensation, and ultimately,

removal of the apoptotic cells by phagocytosis (Gupta, 2001)).

To detect apoptosis, several techniques have been developed based on the understanding of morphological, biochemical and molecular mechanism involved. Changes in the phospholipid bilayers of cell membranes are observed early in the apoptosis process. The phosphatidylserine (PS) component of the phospholipid bilayer is externalized and can be detected by fluorescence labeling (Martin et al., 1996; Bratton et al., 1997). Annexin V (AV), a member of the annexin family of calcium-dependent phospholipid-binding proteins, has a high affinity for PS-containing phospholipid bilayers. FITC-conjugated AV is used as a fluorescent dye to detect this early event in apoptotic cells.

As the apoptotic process progresses, cell membranes lose integrity, allowing chromosomal DNA to be exposed. Propidium iodide, a fluorescent dye that binds to DNA can be used in conjunction with FITC-conjugated AV to identify subpopulations of cells with end-stage apoptotic changes (Bacso and Eliason, 2001).

The TUNEL enzymatic labeling assay is another method used to detect apoptosis in individual cells (). Extensive DNA fragmentation/degradation is a characteristic event that occurs in apoptosis. The TUNEL assay is used to detect DNA strand breaks by labeling the free 3'-OH ends.

Both of these assays can be used in conjunction with laser scanning cytometry (LSC) to provide both quantitative and morphological analysis of apoptosis (Bacso and Eliason, 2001). Laser Scanning Cytometry uses lasers to excite fluorochromes in cellular specimens and detects the fluorescence in discrete wavelengths with multiple photomultiplier tubes (PMT's). Data are collected on heterogeneous populations of cells, and software analysis tools are used to obtain statistical analysis of the populations. LSC also creates temporary digital images of the specimens

on microscope slides and employs image processing algorithms to identify and segment the "events" (e.g., individual cells). LSC can additionally find and quantitate events by multiple filter setting, for example, making it possible to distinguish cytoplasmic fluorescence from nuclear fluorescence. Finally, LSC generates high resolution images that allow visual inspection of individual cells of interest.

In this study, we used LSC to investigate the progression of apoptosis in adipocytes treated with TNF- α in vitro over a 24 h period. Our findings indicate that LSC is an effective tool for studying the progression of apoptotic changes in different populations of adipocytes in response to an apoptotic stimulus.

Materials and Methods

Rat primary adipocyte culture

Inguinal fat pads from 8 week-old male Sprague-Dawley rats (~100 g body weight) were excised aseptically. Adipose tissues from pairs of rats were pooled, minced and incubated with digestion buffer (0.1 M HEPES, 1.5% bovine serum albumin with 3.2 mg/ml collagenase (Sigma, St. Louis, MO)) in a shaking water bath at 37 °C for 2h, followed by filtration through double filters with 180- and 20- μ m nylon net (Millipore, Bedford, MA). Filtered cells then underwent brief centrifugation and were incubated with erythrocyte lysis buffer (154mM NH₄Cl, 10nM KHCO₃, 0.1mM EDTA) (7) for 5 minutes. Cells were washed with DMEM/F12 medium, resuspended in 10% FBS/DMEM/F12 medium and seeded onto either 35 mm culture dish at a density of 5×10^4 cells or 2 well chamber slide (1×10^4 /well density). To allow differentiation to mature adipocytes, one day after seeding, the medium was changed to serum free DMEM/F12 with ITTS (Sigma, containing 850 nM insulin, 64 nM transferrin, 29 nM sodium selenite and 2 nM T₃) for 6-8 days. Cells were then treated with low level insulin (8.5 nM) ITTS medium for 12 hr

prior to TNF- α treatment.

3T3-L1 cell culture

3T3-L1 mouse embryo fibroblasts were obtained from American Type Culture Collection (ATCC, Manassas, VA) and cultured as described elsewhere (14). In brief, cells were grown in 10% FCS/DMEM medium. After inducing confluent preadipocytes for 2 days (Day 0), cells were cultured with 10% FBS/DMEM culture medium, supplemented with 1 mM insulin, 0.5 mM isobutylmethylxanthine (IBMX) and 1 mM dexamethasone for two days (Day 2). Cells were then maintained in culture medium with 1 mM insulin supplement for another two days (Day 4), followed by culturing with 10% FBS/DMEM medium for additional 4 days, at which time more than 90% of cells were mature adipocytes that accumulated fat droplets and were ready for TNF- α incubation.

Cells were cultured at 37C in a humidified 5% CO₂ atmosphere. All media contained 100 U/ml of penicillin, 100 μ g/ml of streptomycin, and 292 μ g of L-glutamine/ml (Invitrogen, Carlsbad, CA).

TNF- α incubation experiments

All experiments were performed in duplicate or triplicate on two occasions. Twenty five (25) nM rat recombinant TNF- α (Sigma, in PBS/0.1% bovine serum albumin) was added to the culture medium (in DMEM/F12 for rat adipocyte culture and 10%FBS/DMEM for 3T3-L1) for up to 24h. In a separate experiment, cells were treated similarly, except without the addition of TNF- α , for 0, 12 and 24 h.

Annexin V/propidium iodide (AV/PI) assay for apoptosis

Monolayer cells were washed twice with cold PBS and once in binding buffer, then incubated for 10 minutes with 5 μ l AV-FITC and 5 μ l Propidium Iodide (PI) in 400 μ l binding buffer (BD Biosciences, San Diego, CA) at ambient temperature in dark with gentle agitation for 10 minutes.

TUNEL assay for apoptosis

APO-BrdU TUNEL (Terminal deoxynucleotide transferase dUTP nick end labeling) kit was obtained from Molecular Probes (Eugene, OR). Monolayer cells were fixed with 1% paraformaldehyde for 15 minutes on ice, washed twice with cold PBS, then stored in 70% ethanol at -30°C freezer for 24 h. Cells were then washed twice in washing buffer, followed by incubation with 150 μ l DNA-labeling solution (containing 30 μ l reaction buffer, 2.25 μ l terminal deoxynucleotidyl transferase (TdT), 24 μ l BrdUTP with 93.75 μ l dH_2O) covered with parafilm at 37°C in a humidity box with gentle agitation for 1h, followed by 30 minutes incubation with Alexa Fluor 488 dye-labeled anti-BrdU antibody (1:20 dilution) and an additional 30 minutes with PI/RNase buffer to stain the nucleus at room temperature in dark.

Laser Scanning Cytometry (LSC)

Fluorescence of gated cell populations was measured by LSC (CompuCyte, Cambridge, MA). Slides (trimmed dishes) were positioned on the microscope stage, excited by an argon laser at 488 nm and scanned stepwise using a 20x objective lens. Fluorescence emitted by the cells was collected through green (for AV/FITC or TUNEL/Alexa-Fluor) and long red (for PI) filters. Cell population data (fluorescent intensity, expressed as maximum pixel value of fluorescence) were analyzed by WinCyte and CompuSort software for sorting and morphological relocation. The scanning process on the user-defined region of interest took about 30 minutes to finish or stopped

automatically when 5000 events were collected.

Statistical analysis

Data were analyzed by one-way ANOVA according to the general linear model procedure using SAS (SAS, 1999) and were expressed as least square means \pm SEM. $P < 0.05$ was considered significant.

Results

The AV/PI combination assay detected apoptotic cell membrane phosphatidyl serine (PS) externalization and served as a measure of adipocyte viability. Utilizing these two stains, the LSC system can provide information about the progression from early apoptotic events to end stage apoptosis by measuring the relative changes in percent of cells stained with AV and PI over time (Fig. 1). In each scattergraph, cells in the lower left quadrant (Q1) have a low intensity of staining with either AV or PI, and are considered to be normal cells. Cells in the upper left quadrant (Q2) are stained primarily with AV, indicating early apoptosis. Cells with both AV and PI staining are entering a later stage of apoptosis and appear in the upper right quadrant (Q3). Cells with only PI staining appear in the lower right quadrant (Q4). These cells are dead, but at this stage death by necrosis cannot be differentiated from death by apoptosis. It is the progression of changes over time that indicates that cells are becoming apoptotic and dying. In this study, the number of apoptotic cells at each time point was determined by the total number of cells in quadrants 2,3 and 4. Quadrant settings are determined by the software, using intensity value criteria for each channel that are set by the user.

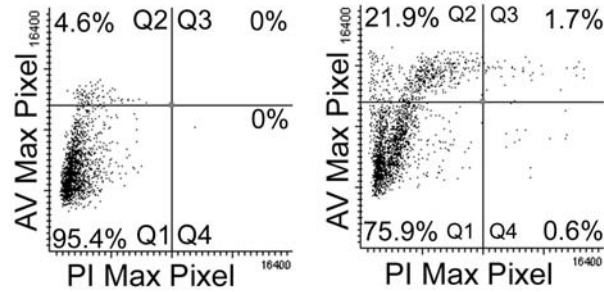


Figure 1. Example of LSC-generated scattergraph. Graphs are divided into four quadrants based on differences in intensity of AV and PI fluorescence. Increased AV fluorescence only (Q1) indicates cells undergoing early apoptotic events. As apoptosis progresses, more cells are stained with both AV and PI (Q3). End-stage apoptosis (cell death) is indicated by PI staining alone (Q4).

In control 3T3-L1 cells, the percent of apoptosis was low, as indicated by low levels of both AV and PI fluorescence (Fig. 3, 0 h), and apoptosis did not increase significantly over time (Fig. 2; 3T3-L1 adipocytes: $F[2,11]=2.46$, NS). In rat adipocytes, the basal level of apoptosis was higher than in 3T3-L1 cells, most likely a result of the reduction in insulin concentration in the incubation medium after cells reached maturity. However, as with the 3T3-L1 adipocytes, the percent apoptotic cells did not increase over the 24 hr period ($F[2,9]=0.95$, NS; Fig. 2).

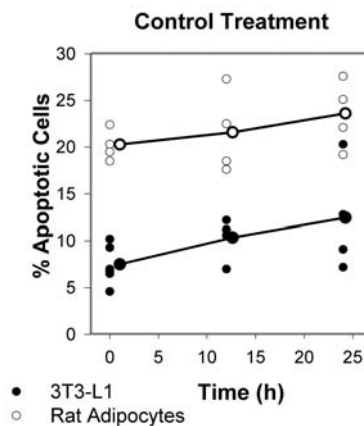


Figure 2. Percentage of apoptotic cells at 0, 12 and 24 hr in murine 3T3-L1 and rat primary adipocytes cultured in the absence of $TNF-\alpha$. Scattergraph of % apoptosis from individual dishes. Lines show mean % apoptosis at each time period.

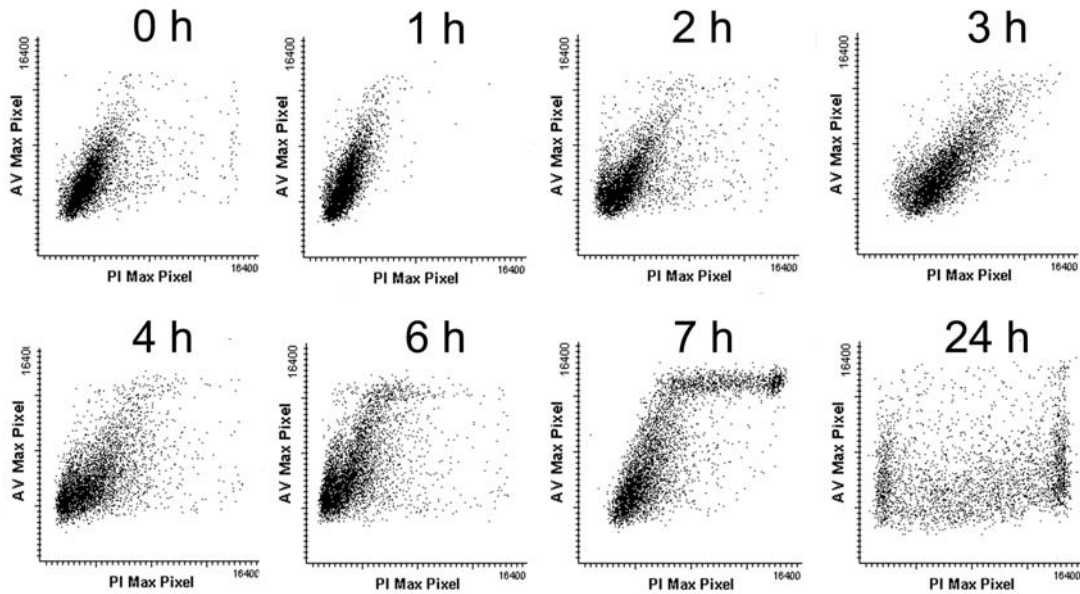


Figure 3. LSC-generated scattergraph series of AV/PI fluorescent intensity in adipocytes treated with 25 nM TNF- α for 0, 1, 2, 3, 4, 6, 7 and 24 h. Note that there was a shift of AV/PI intensity associated with development of apoptosis over time.

TNF- α (25 nM) induced apoptosis in both rat primary adipocytes and murine 3T3-L1 adipocytes, as detected with both AV/PI and TUNEL methods (Figs. 3 - 5). With increased TNF- α incubation time, the percentage of apoptotic 3T3-L1 cells increased, as indicated by the gradual increase in AV fluorescence (Fig. 3, Y axis). After 2 h, there were still relatively few cells with PI fluorescence, indicating that the cell membrane was intact (Fig. 3, 2h). As incubation proceeded, however, PI fluorescence increased in the cell population, demonstrating a shift in the number of cells in late-stage apoptosis (Fig. 3, 7h). By 24 h, more than half of the cells were at late-stage apoptosis, as characterized by high intensity of PI fluorescence with reduced AV fluorescence (Fig. 3, 24h and Fig. 4a). Figure 6 shows fluorescent images of 3T3-L1 adipocytes with different AV/PI fluorescent intensity, captured after LSC scanning using relocalization through CompuSort software.

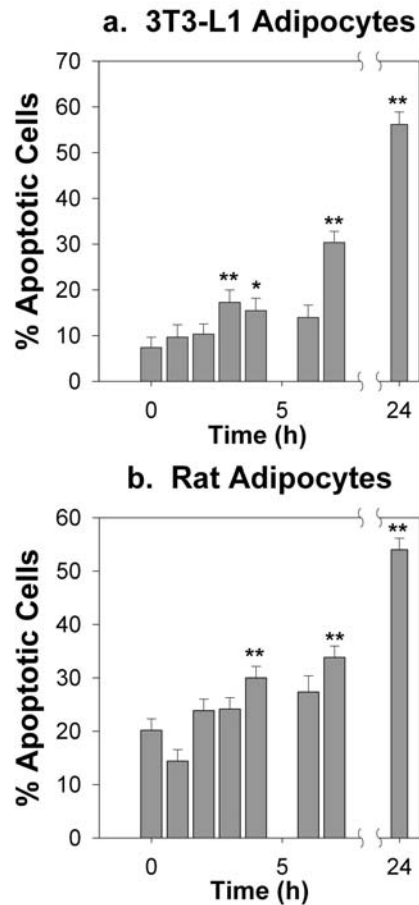


Figure 4. Percentage of apoptotic 3T3-L1 adipocytes (a) and apoptotic rat adipocytes (b) incubated with 25 nM TNF- α for 0, 1, 2, 3, 4, 6, 7 and 24 h. * $P < 0.05$, ** $P < 0.01$ compared to 0 h. N= 4-6.

Rat adipocytes responded to TNF- α with the same temporal pattern of apoptosis (Fig. 4b). Compared with 3T3 L1 adipocytes, the basal apoptotic percentage was higher in rat adipocytes (Fig. 2), which could be a result of using serum free medium and decreased insulin concentration in the rat adipocyte culture, as well as the fact that it was a more variable cell population. We also noticed that in rat adipocyte culture, some cell clusters were excluded from LSC analysis. Because the AV/ PI assay was used with live cells and the staining procedure was short, the threshold

fluorescence intensity may not have been reached for those cells.

TUNEL method analysis by LSC yielded results similar to those using the AV/PI method. One hour incubation with TNF- α produced both weak fluorescent TUNEL signals and low cell counts. After 4h TNF- α incubation, TUNEL fluorescence significantly increased (Fig. 5), along with increased cell counts, indicating that more cells were undergoing DNA fragmentation.

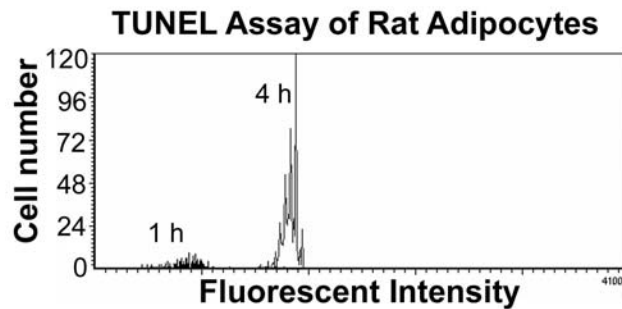


Figure 5. Histogram overlay of two time periods (1 h TNF- α incubation vs 4 h TNF- α incubation) of TUNEL intensity/counts in rat adipocytes. Note the weak signal and lower cell numbers at 1 h (left small peak) vs the intense signal and counts after 4 h incubation (4 h, right side).

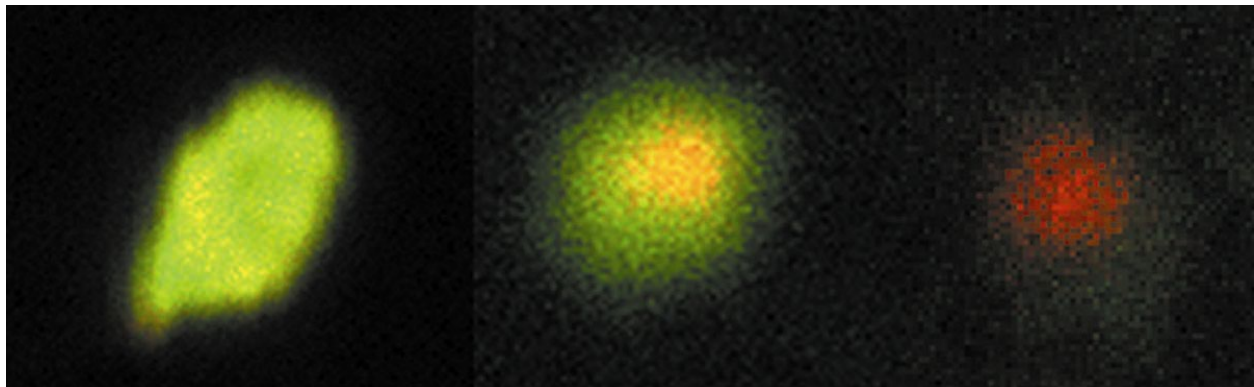


Figure 6. Fluorescent images showing cells with differences in AV/PI fluorescent intensities, captured after LSC scanning using relocalization through CompuSort software. From left to right: AV⁺PI⁻ cell, showing only green staining of the cell membrane; AV⁺PI⁺ cell, showing both green staining of the membrane and red staining of the nucleus; and AV⁻PI⁺ cell, showing only red staining of the nucleus (late stage of apoptosis).

After 24 hr TNF- α treatment, some cells had detached and were floating in the medium. These were washed out prior to LSC analysis. This could result in an underestimation of total percent of apoptotic cells. Figure 7 shows fluorescent images of rat adipocytes captured through CCD camera demonstrating TUNEL labeled fragmented DNA (green) in apoptotic cells compared to intact nuclei (PI, red) of nearby normal cells.

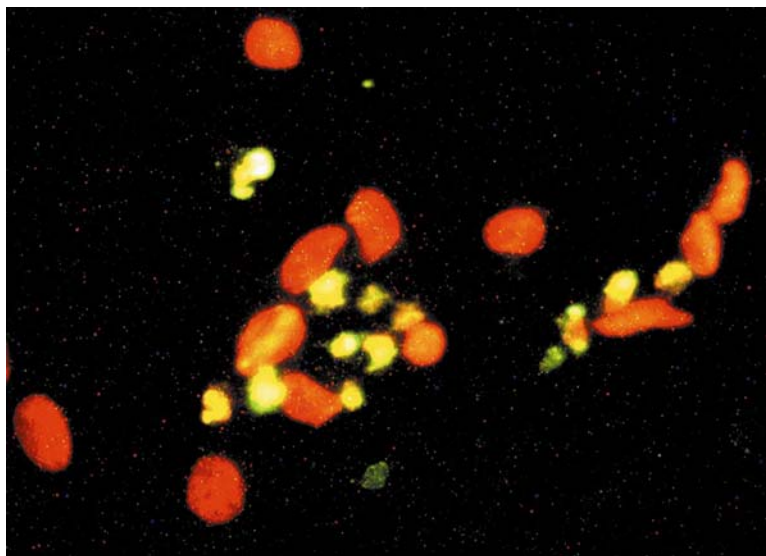


Figure 7. Fluorescent image captured through CCD camera shows TUNEL labeled fragmented DNA (green) in apoptotic cells compared to intact nuclei (PI, red) of nearby normal cells.

Discussion

Our study demonstrated TNF- α induced adipocyte apoptosis in vitro, as measured by LSC. Several techniques have been developed to detect apoptosis that are based on morphological, biochemical or molecular mechanisms of the apoptosis process, including light and electron microscopy, laser scanning confocal microscopy, flow cytometry, gel analysis of DNA fragmentation, and certain apoptotic factor assays. All of these assays have some advantages and

limitations (Watanabe et al., 2002). Laser scanning cytometry has recently been developed and is a microscope-based cytofluorometry method (Bacso Z and Eliason, 2001; Verdaguer et al., 2002; Bollmann et al., 2002) The LSC includes a digital microscope and an image processor to automatically segment cells and measure stoichiometric quantitative and morphological features of each cell. The LSC applies user-defined sets of rules to segment cells, and the image processing software extracts measurements for a variety of event features, including total fluorescence at each detector wavelength, peak brightness of each detector's signal, absolute position of the event, nuclear vs. peripheral fluorescence, etc. A unique feature of LSC is that every event (cell) recorded with fluorescence can be visualized after the completion of the analysis using Compusort software; thus LSC allows the analysis of a cell population quantitatively and with morphological evidence, as seen in this study (Fig 6-7).

By applying LSC in conjunction with AV/PI, we developed a method to evaluate apoptotic progress in adipocyte cultures. Annexin V is a Ca^{2+} dependent phospholipid binding protein that has a high affinity for PS, a membrane phospholipid. Under normal conditions, PS is distributed towards the intracellular leaflet of the cell membrane. During apoptosis, PS is translocated to the outer leaflet of the membrane, where it is exposed to AV. The externalization of PS requires the activation of caspase 3 and calcium flux (Martin et al., 1996; Bratton et al., 1997), both important factors in the apoptotic process. In our study, the percent of AV positive cells increased with increased TNF- α incubation time, indicating more adipocytes were undergoing the apoptotic process.

PI, a fluorescent dye that binds to DNA, is not able to permeate normal live cells; thus, it is used to distinguish end stage apoptotic cells from normal viable cells in live cell cultures. In our study, PI intensity was low in controls, but as TNF- α incubation time increased, PI level

significantly increased, indicating that an increased number of cells were undergoing late stage apoptosis. PI intensity does not differentiate apoptotic cells from necrotic ones; however, together with the temporal shift and AV intensity, it was clear that apoptosis, not necrosis, resulted in the death process triggered by TNF- α in this study.

We also used the TUNEL method to detect DNA fragmentation in apoptotic cells. Terminal deoxynucleotidyl transferase (TdT) recognizes 3'-hydroxyl ends of DNA fragments, and adds deoxyribonucleotides in a template-independent fashion. In our study, 5-bromo-2'-deoxyuridine 5'-triphosphate (BrdUTP) was used as a substrate (deoxythymidine analog) to the TdT reaction to label the break sites. Once incorporated into the DNA, it is detected by anti-BrdU antibody labeled with Alexa Fluor 488 dye. We found that treatment of adipocytes by 25 nM TNF- α for just 4h resulted in significantly increased DNA fragmentation (Fig. 4).

TNF- α is a cytokine that is mainly produced by macrophages but also by lymphoid cells, endothelial cells, fibroblasts and adipocytes (Kern et al., 1995). TNF- α has a wide range of bioactivities and plays key roles in pro-inflammatory regulation and cachexia. In adipose cells, TNF- α stimulates lipolysis (Gasic et al., 1999; Green et al., 1994), inhibits preadipocyte differentiation and causes delipidation of newly developed adipocytes (Green et al., 1994; Petruschke and Hauner, 1993). TNF has also been shown to induce adipocyte apoptosis (Prins et al., 1997; Qian et al., 2001). TNF- α induced apoptosis involves binding to TNF-receptor 1, which results in recruitment of TNF receptor-associated death domain (TRADD) and activation of the cascade of caspases that lead to cell death and phagocytosis by macrophages (for reviews, see (Ashe and Berry, 2003; Schultz and Harrington, 2003).

In obesity expression of TNF- α in adipocytes is increased, and this is believed to be a major factor in the development of insulin resistance and Type II diabetes (Hotamisligi et al., 1993).

TNF- α directly interferes with the insulin signaling cascade, impairs insulin-stimulated glucose transport and may act as an important autocrine/paracrine regulator of fat cell function to limit adipose tissue expansion. This could be, at least in part, though triggering adipocyte apoptosis.

Change in adipose tissue mass involves change in adipocyte number or volume or both (Krotkiewski et al., 1983; Gullicksen et al., 2003). Because apoptosis is an important mechanism in regulating adipose cell number, a better understanding of the mechanisms involved could lead to development of more effective treatment strategies for obesity and related metabolic disorders. LSC provides a relatively fast method for obtaining both quantitative and morphological information about the apoptotic process in adipocytes; therefore it can serve as a valuable tool, both to study the molecular mechanisms and to screen potential new drugs for activity in inducing adipocyte apoptosis.

Acknowledgments

This work was supported in part by the Georgia Research Alliance Eminent Scholar endowment held by CAB.

References

- Ahima RS and Flier JS. Adipose tissue as an endocrine organ. *Trends Endocrinol.Metab* 2000; 11: 327-332.
- Ailhaud G, Grimaldi P and Negrel R. Cellular and molecular aspects of adipose tissue development. *Annu Rev Nutr* 1992; 12: 207-233.
- Ashe PC and Berry MD. Apoptotic signaling cascades. *Prog.Neuropsychopharmacol.Biol.Psychiatry* 2003; 27: 199-214.
- Bacso Z and Eliason JF. Measurement of DNA damage associated with apoptosis by laser scanning cytometry. *Cytometry* 2001; 45: 180-186.
- Bollmann R, Torka R, Schmitz J, Bollmann M and Mehes G. Determination of ploidy and steroid receptor status in breast cancer by laser scanning cytometry. *Cytometry* 2002; 50: 210-215.
- Bratton DL, Fadok VA, Richter DA, Kailey JM, Guthrie LA and Henson PM. Appearance of phosphatidylserine on apoptotic cells requires calcium-mediated nonspecific flip-flop and is enhanced by loss of the aminophospholipid translocase. *J.Biol.Chem* 1997; 272: 26159-26165.
- Gasic S, Tian B and Green A. Tumor necrosis factor alpha stimulates lipolysis in adipocytes by decreasing Gi protein concentrations. *J.Biol.Chem* 1999; 274: 6770-6775.
- Green A, Dobias SB, Walters DJ and Brasier AR. Tumor necrosis factor increases the rate of lipolysis in primary cultures of adipocytes without altering levels of hormone-sensitive lipase. *Endocrinology* 1994; 134: 2581-2588.
- Gullicksen PS, Hausman DB, Dean RG, Hartzell DL and Baile CA. Adipose tissue cellularity and apoptosis after intracerebroventricular injections of leptin and 21 days of recovery in rats. *Int.J.Obes.Relat Metab Disord.* 2003; 27: 302-312.
- Gupta S. Molecular steps of death receptor and mitochondrial pathways of apoptosis. *Life Sci* 2001; 69: 2957-2964.
- Hemati N, Ross SE, Erickson RL, Groblewski GE and MacDougald OA. Signaling pathways through which insulin regulates CCAAT/enhancer binding protein alpha (C/EBPalpha) phosphorylation and gene expression in 3T3-L1 adipocytes. Correlation with GLUT4 gene expression. *Int.J.Obes.Relat Metab Disord.* 1997; 272: 25913-25919.
- Hotamisligil GS, Shargill NS and Spiegelman BM. Adipose expression of tumor necrosis factor-alpha: direct role in obesity-linked insulin resistance. *Science* 1993; 259: 87-91.
- Kern PA, Saghizadeh M, Ong JM, Bosch RJ, Deem R and Simsolo RB. The expression of tumor necrosis factor in human adipose tissue. Regulation by obesity, weight loss, and relationship to lipoprotein lipase. *J.Clin.Invest* 1995; 95: 2111-2119.
- Kim S and Moustaid-Moussa N. Secretory, endocrine and autocrine/paracrine function of the adipocyte. *J Nutr* 2000; 130: 3110S-3115S.
- Krotkiewski M, Bjorntorp P, Sjostrom L and Smith U. Impact of obesity on metabolism in men and women. Importance of regional adipose tissue distribution. *J.Clin.Invest* 1983; 72: 1150-1162.

- Martin SJ, Finucane DM, Amarante-Mendes GP, O'Brien GA and Green DR. Phosphatidylserine externalization during CD95-induced apoptosis of cells and cytoplasts requires ICE/CED-3 protease activity. *J.Biol.Chem.* 1996; 271: 28753-28756.
- Petruschke T and Hauner H. Tumor necrosis factor-alpha prevents the differentiation of human adipocyte precursor cells and causes delipidation of newly developed fat cells. *J.Clin.Endocrinol.Metab* 1993; 76: 742-747.
- Prins JB, Niesler CU, Winterford CM, Bright NA, Siddle K, O'Rahilly S, Walker NI and Cameron DP. Tumor necrosis factor-alpha induces apoptosis of human adipose cells. *Diabetes* 1997; 46: 1939-1944.
- Prins JB and O'Rahilly S. Regulation of adipose cell number in man. *Clin Sci (Lond)* 1997; 92: 3-11.
- Prins JB, Walker NI, Winterford CM and Cameron DP. Apoptosis of human adipocytes in vitro. *Biochem Biophys Res Commun* 1994; 201: 500-507.
- Qian H, Hausman DB, Compton MM, Martin RJ, Della-Fera MA, Hartzell DL and Baile CA. TNFalpha induces and insulin inhibits caspase 3-dependent adipocyte apoptosis. *Biochem.Biophys.Res.Commun.* 2001; 284: 1176-1183.
- Rosen ED and Spiegelman BM. Molecular regulation of adipogenesis. *Annu Rev Cell Dev Biol* 2000; 16: 145-171.
- SAS. *SAS User's Guide*. Statistical Analysis Systems Institute, Inc.: Cary, NC, 1999.
- Schultz DR and Harrington WJ, Jr. Apoptosis: programmed cell death at a molecular level. *Semin.Arthritis Rheum.* 2003; 32: 345-369.
- Smolewski P, Bedner E, Du L, Hsieh TC, Wu JM, Phelps DJ and Darzynkiewicz Z. Detection of caspases activation by fluorochrome-labeled inhibitors: Multiparameter analysis by laser scanning cytometry. *Cytometry* 2001; 44: 73-82.
- Verdaguer E, Pubill D, Rimbau V, Jimenez A, Escubedo E, Camarasa J, Pallas M and Camins A. Evaluation of neuronal cell death by laser scanning cytometry. *Brain Res.Brain Res.Protoc.* 2002; 9: 41-48.
- Watanabe M, Hitomi M, van der WK, Rothenberg F, Fisher SA, Zucker R, Svoboda KK, Goldsmith EC, Heiskanen KM and Nieminen AL. The pros and cons of apoptosis assays for use in the study of cells, tissues, and organs. *Microsc.Microanal.* 2002; 8: 375-391.

APPENDIX D

COMPARATIVE 2D DIFFERENCE GEL ANALYSIS OF HYPOTHALAMUS PROTEIN EXPRESSION PATTERN OF MYOSTATIN KNOCKOUT MICE WITH CLENBUTEROL TREATMENT⁶

⁶Lin, J., K. A. Page, T. M. Andacht, M A. Della-Fera, D. L. Hartzell, and C. A. Baile. Comparative 2D Difference Gel Analysis of Hypothalamus Protein Expression Pattern of Myostatin Knockout Mice with Clenbuterol Treatment. *Endocrinology Abstract* 2004.

Abstract

Myostatin (growth and differentiation factor-8, GDF-8) is a member of the TGF- β family of growth factors that inhibits muscle growth. Knockout of the myostatin gene results in increased skeletal muscularity and decreased adiposity. In this study we used two-dimensional difference gel electrophoresis (DIGE) analysis to compare the global hypothalamic protein expression patterns in myostatin knockout (KO) and wild type (WT) mice treated with clenbuterol, a β 2-adrenergic receptor agonist, or control. Four groups (N=5) were selected from 10 WT and 10 KO adult mice. They were given either 0 or 200 ppm clenbuterol in their food for 3 weeks. After the mice were killed, brains were removed and hypothalami were collected. Proteins were extracted in 5 M urea, 2 M thiourea, 4% CHAPS and 15mM Tris buffer at pH8.3 with sonication, followed by further cleaned-up and concentrated through filter centrifugation. Prior to electrophoresis, 50 :g of hypothalamic protein samples were labeled with 3 different fluorescent CyDyes: Cy3 for WT, Cy5 for KO samples and a pooled sample, labeled with Cy2, that included equal amounts of protein from all 20 hypothalamic samples and served as internal standard to improve the accuracy of protein quantification between samples from different gels. A pair of the differently labeled samples was then co-separated on the same 2D gel (pH 3-10, 8-15% gradient) in addition to the pooled sample. Two way ANOVA analysis plus 3D image view indicated that 82 spots ($P<0.05$) had significant differences between genotypes in protein quantity. In myostatin KO mice, 46 proteins had increased levels and 36 proteins had decreased levels compared to WT. Forty proteins showed a difference in quantity between clenbuterol and control treatments ($P<0.05$). In clenbuterol treated mice, 14 proteins had reduced levels and 26 proteins had increased levels compared to control. Our results indicate that hypothalamic protein expression pattern is affected by both myostatin gene knockout and clenbuterol treatment, and demonstrate

that alterations in muscle and fat mass can affect hypothalamic protein expression patterns. In addition, this study shows that DIGE analysis provides a powerful tool for comparative proteomics. Further downstream protein identification will be carried out by mass spectrometry. Supported in part by the Georgia Research Alliance Eminent Scholar endowment held by CAB.